



University of  
Stavanger

**Faculty of Science and Technology**

## MASTER'S THESIS

Study program/Specialization:

Petroleum Geosciences Engineering

Spring, 2018

Open

Writer:

Tonje Iren Braut

(Writer's signature)

Faculty supervisor: Alejandro Escalona  
Carita Augustsson

External supervisor(s):

Title of thesis:

Middle to Upper Jurassic Depositional Setting in the Hammerfest Basin, Southwestern Barents Sea

Credits (ECTS): 30

Keywords:

Hammerfest Basin  
Fuglen and Hekkingen Formations  
Facies Associations  
Rift Basin

Pages: 106

+enclosure:

Stavanger, July 6, 2018.

Copyright  
by  
Tonje Iren Braut  
2018

**Middle to Upper Jurassic Depositional Setting in the Hammerfest Basin,  
Southwestern Barents Sea**

**by**

**Tonje Iren Braut**

**MSc Thesis**

Presented to the Faculty of Science and Technology

The University of Stavanger

**The University of Stavanger**

**July 2018**

## **ACKNOWLEDGEMENTS**

I would like to express my sincere gratitude to my supervisors Alejandro Escalona and Carita Augustsson for their valuable guidance and support throughout this project.

A great thanks also goes to Dora Marín for guidance during the core viewing, and technical support with the Landmark Decisionspace software.

Acknowledgement also goes to the JuLoCrA project sponsors for the financial support, Halliburton Landmark for the Decisionspace software, Lundin Norway AS and PGS for permission to use the information of the OMV0801LNR14 and LN12M01 three-dimensional seismic cubes, and the Norwegian Petroleum Directorate for organizing the core viewing.

Furthermore, a great thanks to my fellow students at the University of Stavanger, these two years of studying would not have been the same without you!

Lastly, I thank my family and friends for endless support through the duration of my studies. I could not have done this without you.

## **ABSTRACT**

### **Middle to Upper Jurassic Depositional Setting in the Hammerfest Basin, Southwestern Barents Sea**

Tonje Iren Braut, MSc

The University of Stavanger, 2018

Supervisor: Alejandro Escalona and Carita Augustsson

The Middle to Upper Jurassic Fuglen and Hekkingen formations of the southwestern Barents Sea represents both important source rocks and seals in several petroleum plays in the region. The current understanding of this time interval is that deposition occurred during a time of regional transgression and active rifting, in an oxic to restricted marine setting. The depositional setting and controls of deposition in the Middle to Upper Jurassic is still poorly understood, as few studies have evaluated this time interval from the basin evolution point of view. Throughout the Hammerfest Basin, the Fuglen and Hekkingen formations display great variability, both in facies and distribution. This study aims to improve the understanding of the depositional setting, the palaeogeography and the controlling factors on the lateral and vertical variabilities of the Middle to Upper Jurassic interval in the Hammerfest Basin. This is achieved by utilizing and integrating an extensive dataset comprising core data, 2D and 3D reflection seismic, and petrophysical data. Main findings includes five different facies associations, where shallow marine, restricted anoxic and mass flow deposits dominate. A time significant sequence stratigraphic framework is defined, comprising the sequences J1-J5, that are bound by regional unconformities and flooding surfaces. The

sequences provides a good correlation with the existing lithostratigraphic framework, and the facies associations defined in this study. Local tectonic activity acts as the main control on the deposition of the sequences J1-J5. Diachronous fault activity led to the formation of local isolated depocenters, where the accommodation creation was controlled by differential subsidence along the different fault segments. Areas of erosion or non-deposition were present over structural high, however, clastic sediment sources were not emergent until the deposition of sequences J4-J5. The deposition of the sequences correlates with a regional sea-level rise, where the transgressional processes observed in the study area were most likely further amplified by local tectonics.

## Table of Contents

<b>ACKNOWLEDGEMENTS</b> .....	<b>IV</b>
<b>ABSTRACT</b> .....	<b>V</b>
<b>LIST OF TABLES</b> .....	<b>X</b>
<b>LIST OF FIGURES</b> .....	<b>XI</b>
<b>1. INTRODUCTION</b> .....	<b>19</b>
1.1. Motivation and Objectives .....	1
<b>2. GEOLOGICAL SETTING</b> .....	<b>3</b>
2.1. Structural Framework of the Hammerfest Basin .....	5
2.2. Lithostratigraphy .....	8
2.2.1. Stø Formation: .....	9
2.2.2. Fuglen Formation:.....	10
2.2.3. Hekkingen Formation: .....	10
<b>3. DATA AND METHODOLOGY</b> .....	<b>12</b>
3.1. Data .....	12
3.2. Methodology .....	14
3.2.1. Core logs: .....	14
3.2.2. Framework .....	14
3.2.3. Seismic:.....	15
3.2.4. Limitations: .....	16
<b>4. OBSERVATIONS AND INTERPRETATION</b> .....	<b>19</b>
4.1. Core and GR analysis – Facies and depositional processes.....	19
4.1.1. Facies Association 1 (FA1) – Transgressive Shelf.....	23
Observations from cores: .....	23
Correlation with GR:.....	27
Interpretation:.....	28
4.1.2. Facies Association 2 – Lower Shoreface to Offshore Transition .....	30
Observations from core:.....	30

Correlation with GR:.....	33
Interpretation.....	34
4.1.3. Facies Association 3 – Offshore .....	36
Observations from core:.....	36
Correlation with GR:.....	39
Interpretation.....	40
4.1.4. Facies Association 4 – Restricted Anoxic .....	41
Observations from core:.....	41
Correlation with GR:.....	42
Interpretation:.....	43
4.1.5 Facies Association 5 – Mass Flow.....	45
4.1.5.1 Sub-association 5a – Distal basin floor fan.....	45
Observations: .....	45
Correlation with GR:.....	46
Interpretation:.....	47
4.1.5.1 Sub-association 5b – Proximal basin floor fan .....	48
Observations: .....	48
Correlation with GR:.....	49
Interpretation:.....	50
4.2 Genetic Sequences and Age Control.....	52
4.2.1. Sequence J1:.....	54
4.2.2. Sequence J2:.....	54
4.2.3. Sequence J3:.....	55
4.2.4. Sequence J4:.....	55
4.2.5. Sequence J5:.....	56
4.3. Seismic Interpretation .....	60
4.3.1 Structural Configuration .....	60
4.3.2. Vertical and Lateral Distribution .....	65
<b>5. DISCUSSION.....</b>	<b>67</b>
5.1. Controlling Factors on Basin Fill.....	67
5.1.1. Sediment supply:.....	67
5.1.2. Eustasy .....	69



5.1.3. Subsidence .....	71
5.2. Depositional Evolution .....	74
5.2.1. Stage 1: Late Bathonian – Oxfordian (Sequences J1 and J2).....	74
5.2.2. Stage 2: Kimmeridgian – Ryazinian (Sequences J3-J5).....	76
<b>6. CONCLUSIONS.....</b>	<b>78</b>
<b>REFERENCES: .....</b>	<b>80</b>

## LIST OF TABLES

Table 1: Wells with available core data from the Middle to Upper Jurassic interval in the Hammerfest Basin.....	12
Table 2: Key wells and available data used in this study for facies analysis and correlations.....	13
Table 3: Facies description and process interpretation for the lithofacies observed in the Middle to Upper Jurassic core sections in the Hammerfest Basin. ....	20
Table 4: Facies associations.....	21
Table 5: Correlation of facies associations observed in core sections with GR signature. Scale bars represents 10 m. ....	22

## LIST OF FIGURES

- Figure 1: A) Bathymetric map of the Arctic from Jakobsson et al. (2012), with the southwestern Barents Sea outlined. B) Main structural elements of the southwestern Barents Sea. Study area is outlined in red together with key wells used in this study. ....21
- Figure 2: Main structural elements of the southwestern Barents Sea as defined by Gabrielsen et al. (1990). Colours reflect the focus of tectonic activity during the three rift phases. Abbreviations: BB = Bjørnøya Basin, HB = Harstad Basin, HfB = Hammerfest Basin, LH = Loppa High, MB = Maud Basin, NB = Nordkapp Basin, NH = Norsel High, OB = Ottar Basin, PSP = Polheim Sub-platform, SB = Sørvestnaget Basin, SR = Senja Ridge, TB = Tromsø Basin, VH = Veslemøy High. Modified from Faleide et al. (2010). ....4
- Figure 3: A) NNW-SSE regional line across the western part of the Hammerfest Basin illustrating the basin configuration and main structural elements. Note the thinning of the Middle to Upper Jurassic strata towards the Central High. B) NNW-SSE regional line across the central part of the Hammerfest Basin illustrating the general basin configuration and main structural elements. Note that the Loppa High is not faulted in this area. C) NW-SE regional line across the eastern part of the Hammerfest Basin illustrating the basin configuration and main structural elements. Note the decrease in fault activity from west to east. D) Time structural map of the Base Cretaceous unconformity, location of regional lines and the main structural elements of the Hammerfest Basin. Lower Cretaceous seismic sequences are defined according to Marín (2017). ....7

Figure 4: General Jurassic and Cretaceous lithostratigraphy of the southwestern Barents Sea. Modified from Nøttvedt et al. (1993). Geodynamic events from Worsley (2008) and Smelror et al. (2009). .....	9
Figure 5: Overview of the seismic coverage, well distribution and location of wells with core sections from the Middle and Upper Jurassic interval in the study area. ....	13
Figure 6: NW-SE regional seismic line illustrating Middle to Upper Jurassic seismic sequence with well 7120/2-2 drilled on the northern basin margin. The GR-log illustrates the five Middle to Upper Jurassic genetic sequences. The figure also illustrates the scale differences of the data utilized in this study, ranging from several kilometers basin wide, to mm scale within the cored intervals. Note the thickness of the cored section of well 7120/2-2 compared to the overall thickness of the Middle to Upper Jurassic sequences, and the limited coverage of the overall study area the core data provides.....	17
Figure 7: Synthetic seismograms for wells 7120/6-1 and 7120/2-2. Note the thickness and low seismic resolution of the Middle to Upper Jurassic seismic sequence.....	18
Figure 8: Location of the logged wells and the distribution of facies associations observed in cores.....	21

Figure 9: Facies observed in FA1. A) Red coloured mudstones with brecciated contact and possible root traces, grading into a silty fine grained sandstone towards the top. From well 7122/7-3, depth 1088.5. B and C) Well rounded, pebble sized grains, in a medium-grained sandstone matrix (F6). The upper interval consists of alternating layers of light and dark brown mudstones (F1) with possible glossifungites trace fossils just below the upper contact. From well 7122/7-2, depth 1077.5 D) Grey to dark grey clast supported conglomerate (F6) overlying a massive sandstone (F12), with an erosive contact. From well 7121/4-2, depth 2481 m. E) Very fine grained, erosive-based sandstone with mud rip-up clasts and large pyrite nodules. From well 7120/6-1, depth 2388.5 m. Scale bars are 1 cm.....24

Figure 10: Core logs and associated GR logs for wells 7120/6-1 and 7121/4-2 located in the central part of the Hammerfest Basin. Ages for well 7121/4-2 is from the biostratigraphic report from the Petrobank database, conducted by Gearhart Geo Consultants LTD for Statoil (1985). Ages for 7120/6-1 is from the final well report (NPD, 2018). .....25

Figure 11: Core logs and associated GR log for wells 7122/7-3 and 7122/7-2 located on the Goliat Anticline. No age control was available for these wells. ....26

Figure 12: Distribution of FA1 observed from core data. ....27

Figure 13: Facies observed in FA2. A and B) Very fine grained, highly bioturbated silty sandstones (F5) displaying faint, low angle cross-stratification. From well 7122/7-3, depth 1084.6 m. C) Very fine grained, micaceous, highly bioturbated silty sandstone with high trace fossil diversity. From well 7120/12-1, depth 2047 m. D) Very fine grained to silty sandstone with faint ripple lamination (lower arrows) and large coal fragment (upper arrow). From well 7120/12-1, depth 2046 m. Scale bars are 1 cm. ....31

Figure 14: Core logs and the associated GR-log from well 7120/12-1 located on the southwestern basin margin. Ages are sourced from the final well report (NPD, 2018). ....32

Figure 15: Distribution of FA2 observed from core data and well-logs.....34

Figure 16: Facies observed in FA3. A) Horizontal burrow in a thin, very fine-grained light coloured sandstone. The sandstone is encased in a dark grey, micaceous and structureless mudstone. From well 7120/12-1, depth 1665.65 m. B and D) Dark grey to black, structureless mudstone with pyritized burrows. From well 7121/4-2 and 7120/6-1, depths 2473.7 m, and 2387.9 m., respectively. C) Dark grey micaceous mudstone with interbedded, very fine grained sandstone, sand-filled burrow, possible bivalve fossil and carbonate filled fractures. From well 7120/12-1, depth 1663.5 m. E) Very well preserved bivalve fossils in dark grey, micaceous mudstone. From well 7120/12-1, depth 1662 m. Scale bars are 1 cm. ....37

Figure 17: Core logs and gamma ray logs from wells 7120/2-2 and 7120/2-3-S located on the northern Hammerfest Basin margin. Ages for well 7120/2-2 is from the final well report (NPD). Ages for well 7120/2-3-S is from the biostratigraphic report available from the Petrobank database, conducted by Fugro Robertson Ltd. (2012). Ages for well 7120/2-2 is from the final well report (NPD, 2018). .....38

Figure 18: Distribution of FA3 observed in cores and well-logs.....39

Figure 19: Facies observed in FA4. A) Ptygmatically folded, vertical to sub-vertical sandstone beds encased in organic rich, black shale. From well 7120/2-3-S, depth 2017 m. B) Angular shale clasts in light grey, non-calcareous, well cemented sandstone. From well 7120/2-3-S, depth 2010 m. C and D) Parallel laminated to low-angle laminated dark coloured shales with carbonate filled fractures. From well 7120/2-3-S, depths 2004 m. E) Large pyrite nodule with well developed zonation in black shale. From well 7120/2-2, depth 2636.6 m. F) Poorly consolidated mudstone with euhedral pyrite crystals. From well 7120/2-2, depth 2023.5 m. Scale bars are 1 cm. ....42

Figure 20: Distribution of FA4 based on observations from cores and well-logs. 43

Figure 21: Facies observed in FA5a. A) Parallel laminated, very fine grained sandstone with interbedded mudstone and siltstone. B) Erosive contact in F11, overlain by soft sediment deformed sandstone and siltstone. A lithoclast with glauconite fragments (Lower arrow), and possibly authigenic glauconite (Upper arrow) is also observed. C) Parallel laminated, and ripple laminated sandstone and siltstone with micro-normal faults. All images are from well 7120/2-2, at depths 2637.5 m, 2637.1 m, and 2636.3 respectively. Scale bars are 1 cm. 46

Figure 22: Facies observed in FA5b. A) Chaotic medium grained sandstone with angular coal clasts (upper arrows) and glauconitic clast (lower arrow) (F8). B) Heterolithic bedding, fining upwards from medium grained sandstone to mudstone and slightly offset by micro-normal fault (F8 and F9). C) Ripple laminated, medium-grained sandstone (F9) D) Ripple laminated sandstone capped by dark brown mudstone, offset by micro-normal faults (F8 and F10) E) Medium-grained ripple laminated sandstone with erosive base and fining upwards (F9). All images are from well 7120/12-1 at depths, 1703.4 m, 1703 m, 1702 m, 1702.9 m, and 1703.2 m, respectively. Scale bars are 1 cm. ....49

Figure 23: Left: Coarse-grained clastic packages observed in well 7120/1-2, possibly belonging to FA5. Right: Distribution of FA5 based on observations from cores and well logs. ....50

Figure 24: Six selected wells and their correlation across the Hammerfest Basin illustrating the five third order sequences (J1-J5). The sequences are bound by flooding surfaces (FS1-FS4). The base of J1 and top of J5 are bound by the regional unconformities, the Upper Jurassic Unconformity (UJU) and Base Cretaceous Unconformity (BCU) respectively. Note the time transgressive relationship between the different sequences and their respective bounding surfaces, and the correlation between the sequences and the lithostratigraphy. Abbreviations: Cret=Cretaceous. Mb=Member. ....53

Figure 25: Chronostratigraphic correlation compared to the sequence stratigraphic framework and the lithostratigraphy along the northern Hammerfest Basin margin. Note the variability of ages within similar lithostratigraphic units. ....57



Figure 26: Chronostratigraphic correlation compared to the sequence stratigraphic framework and the lithostratigraphy along the northern Hammerfest Basin margin. Note the variability of ages within similar lithostratigraphic units. ....58

Figure 27: Chronostratigraphic correlation compared to the sequence stratigraphic framework and the lithostratigraphy across the Central High. Note the variability of ages within similar lithostratigraphic units. ....59

Figure 28: Time structural map of the Upper Jurassic Unconformity and the four different fault families identified. ....61

Figure 29: Upper: Un-interpreted NNW-SSE regional line. Middle: Interpreted NNW-SSE regional line illustrating the basin configuration of the southern central part of the study area. Note the diachronous fault activity and thinning of strata over the Central High. Lower: Close up of the Central High, where the line is flattened to the BCU surface. Internal reflectors of the Middle to Upper Jurassic seismic sequence are onlapping the structure. Location of the line is indicated in Figure 28. ....63

Figure 30: Upper: Interpreted NNW-SSE seismic line through the Goliat Anticline illustrating the structural configuration of the Goliat Anticline. Note the thinning of strata towards the structure. Lower: Close up of the flank of the Goliat Anticline flattened to the BCU surface, where the Middle to Upper Jurassic seismic sequence is seen onlapping the anticline. Location of the line is indicated in Figure 28. ....64

Figure 31: E-W regional line illustrating the basin configuration in southeastern part of the study area. Note the depocenter associated with FF4, and how some of the faults offset the entire seismic sequence, whereas others terminate before the BCU. Location of the line is indicated in Figure 28. ....	65
Figure 32: Time thickness map of the Middle to Upper Jurassic seismic sequence. Note how the depocenters are isolated and restricted to areas of more fault activity. ....	66
Figure 33: Composite sea level charts of the Jurassic to Lower Cretaceous, including transgressive-regressive cycles from Hardenbol et al. (1998). Modified from Haq et al. (1988), Surlyk (1990), and Hardenbol et al. (1998). ....	70
Figure 34: Subsidence plots generated for wells 7121/4-2, 7120/6-3-S, 7120/12-1, 7120/2-3-S and 7121/9-1. Note the large variability in subsidence at different locations. Locations of wells are indicated in insert map. .	72
Figure 36: Paleogeographic interpretation of sequences J1 and J2. ....	75
Figure 37: Paleogeographic interpretation of sequences J3-J5. Note the more widespread deposition of offshore and anoxic facies during this stage. ....	77

## 1. INTRODUCTION

The Barents Sea Shelf, offshore Northern Norway (Figure 1), has been the focus of extensive exploration activity since the first licenses in the region were awarded in the early 1980's. To date, the Jurassic interval has proven to be the most prolific, comprising both the most successful reservoir rock (Stø Formation) and the richest source rock (Hekkingen Formation) (Berglund et al., 1986; Stewart et al., 1991; Leith et al., 1993; Henriksen et al., 2011). Several play models are confirmed in the region; however, the Jurassic is the only proven commercial model that is currently in production. The more recent technical discoveries (e.g. Skalle, Salina and Nunatak wells) within the Lower Cretaceous interval have led to a renewed interest and motivation for further exploration of the Lower Cretaceous in the area. Despite the extensive exploration activity over the last 30 years, the Barents Sea region (Figure 1) is still regarded as an immature petroleum province, and several elements of the Jurassic to Lower Cretaceous petroleum systems are still poorly understood.

The Jurassic of the southwestern Barents Sea comprises the Stø, Fuglen and Hekkingen formations (Dalland et al., 1988). These successions represents a relatively thin transition from the sand-rich, continental to marginal marine deposits of the Triassic (Dalland et al., 1988; Mørk et al., 1999; Riis et al., 2008; Smelror et al., 2009), to the thick, mud-dominated, marine deposits of the Lower Cretaceous (Dalland et al., 1988; Mørk et al., 1999; Smelror et al., 2009; Marín, 2017). In the Hammerfest Basin (Figure 1), the Jurassic formations are bound by regional unconformities, and show great variability in both lithology and distribution (Dalland et al., 1988; Mørk et al., 1999;

Worsley, 2008; Henriksen et al., 2011). Based on the tectonic regime and depositional settings, the Late Pliensbachian to Bajocian Stø Formation has been described as comparable to the Triassic successions, deposited during a time of relative tectonic quiescence, in a shallow marine environment (Olaussen et al., 1984; Dalland et al., 1988; Smelror et al., 2009; Henriksen et al., 2011). The Bathonian to Ryazinian Fuglen and Hekkingen formations show more affinity to the Lower Cretaceous, deposited during a time of active rifting in a marine domain (Dalland et al., 1988; Worsley, 2008; Smelror et al., 2009; Henriksen et al., 2011; Marín, 2017).

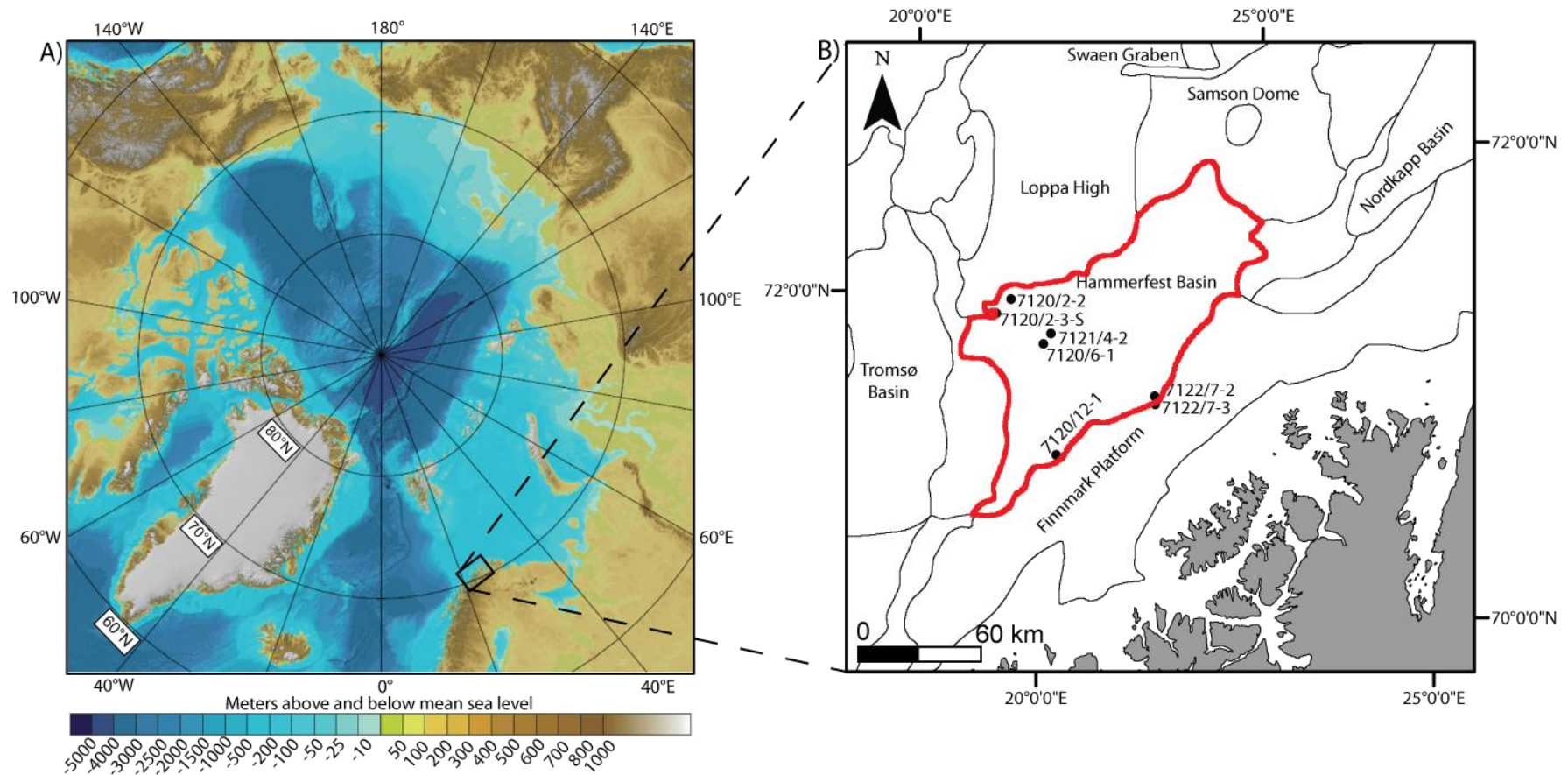


Figure 1: A) Bathymetric map of the Arctic from Jakobsson et al. (2012), with the southwestern Barents Sea outlined. B) Main structural elements of the southwestern Barents Sea. Study area is outlined in red together with key wells used in this study.

## **1.1. Motivation and Objectives**

The current understanding of the Middle to Upper Jurassic successions is that deposition occurred during an early stage of rifting and regional transgression, in a shelfal to deep marine environment with oxic to dysoxic conditions (Dalland et al., 1988; Faleide et al., 1993b; Mørk et al., 1999; Bugge et al., 2002). Palaeogeographic interpretations assume a relatively homogeneous deep-water shelf setting of the southwestern Barents Sea (Nøttvedt and Johannesen, 2008; Smelror et al., 2009; Nøttvedt and Johannesen, 2013). However, the Fuglen and Hekkingen formations display great variability in both distribution and lithology in the Hammerfest Basin (Figure 1). Sand-rich intervals occur as wedges along the basin margins (Henriksen et al., 2011; Marín, 2017), and thinning of strata towards the central part of the basin (Worsley, 2008), suggests that the prevalent interpretations for this time interval might be too general. The controls on deposition, and thus, the lateral and vertical facies variations are still poorly understood.

Consequently, the objectives of this thesis are to;

- Develop a more detailed understanding of the Middle to Upper Jurassic depositional setting and palaeogeography.
- Analyse lateral and vertical facies variations to determine controlling mechanisms on the sedimentation across the study area.

This is achieved by utilizing and integrating an extensive dataset comprising core-, well-log-, and seismic data. Moreover, the results of this study may further aid in improving current exploration models, as facies variations of the Fuglen and Hekkingen formations might be a controlling factor for source rock and seal quality in the Barents Sea region. Additionally, because the geological evolution of the Middle and Upper Jurassic seems to be genetically related to the Lower Cretaceous, investigation of depositional controls might lead to a better understanding of the Lower Cretaceous plays and improve the possibilities for potential plays in the sand-rich facies of the Hekkingen Formation.

## 2. GEOLOGICAL SETTING

The Barents Sea Shelf is bounded by Svalbard and Franz Josefs Land to the north, the Norwegian and Russian mainland in the south, the archipelagos of Novaya Zemlya to the east, and the continental slope of the Norwegian-Greenland Sea to the west (Figure 1). The region makes up a complex structural framework consisting of several basins, platforms and structural highs (Figure 1 Figure 2) (Gabrielsen et al., 1990; Doré, 1995; Henriksen et al., 2011). The present day structural configuration of the Barents Sea is largely a result of two major collisional events, the Caledonian Orogeny (Late Ordovician – Devonian) and the Uralian Orogeny (Late Devonian – Early Permian) (Doré, 1995; Rey et al., 1997; Gudlaugsson et al., 1998; Puchkov, 2009; Henriksen et al., 2011; Puchkov, 2013). The mainly NE-SW to N-S structural trends in the southwestern Barents Sea (Figure 2) are proposed to reflect the remnants of the Caledonian lineaments (Berglund et al., 1986; Doré, 1995; Gudlaugsson et al., 1998).

Following the two compressional events, three stages of rifting, occurring in the late Palaeozoic, Late Jurassic – Early Cretaceous, and Late Cretaceous – Palaeocene, have been proposed (Figure 2) (Gabrielsen et al., 1990; Faleide et al., 1993b; Gudlaugsson et al., 1998; Faleide et al., 2010; Henriksen et al., 2011). The Late Palaeozoic rifting was a result of the initial phase of crustal extension between Norway and Greenland, and led to the formation of several interconnected basins, separated by fault bounded highs (Dengo and Røssland, 1992). Structures such as the Loppa High, Tromsø Basin, Nordkapp Basin, and possibly the Hammerfest Basin (Figure 1 Figure 2) were formed during this stage (Riis et al., 1986; Gabrielsen et al., 1990; Dengo and Røssland, 1992;



Gudlaugsson et al., 1998). During the Middle Jurassic – Lower Cretaceous, widespread rifting occurred over large parts of the Barents Sea shelf, combined with proposed strike-slip adjustments along the older structural lineaments (Faleide et al., 1993a; Faleide et al., 1993b; Gudlaugsson et al., 1998; Faleide et al., 2008). Additionally, the Barents Sea area also underwent times of severe uplift and erosion during the Upper Cretaceous, Upper Eocene, and Pliocene – Pleistocene (Berglund et al., 1986; Gabrielsen et al., 1990; Smelror et al., 2009; Henriksen et al., 2011). These events have been proposed as a main factor for the breaching of hydrocarbon traps and redistributing hydrocarbons within the different basins in the southwestern Barents Sea region (Doré and Jensen, 1996; Ohm et al., 2008).

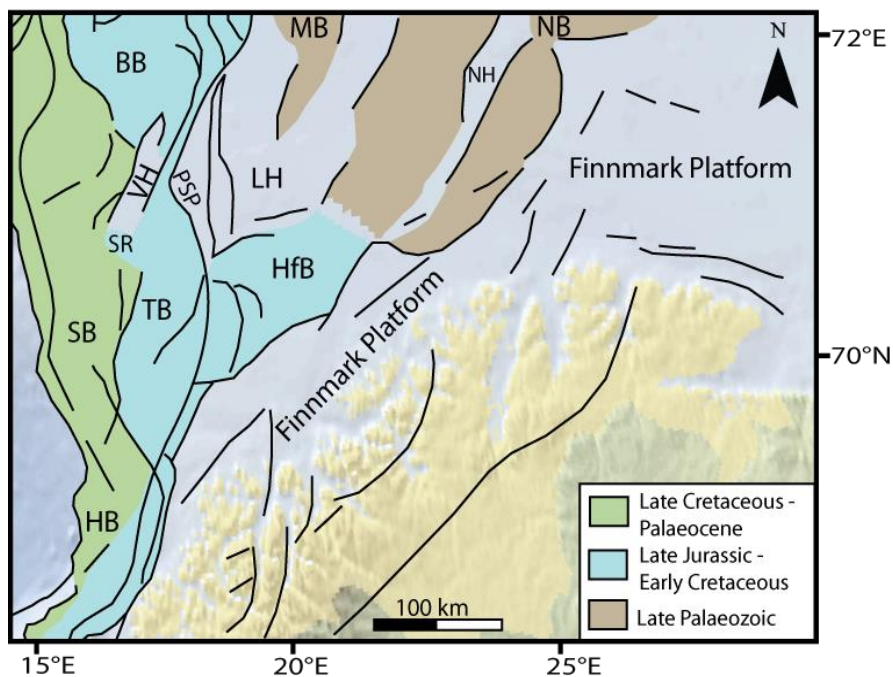


Figure 2: Main structural elements of the southwestern Barents Sea as defined by Gabrielsen et al. (1990). Colours reflect the focus of tectonic activity during the three rift phases. Abbreviations: BB = Bjørnøya Basin, HB = Harstad Basin, HfB = Hammerfest Basin, LH = Loppa High, MB = Maud Basin, NB = Nordkapp Basin, NH = Norsel High, OB = Ottar Basin, PSP = Polheim Sub-platform, SB = Sørvestnaget Basin, SR = Senja Ridge, TB = Tromsø Basin, VH = Veslemøy High. Modified from Faleide et al. (2010).

## **2.1. Structural Framework of the Hammerfest Basin**

The Hammerfest Basin is situated south of the Loppa High, bounded by the Asterias Fault Complex (AFC) to the north, Ringvassøy-Loppa Fault Complex (RLFC) to the west, Troms-Finmark Fault Complex (TFFC) to the south, and the Bjarmeland Platform to the east (Figure 2)(Gabrielsen et al., 1990). It is an ENE-WSW striking basin, with several ENE-WSW to E-W striking faults, mainly in the central and western parts of the basin (Figure 3) (Berglund et al., 1986; Larssen et al., 2002). The eastern part of the basin is shallower and less affected by fault activity (Figure 3). The Hammerfest Basin can be subdivided into a western and eastern sub-basin, proposed to correlate with a possible offshore extension of the onshore Trollfjord-Komagelv Fault Zone (Ziegler et al., 1986; Gabrielsen et al., 1990; Roberts and Lippard, 2005).

From the Late Palaeozoic up until the Middle Jurassic, the Hammerfest Basin was part of an intracratonic basin, during a time of relative tectonic quiescence (Berglund et al., 1986; Worsley, 2008; Smelror et al., 2009). This time of quiescence was later followed by several episodes of rifting from the late Middle Jurassic to Lower Cretaceous, resulting in the present day structural configuration of the Hammerfest Basin (Berglund et al., 1986; Gabrielsen et al., 1990). During this extensional event, a gentle high was formed in the western and central part of the basin, herein referred to as the Central High (Figure 3). This structure is believed to be the result of a flexural rollover, due to fault activity on the northern and southern boundaries of the Hammerfest Basin (Berglund et al., 1986; Sund et al., 1986; Gabrielsen et al., 1990; Faleide et al., 1993b; Larssen et al., 2002). Furthermore, the Palaeozoic Loppa High structure, proposed to

be a result of footwall uplift or lithospheric stretching and flexural isostasy, experienced renewed uplift in the Late Jurassic times as a consequence of this widespread rifting event (Wood et al., 1989; Smelror et al., 2009; Glørstad-Clark, 2010).

Other notable features in the Hammerfest Basin includes the structural high associated with the AFC (Figure 3), herein referred to as the AFC High, and the Goliat Anticline on the southwestern Hammerfest Basin margin (Figure 3). The AFC High has been interpreted as a result of a local compressional event during the Lower Cretaceous, either as a result of dextral strike-slip movement along the AFC (Berglund et al., 1986; Sund et al., 1986; Gabrielsen et al., 1990), or as an inversion structure formed due to differential uplift of the Loppa High (Indrevær et al., 2016). The Goliat High has also been proposed as a Cretaceous inversion structure, active during the early Barremian to Middle Albian (Indrevær et al., 2016; Mulrooney et al., 2017).

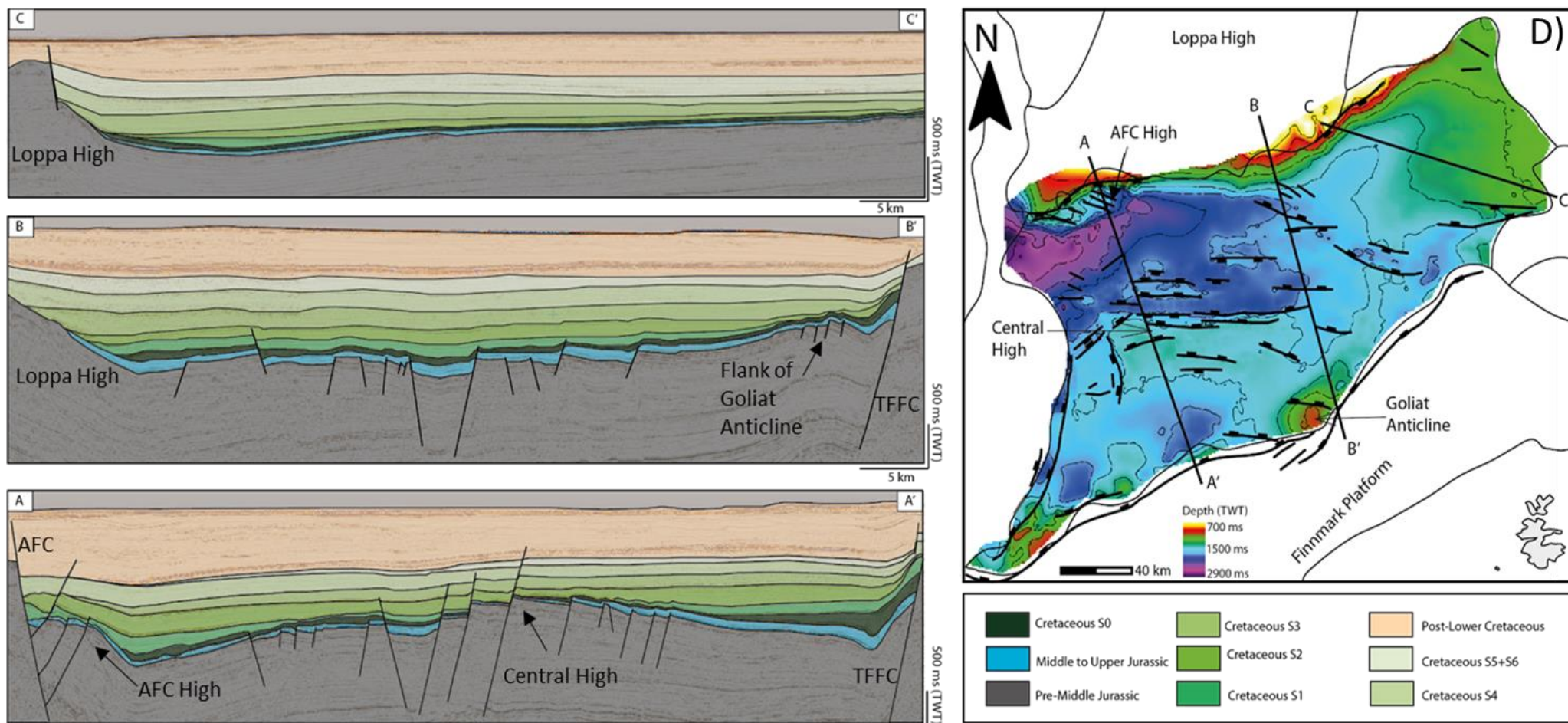


Figure 3: A) NNW-SSE regional line across the western part of the Hammerfest Basin illustrating the basin configuration and main structural elements. Note the thinning of the Middle to Upper Jurassic strata towards the Central High. B) NNW-SSE regional line across the central part of the Hammerfest Basin illustrating the general basin configuration and main structural elements. Note that the Loppa High is not faulted in this area. C) NW-SE regional line across the eastern part of the Hammerfest Basin illustrating the basin configuration and main structural elements. Note the decrease in fault activity from west to east. D) Time structural map of the Base Cretaceous unconformity, location of regional lines and the main structural elements of the Hammerfest Basin. Lower Cretaceous seismic sequences are defined according to Marín (2017).

## **2.2. Lithostratigraphy**

The Middle to Upper Jurassic successions of the southwestern Barents Sea comprises the Stø, Fuglen and Hekkingen formations (Dalland et al., 1988). The main focus of this study is the Fuglen and Hekkingen formations, making up the lower part of the Adventdalen Group (Figure 4). However, a short description of the Stø Formation is also included in this sub-chapter as the cored section of the transition from the Stø Formation to the Fuglen Formation will be covered later in Chapter 4. The Middle to Upper Jurassic interval is generally thickest towards the southwestern part of the Hammerfest Basin, and thins towards the Central High (Figure 3), indicating the active tectonics at the time of deposition. The Adventdalen group represents an approximately 400 meter thick interval in the southwestern part of the Hammerfest Basin, thinning to approximately 100 meter towards the basin axis (Dalland et al., 1988; Worsley, 2008). The Middle to Upper Jurassic succession of the southwestern Barents Sea is confined between two regional unconformities (Dalland et al., 1988; Nøttvedt et al., 1993; Mørk et al., 1999). The basal unconformity is herein referred to as the Upper Jurassic Unconformity (UJU) and defines the boundary between the Kapp Toscana Group and the Adventdalen Group (Figure 4). The upper contact separates the Middle and Upper Jurassic deposits from the overlying Lower Cretaceous sequences by the regional unconformity known as the Base Cretaceous Unconformity (BCU). This boundary was developed during the Valanginian times due to a major break in deposition (Mørk et al., 1999).

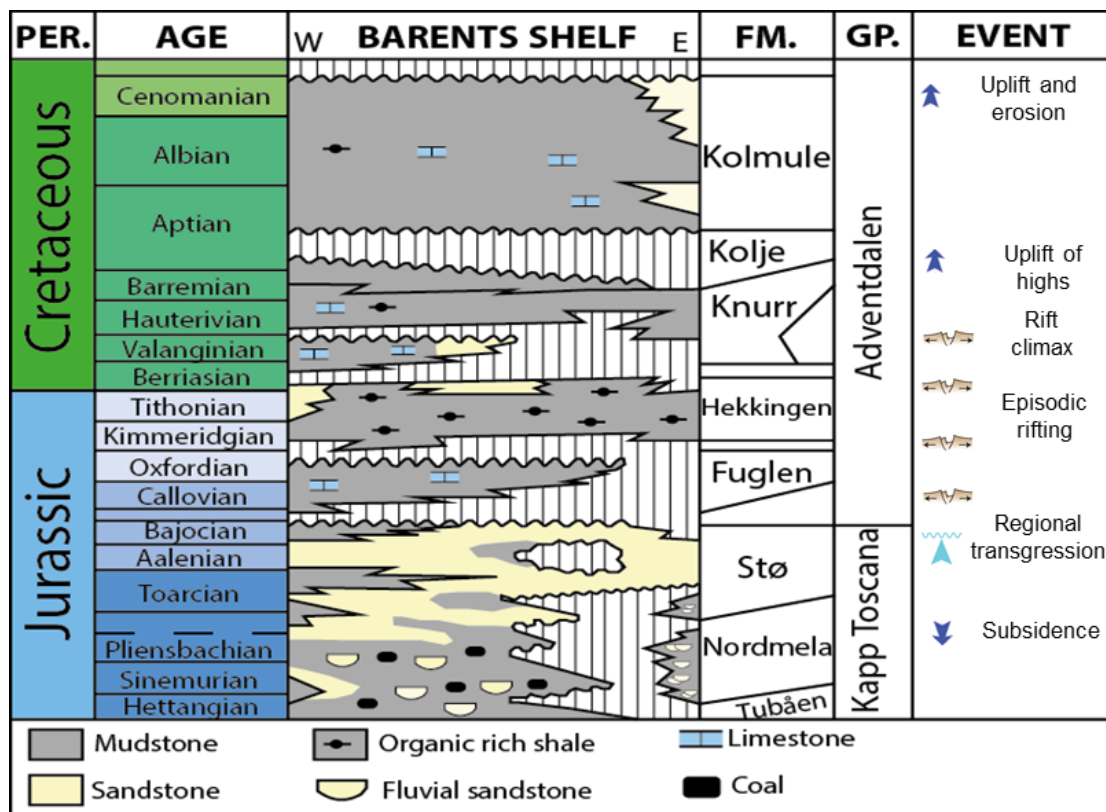


Figure 4: General Jurassic and Cretaceous lithostratigraphy of the southwestern Barents Sea. Modified from Nøttvedt et al. (1993). Geodynamic events from Worsley (2008) and Smelror et al. (2009).

### 2.2.1. Stø Formation:

The Stø Formation (Late Pliensbachian – Bajocian) makes up the upper part of the Kapp Toscana Group (Figure 4). The formation consists of moderately to well sorted, fine to medium grained and mineralogically mature sandstones (Figure 4), and makes up the most prolific reservoir on the Barents Sea shelf to date (Olaussen et al., 1984; Dalland et al., 1988; Stewart et al., 1991; Henriksen et al., 2011). Phosphatic lag conglomerates occur in some wells and are most common in the uppermost parts of the unit (Olaussen et al., 1984; Dalland et al., 1988; Worsley, 2008). The Stø Formation is proposed to have been deposited in a complex setting, with depositional environments ranging from

prograding coastal shallow marine, including shoreface and tidal deltas, to offshore depositional environment (Olaussen et al., 1984; Stewart et al., 1991; Smelror et al., 2009; Henriksen et al., 2011).

### **2.2.2. Fuglen Formation:**

The Fuglen Formation (Late Callovian - Middle Oxfordian) consist of highly fossiliferous and bioturbated dark brown shales of occasionally pyritic composition, with interbeds of white to brownish-grey limestones (Figure 4) (Dalland et al., 1988; Linjordet and Olsen, 1992; Mørk et al., 1999). The abundance of authigenic minerals suggests slow deposition rates in a low-energy environment (Dalland et al., 1988). The formation is proposed to have been deposited in an open marine shelf environment with oxic to dysoxic bottom waters, during a stage of active tectonism (Dalland et al., 1988; Bugge et al., 2002; Nøttvedt and Johannesen, 2008; Worsley, 2008).

### **2.2.3. Hekkingen Formation:**

The Hekkingen Formation (Late Oxfordian/Early Kimmeridgian - Ryazinian) consist of dark coloured shales and mudstones, with occasional interbeds of limestone, dolomite, siltstone and sandstone (Figure 4) (Dalland et al., 1988; Linjordet and Olsen, 1992; Mørk et al., 1999). The coarser clastic deposits have been observed along the Hammerfest Basin margins, along the AFC and TFFC, described as submarine fans of Oxfordian to Barremian age (Henriksen et al., 2011). The Hekkingen Formation is one of the richest source rocks in the Barents Sea region, with TOC values ranging from 1-20 (wt%) and kerogen type II/III, with variable input of terrestrial material (Berglund et al., 1986; Sund et al., 1986; Leith et al., 1993). The Hekkingen Formation is separated

from the overlying Lower Cretaceous sequences by the BCU, and the basal contact of the formation is locally unconformable and most prominent over structural highs (Dalland et al., 1988). The Hekkingen Formation is approximately age equivalent to the organic rich Draupne and Heather Formations of the North Sea and the Spekk Formation of the Norwegian Sea (Berglund et al., 1986; Dalland et al., 1988), and comprises the two members Alge and Krill.

The Alge Member (Late Oxfordian - Kimmeridgian) consist of thinly laminated black shales deposited in a restricted shelf environment, with high values of organic content (Dalland et al., 1988; Stewart et al., 1991; Mørk et al., 1999; Bugge et al., 2002). This member is represented by very high API values in the Gamma-Ray log (GR).

The Krill Member (Kimmeridgian - Tithonian) consists of brownish-grey to dark grey shales and mudstones with interbedded limestone, dolomite siltstone and sandstone (Dalland et al., 1988; Mørk et al., 1999; Henriksen et al., 2011). The unit was deposited during a period of maximum transgression, in an open to restricted shelf environment (Dalland et al., 1988; Smelror et al., 2009).



### 3. DATA AND METHODOLOGY

#### 3.1. Data

The dataset used in this study includes seven wells located in the Hammerfest Basin (Table 1; Figure 5), comprising 105 meters of core data from the Middle to Upper Jurassic interval, logged at the Norwegian Petroleum Directorates (NPD) main offices in Stavanger. 2D and 3D reflection seismic data, well log data and reports covering the Hammerfest Basin and bordering areas is provided by the Norwegian DISKOS database (Figure 5). Full suites of well logs were provided for all wells in the study area. The seismic data are of varying quality, with frequencies ranging between 10-50 Hz. Of the numerous wells drilled in the Hammerfest Basin penetrating the Middle to Upper Jurassic strata, more emphasis were given to wells with available core data and biostratigraphic data of recent age (Table 1; Table 2). Age data was sourced from biostratigraphic reports from the Petrobank database, and final well reports from the public database of the Norwegian Petroleum Directorate (Table 2)(NPD, 2018)

*Table 1: Wells with available core data from the Middle to Upper Jurassic interval in the Hammerfest Basin*

<b>Well</b>	<b>Formation</b>	<b>Core length (m)</b>	<b>Logged interval (m)</b>
7120/2-2	Hekkingen	10	2636 – 2646
7120/2-3 S	Fuglen and Hekkingen	24	2002 – 2025
7120/6-1	Fuglen	20	2370 – 2390
7120/12-1	Fuglen	7	1661 – 1668
7120/12-1	Hekkingen	6	1702 – 1708
7120/12-1	Hekkingen	7	2042 – 2049
7121/4-2	Fuglen	20	2462 – 2482
7122/7-2	Fuglen	3	1075 – 1078
7122/7-3	Fuglen	8	1082 – 1092
	<b>Total</b>	<b>105</b>	

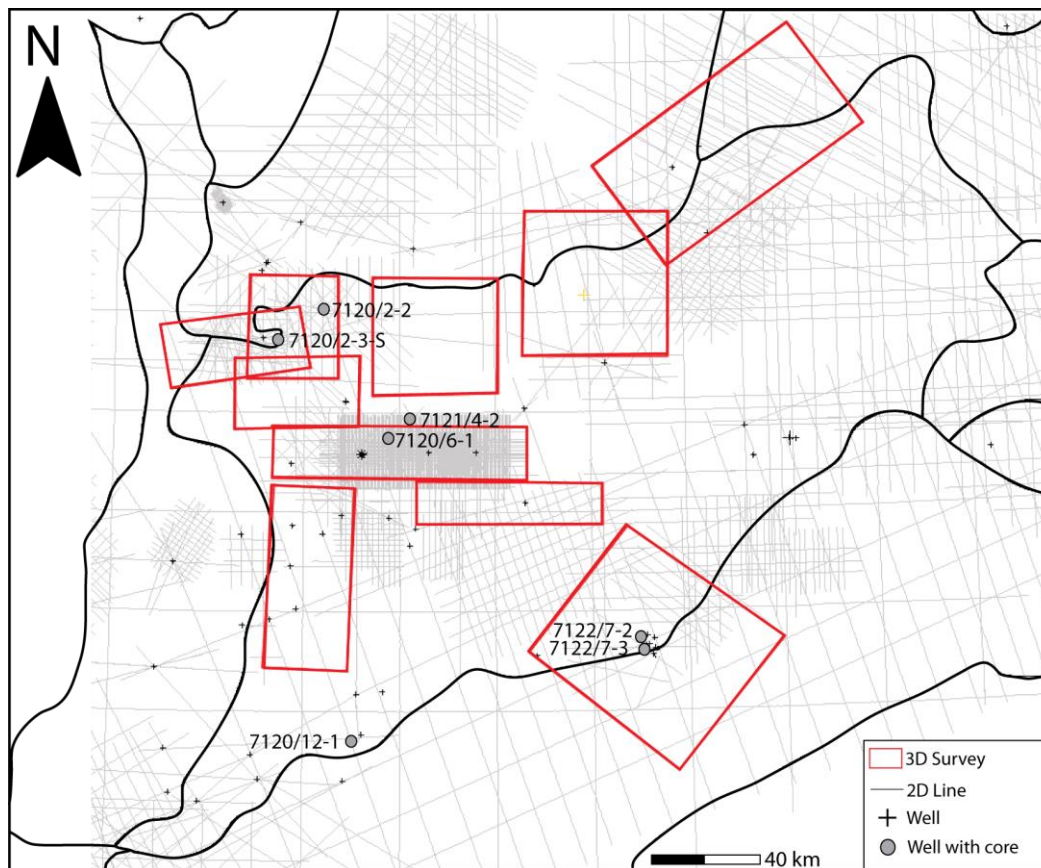


Figure 5: Overview of the seismic coverage, well distribution and location of wells with core sections from the Middle and Upper Jurassic interval in the study area.

Table 2: Key wells and available data used in this study for facies analysis and correlations.

Well	Core	Biostratigraphic report (Year prepared)	Final well report (NPD)
7119/12-1		X (1992)	X
7119/12-2			X
7120/1-2		X (1989)	X
7120/2-2	X		X
7120/2-3-S	X	X (2012)	
7120/5-1			X
7120/6-1	X		X
7120/6-3-S		X (2013)	
7120/9-1			X
7120/12-1	X		X
7121/4-2	X	X (1985)	X
7121/5-2			X
7121/7-2			X
7121/9-1		X (2012)	
7122/2-1			X
7122/4-1		X (1992)	X
7122/7-2	X		
7122/7-3	X		
7123/4-1-A		X (2009)	

## **3.2. Methodology**

### **3.2.1. CORE LOGS:**

The cores were measured at cm scale and lithological facies and depositional process for the sedimentary logs were defined based on grain size, texture, sediment composition, degree of bioturbation, body- and trace fossil distribution and sedimentary structures. The lithological facies were then grouped into facies associations based on the interpreted depositional setting and depositional process. Bioturbation index follows the notation by Taylor and Goldring (1993), where index 1-2 denotes minor bioturbation, index 3-4 denotes medium bioturbation, and index 5-6 indicates heavy bioturbation. Facies association 1 defined in wells 7122/7-2 and 7122/7-3 was based on the interpretation of facies association 8 from Mulrooney et al. (2018).

### **3.2.2. FRAMEWORK**

A chronostratigraphic framework consisting of five third order sequences (J1-J5) bound by flooding surfaces (FS1-FS4) (Galloway, 1989) is defined based on stacking patterns from GR-logs and ages from biostratigraphic reports and final well reports (Figure 6). Wells for correlation purposes are selected based on location and availability of biostratigraphic data. The entire Middle to Upper Jurassic succession is bound at the top and base between regional unconformities, the BCU and UJU. The sequence boundaries were selected due to their regional extent and good lateral continuity (Galloway, 1989). The sequences were then compared to the existing lithostratigraphic framework of the Hammerfest Basin, and the facies associations observed from the core data.

### **3.2.3. SEISMIC:**

The seismic interpretation and generation of synthetic seismograms were performed using the DecisionSpace software from Landmark Halliburton. Synthetic seismograms (Figure 7) were generated for the cored wells (Table 1; Table 2) using an extracted wavelet from the seismic data, in combination with the sonic and density logs. The seismic well tie shows a satisfactory tie between the synthetic and seismic traces (Figure 7). However, as evident from Figure 6 and 7, the Middle to Upper Jurassic is relatively thin, and represents a single seismic sequence (Figure 6 and Figure 7). Hence, only the top and base of the Middle to Upper Jurassic sequence could be confidently mapped throughout the study area. The top and base of the seismic sequence correlates with the BCU (top Hekkingen) and the UJU (top Kapp Toscana Group), respectively (Figure 4). The tied well tops were defined based on the official well tops from the NPD database (NPD, 2018). Time structural maps were generated for the BCU and UJU, to gain an understanding of the structural configuration of the study area. A time thickness map of the studied time interval was constructed to better understand the basin fill and accommodation creation through time.

#### **3.2.4. LIMITATIONS:**

The core data from the studied time interval in the southwestern Barents Sea is limited and the few core samples available are not continuous, which leads to some degree of uncertainty regarding the lateral and vertical distribution of facies. Furthermore, all the examined wells are drilled on structural highs, and the lithological facies observed in these core sections might not be representative for the studied time interval across the entire basin. Moreover, age control is scarce, and is often noted as uncertain in the biostratigraphic reports. Seismic interpretation is also limited for this time interval in the area, and only one seismic sequence could be differentiated. Hence, no internal seismic characteristics, nor the full lateral and vertical extent of sequences J1-J5 are described from seismic. Moreover, this study includes data from different scales, ranging from mm scale in the core data, to several km on the full basin scale (Figure 6). Integration of data of various scales with lateral and vertical limitations leads to a high degree of uncertainty regarding the interpreted depositional settings for the defined sequences, and their lateral and vertical distributions.

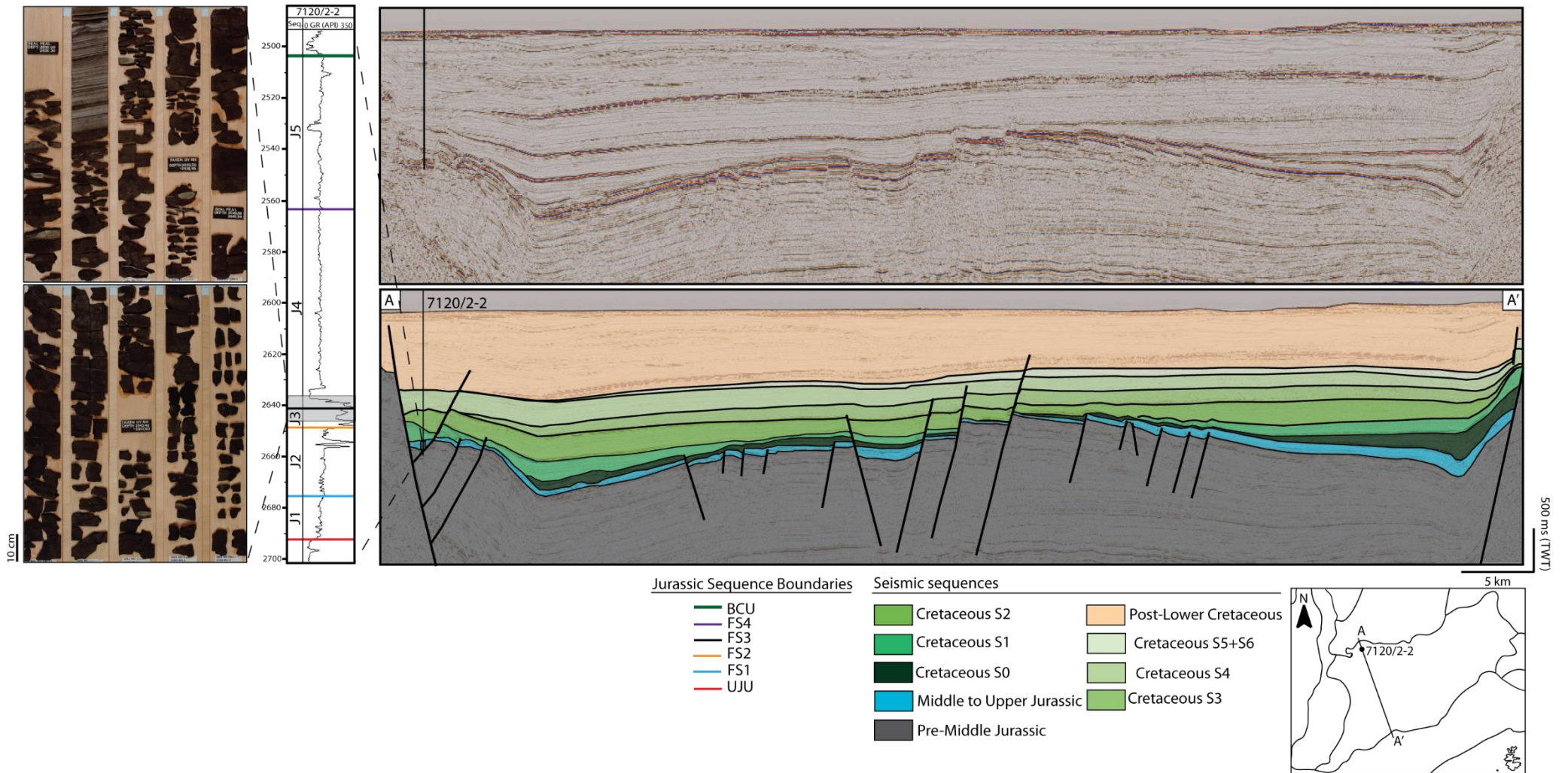


Figure 6: NW-SE regional seismic line illustrating Middle to Upper Jurassic seismic sequence with well 7120/2-2 drilled on the northern basin margin. The GR-log illustrates the five Middle to Upper Jurassic genetic sequences. The figure also illustrates the scale differences of the data utilized in this study, ranging from several kilometers basin wide, to mm scale within the cored intervals. Note the thickness of the cored section of well 7120/2-2 compared to the overall thickness of the Middle to Upper Jurassic sequences, and the limited coverage of the overall study area the core data provides.

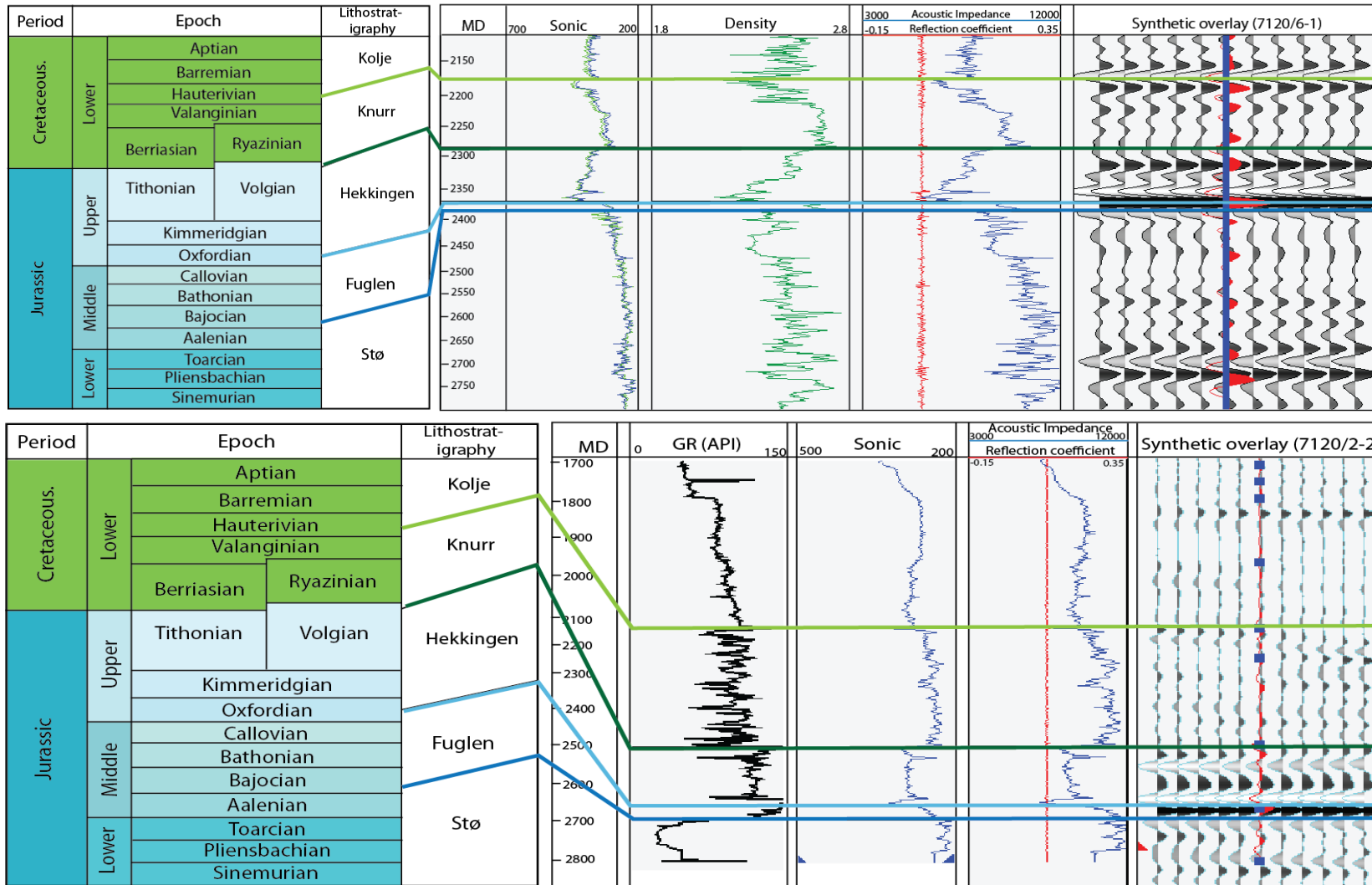


Figure 7: Synthetic seismograms for wells 7120/6-1 and 7120/2-2. Note the thickness and low seismic resolution of the Middle to Upper Jurassic seismic sequence.

## **4. OBSERVATIONS AND INTERPRETATION**

### **4.1. Core and GR analysis – Facies and depositional processes**

The Middle to Upper Jurassic Fuglen and Hekkingen formations were the main focus of the core interpretation. Where available, the transition from the underlying Kapp Toscana Group was also included in order to gain a better understanding of the evolution of the depositional setting. Eleven lithofacies (Table 3) are identified and grouped together as five different facies associations (Table 4; Figure 8), reflecting distinct depositional elements or depositional environments. The interpreted facies associations includes shallow marine, restricted anoxic and mass flow groups (Table 4). Facies association 5 was divided into two different sub-associations (Table 4; FA5a and FA5b) based on the inferred dominant depositional process and location within the depositional system. The distribution of facies associations from the cored wells is indicated in Table 4 and Figure 8, and a detailed summary and description is given in the following sub-chapters. The defined facies associations are also correlated to the GR-logs and mapped in several wells across the basin to get an overview of the lateral distribution of facies (Table 5). Maps are constructed to better understand the relative distribution of the different facies associations.



Table 3: Facies description and process interpretation for the lithofacies observed in the Middle to Upper Jurassic core sections in the Hammerfest Basin.

Facies	Grain size	Description	Interpretation
<b>F1: Bioturbated mudstone</b>	Clay to silt	Light brown to black. Subfissile to blocky. Often appear homogeneous and structureless. Often very micaceous. Occasionally calcareous. Pyrite nodules and pyritized burrows are common. Siderite cement and carbonate filled fractures occur. Shells and shell fragments appear sporadically. Coalified wood occur but is rare.	Deposition from suspension fallout of pelagic and hemipelagic sediments in a low energy, oxic to dysoxic environment.
<b>F2: Parallel laminated mudstone</b>	Clay to silt	Dark brown to black. Fissile to blocky. Often very micaceous. Laminae commonly silty and lined with pyrite. Pyrite crystals and nodules common. Siderite cement and carbonate filled fractures occur.	Deposition from suspension fallout of pelagic and hemipelagic sediments in a low energy, dysoxic to anoxic environment
<b>F3: Black shales</b>	Clay	Black. Fissile. Mainly homogeneous and structureless. Parallel lamination occurs, and laminae often show greenish tint. Pyrite crystals and carbonate-filled fractures are common.	Deposition from suspension fallout of pelagic and hemipelagic sediments in a low energy, anoxic environment
<b>F4: Bioturbated calcareous sandstone</b>	Fine to medium sand	Light grey to brown, occasionally red stained. Often silty. Very micaceous. Coal clasts and coal fragments common. Occasional carbonate filled fractures. Fossils abundant. Large trace fossil diversity, primary structures disrupted by intense bioturbation.	Slow deposition in well-oxygenated, low-energy environment. Possibly in proximity to a terrestrial source.
<b>F5: Bioturbated silty sandstone</b>	Very fine sand	Light grey to light brown. Non-calcareous. Very micaceous. Primary structures completely obliterated. Intensely bioturbated and high trace fossil diversity. Lower boundary often erosive.	Slow deposition in well-oxygenated, low-energy environment.
<b>F6: Normally graded conglomerate</b>	Granules	Grey to dark grey. Clast supported and matrix supported. Grains angular to rounded. Lower boundary erosive. Contains phosphatic nodules and pebble sized, well-rounded quartz grains.	Transgressive lag deposits. Progressive reworking and removal of fine-grained matrix caused by wave action and wave induced currents.
<b>F7: Siltstone</b>	Silt	Grey to brown. Often bioturbated and fossiliferous. Occasionally parallel laminated.	Fallout from suspension in low-energy, well-oxidized environment.
<b>F8: Soft sediment deformed sandstone</b>	Very fine to medium sand	Light brown to light grey. Coal clasts and glauconite clasts common. Water escape structures are present. Includes slump folds, sand injectites, convoluted beds, rip up clasts and micro normal faults.	Rapid deposition of reworked material. Deformation due to fluid migration and shearing from currents.
<b>F9: Ripple laminated sandstone</b>	Very fine to fine sand	Light brown to light grey. Both symmetrical and asymmetrical ripples occur. Ripples are often draped by mudstone, displaying lenticular bedding.	Deposition in the lower flow regime by both unidirectional and oscillatory flows.
<b>F10: Parallel laminated sandstone</b>	Very fine to fine sand	White to light grey. Laminae ranges from 1 mm to 1 cm thick, with interbedded dark mudstone and siltstone. The base of the sandstones is weakly erosive and shows a faint fining upwards trend.	Fallout from suspension from low density turbidity current or turbulent flow (Td; Bouma, 1962)
<b>F11: Massive sandstone</b>	Very fine to medium sand	White to light grey. Mainly structureless and homogeneous. Upper boundary often erosive.	Reworking of previously deposited sediments by wave and current action in a transgressive shelfal setting.

Table 4: Facies associations.

Facies Association	Facies	Group	Wells
<b>FA1. Transgressive shelf</b>	F2, F6, F12	Shallow marine	7120/6-1, 7121/4-2, 7122/7-3, 7122/7-2
<b>FA2. Lower shoreface to offshore transition zone</b>	F4, F5, F7	Shallow marine	7120/12-1, 7122/7-2, 7122/7-3
<b>FA3. Offshore</b>	F1-F3, F5, F7	Shallow marine	7120/2-2, 7120/6-1, 7120/12-1, 7121/4-2.
<b>FA4. Restricted anoxic</b>	F1-F3, F5, F7, F8	Undifferentiated	7120/2-2, 7120/2-3-S
<b>FA5. Basin floor fan</b>		Mass flow	
FA5a. Distal basin floor fan	F1-F3, F7-F9, F11		7120/2-2
FA5b. Proximal basin floor fan			7120/12-1

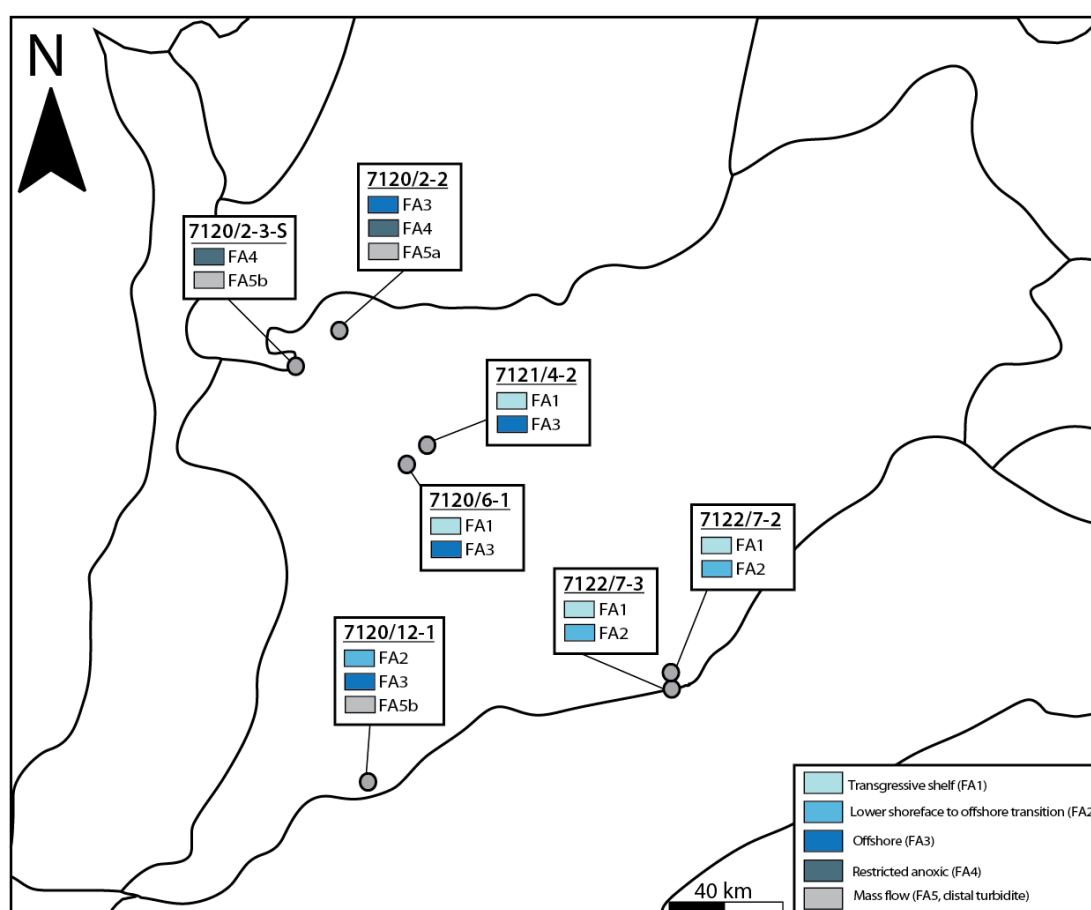




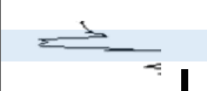



Figure 8: Location of the logged wells and the distribution of facies associations observed in cores.

Table 5: Correlation of facies associations observed in core sections with GR signature. Scale bars represents 10 m.

Facies Association	Well-log signature	Description	Example
FA1 – Transgressive shelf	Blocky	Overall low GR values and a coarsening upwards trend, followed by a rapid increase in GR.	
FA2 – Lower shoreface to offshore transition zone	Spiky to erratic	Highly serrated GR pattern with an overall coarsening upwards trend. Occasionally displays fining upwards trend. Lower contact transitional, upper contact marked by rapid increase in GR.	
FA3 – Offshore	Erratic	High GR values with a weakly serrated log motif. Overall aggradational pattern, occasionally with a coarsening upwards trend.	
FA4 – Restricted anoxic	N/A	High to extremely high GR values (>250 API). Lower contact marked by rapid increase in GR, upper contact marked by rapid decrease in GR.	
FA5a – Distal basin floor fan	Blocky	Lower contact marked by rapid decrease in GR, upper contact marked by rapid increase in GR. Aggradational to slightly fining upwards.	
FA5b – Proximal fan	Bell shaped to slightly spiky	Coarsening upwards, followed by fining upwards trend. Upper and lower contact marked by high GR values.	

#### **4.1.1. FACIES ASSOCIATION 1 (FA1) – TRANSGRESSIVE SHELF**

##### **Observations from cores:**

Facies association 1 consists of a 10 cm to 2.5 m thick interval observed at the boundary between the Fuglen Formation and the underlying Kapp Toscana Group (Stø or Tubåen formations; Figure 4). This unit is observed close to the Central High in wells 7120/6-1 and 7121/4-2, and on the Goliat Anticline on the southwestern basin margin (Figure 3 Figure 8).

In well 7121/4-2, the interval consists of poorly sorted, grey-coloured, angular to sub-angular, clast-supported erosive conglomerates (F6; Table 3; Figure 9), overlain by a 10 cm thick, dark brown, fissile mudstone layer (Figure 10). The mudstone layer is followed by a 2.5 m thick sandstone interval, with interbedded silt, mud rip-up clasts, and intense bioturbation at the base, grading into a massive, homogeneous sandstone towards the top (F12; Table 3; Figure 10). The upper contact of the sandstone is sharp and erosive, and contains large pyrite nodules and authigenic glauconite (Figure 10). In the nearby 7120/6-1 well (Figure 8), FA1 is represented by a 10 cm thick interval of very fine grained sandstone containing abundant mud rip-up clasts (Figure 9; Figure 10). The lower contact of FA1 is erosive, and the upper contact contains macro-sized (2-5 cm), rounded, and elongated pyrite nodules (Figure 9; Figure 10).

On the southwestern margin, in wells 7122/7-2 and 7122/7-3 (Figure 8), FA1 makes up a 15-20 cm thick interval, with different lithological facies compared to the Central High area. In well 7122/7-2 the lower boundary of FA1 is sharp and contains a thin (2-5 cm) conglomeratic interval, overlain by thinly laminated (1 mm – 1 cm) alternating red and grey coloured mudstones (Table 3; Figure 9 and Figure 11). The laminae are sub-horizontal and slightly undulating (Figure 9). The conglomeratic interval is matrix supported and contains pebble sized, well rounded phosphatic and quartzitic grains

(Figure 9). The upper boundary is erosive and contains vertical to sub-vertical burrows. The burrows appear to be passively filled, and there is little to no deformation of the primary sedimentary structures in the vicinity of the burrows (Figure 9). In well 7122/7-3, conglomeratic facies are absent, and the lower contact is marked by a brecciated light-coloured mudstone interval (Figure 9 and Figure 11).



*Figure 9: Facies observed in FA1. A) Red coloured mudstones with brecciated contact and possible root traces, grading into a silty fine grained sandstone towards the top. From well 7122/7-3, depth 1088.5. B and C) Well rounded, pebble sized grains, in a medium-grained sandstone matrix (F6). The upper interval consists of alternating layers of light and dark brown mudstones (F1) with possible glossifungites trace fossils just below the upper contact. From well 7122/7-2, depth 1077.5 D) Grey to dark grey clast supported conglomerate (F6) overlying a massive sandstone (F12), with an erosive contact. From well 7121/4-2, depth 2481 m. E) Very fine grained, erosive-based sandstone with mud rip-up clasts and large pyrite nodules. From well 7120/6-1, depth 2388.5 m. Scale bars are 1 cm.*

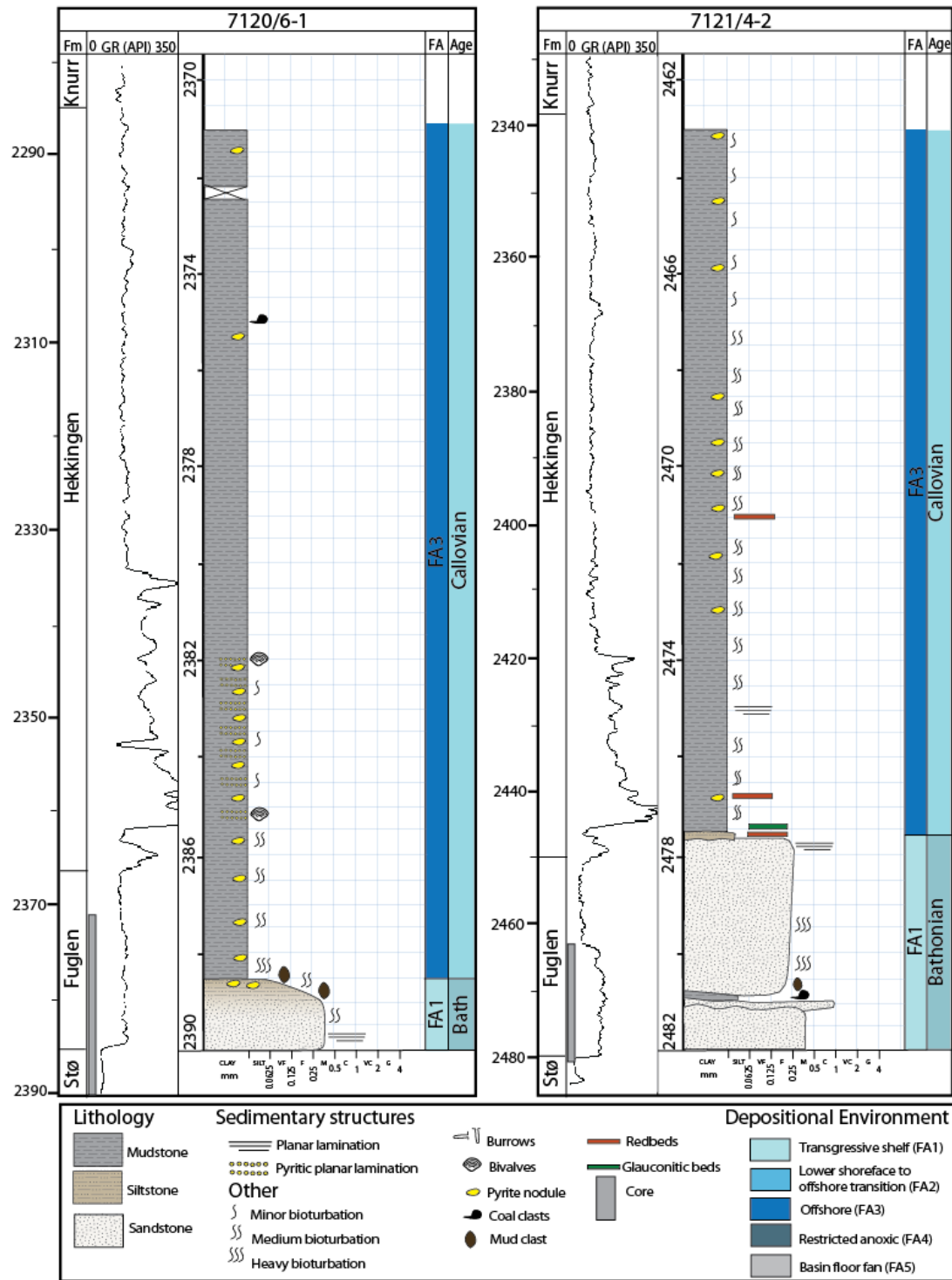


Figure 10: Core logs and associated GR logs for wells 7120/6-1 and 7121/4-2 located in the central part of the Hammerfest Basin. Ages for well 7121/4-2 is from the biostratigraphic report from the Petrobank database, conducted by Gearhart Geo Consultants LTD for Statoil (1985). Ages for 7120/6-1 is from the final well report (NPD, 2018).

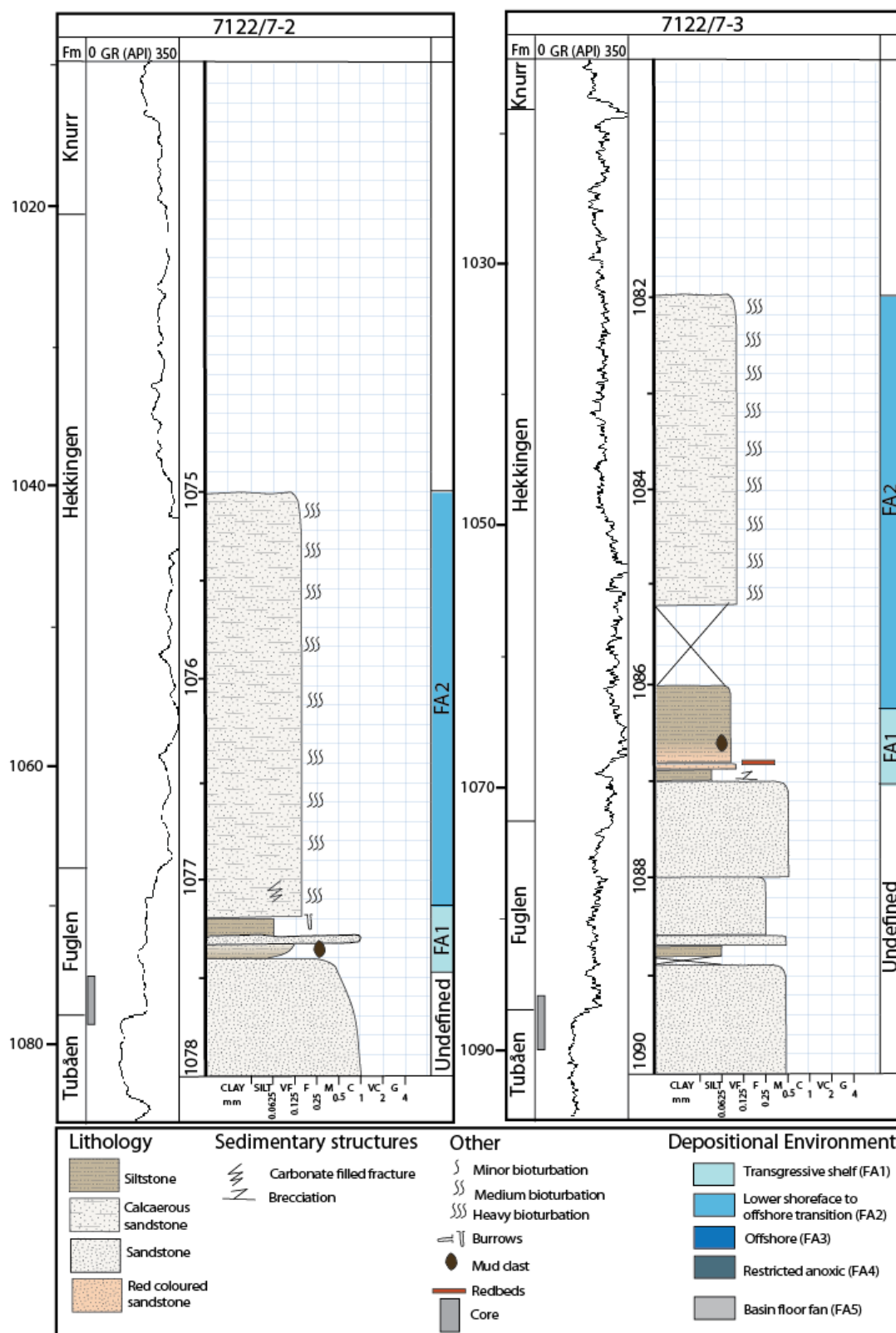


Figure 11: Core logs and associated GR log for wells 7122/7-3 and 7122/7-2 located on the Goliat Anticline. No age control was available for these wells.

### Correlation with GR:

In wells 7120/6-1, 7122/7-2 and 7122/7-3 this association comprises a 15-20 cm thick interval, and is therefore below resolution of the GR log. In well 7120/4-2 FA1 is represented by a blocky GR signature, medium to low GR values (0-50 API) and an overall coarsening upwards trend (Table 5; Figure 10). Both the lower and upper contacts are marked by a rapid increase in GR. Due to the low resolution of this association, and thus, the high uncertainty regarding the well-log response, the distribution of FA1 in Figure 13 is solely based on observations from cores.

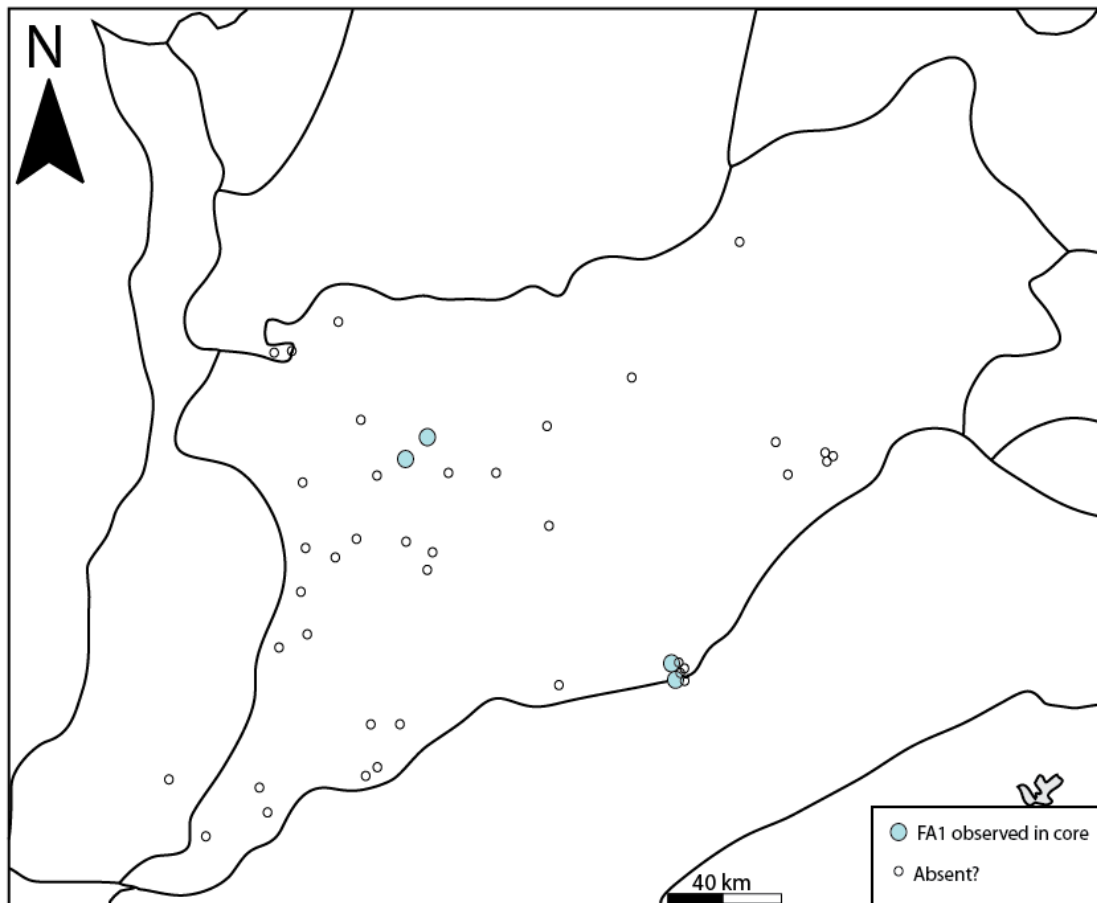


Figure 12: Distribution of FA1 observed from core data.



**Interpretation:**

In the Central High area, FA1 shows evidence of overall decreasing depositional energy and a deepening upwards trend based on the transition from the well-sorted, medium-grained sandstones to the overlying dark mudstones (Figure 10). The overall fining upwards trend in the GR logs (Table 5; Figure 10; Figure 11), and its stratigraphic position at the boundary between the continental to shallow marine Kapp Toscana Group and the marine Adventdalen Group (Figure 4) further support the interpreted transgressive nature of the unit. The sharp based and occasionally erosional contacts (Figure 9) indicates multiple events of erosion or depositional hiatus. The conglomeratic intervals are interpreted as transgressive lag deposits, commonly developed in coastal, foreshore, inner shelf zones or isolated subaqueous highs (Einsele, 2000b). They can be formed by wave action and wave induced currents that erode and rework the existing sediments, where the repeated reworking allows for the finer sediments to be transported away, leaving behind the coarser and more resistant sediments (Einsele, 2000b; Cattaneo and Steel, 2003). The presence of glauconite indicates slightly reducing conditions either in the water column or sediment water interface, which is further supported by the presence of pyrite, commonly formed under dysoxic to anoxic conditions (Potter et al., 2005a; Potter et al., 2005d). Moreover, glauconite is formed when sedimentation rates are low, and tend to be typical of continental shelf to shallow marine environments (Cloud, 1955; Blatt et al., 1972a; Einsele, 2000c; Potter et al., 2005a; Nichols, 2009c; Bonewitz, 2012).

The brecciated interval in well 7122/7-3 is interpreted as desiccation cracks, formed as a result of fluid loss within clay rich sediment, and are good indicators of subaerial exposure (Nichols, 2009b). Furthermore, the presence of root traces below the brecciated unit, in combination with the light reddish colour of the mudstone, suggests an overall oxidising environment (Potter et al., 2005d). The burrowed mudstone

observed towards the top of FA1 in well 7122/7-2 (Figure 9) was most likely cemented prior to burrowing activity, suggested by the passive infilling of the burrows and the absence of deformation of the primary lamination. The burrows are interpreted as part of the *glossifungites/trypanites* ichnofacies and represents hardground or firmground formation during non-deposition in a marginal marine to marine setting (MacEachern et al., 1992; Reading and Collinson, 1996; Einsele, 2000b; Cattaneo and Steel, 2003; Catuneau, 2006; Nichols, 2009a).

In summary, the lithological characteristics of FA1 from the Goliat Anticline suggest deposition during an overall transgressional setting in the marine environment, where reworking processes and low sedimentation rates were dominant controls. Moreover, as this area shows evidence of multiple episodes of erosion or non-deposition, it was most likely subaerially exposed for a significant amount of time, or acted as an area of bypass. FA1 close to the Central High was most likely more distal compared to the Goliat Anticline, where reworking processes dominated in a shallow marine, transgressional setting, and possibly a paralic setting on the Goliat Anticline. FA1 also shows evidence of low-sedimentation rates and possibly times of non-deposition.

#### **4.1.2. FACIES ASSOCIATION 2 – LOWER SHOREFACE TO OFFSHORE TRANSITION**

##### **Observations from core:**

Facies association 2 is observed at the southern margin of the Hammerfest Basin (Figure 8), and consists of very fine to fine grained, slightly silty, occasionally calcareous, and intensely bioturbated sandstone (F4 and F5; Table 3) (Figure 13). The sandstones are light grey to light brown in colour and very micaceous (F3 and F4; Table 3). Primary sedimentary structures are rarely preserved; however, faint low angle cross-stratification and faint ripple lamination is observed in a few intervals (Figure 13; Figure 14). Trace fossil diversity is high, with vertical to sub-vertical burrows being most abundant, and some sub-horizontal burrows present (Figure 13). Some body fossils are recognized, including belemnites and bivalves. Coal clasts, well preserved coal fragments and coalified wood occurs frequently (Figure 13). Carbonate filled fractures occur sporadically and are most often observed towards the boundary with FA1. In wells 7122/7-2 and 7122/7-3, located on the Goliat Anticline, the lower boundary of FA2 is erosively overlying FA1 (Figure 9). In well 7120/12-1, the lower boundary is represented by a more gradual change from medium grained sandstones to very fine-grained, silty sandstones (Figure 14). Siderite cement is observed towards the base of FA2 in well 7120/12-1.

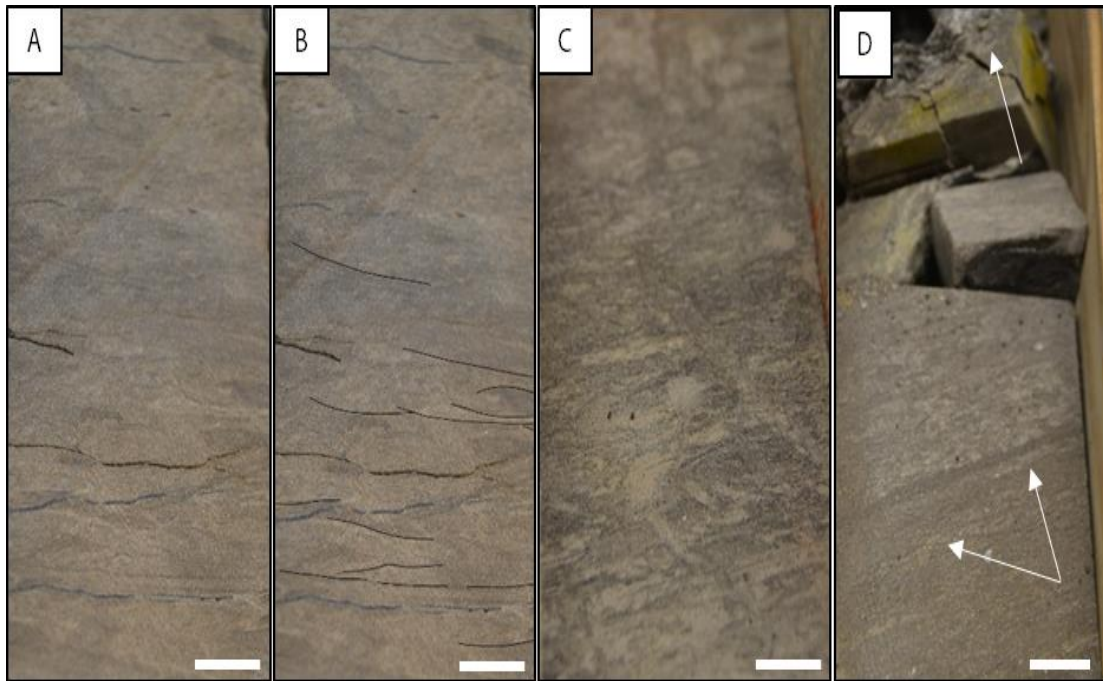


*Figure 13: Facies observed in FA2. A and B) Very fine grained, highly bioturbated silty sandstones (F5) displaying faint, low angle cross-stratification. From well 7122/7-3, depth 1084.6 m. C) Very fine grained, micaceous, highly bioturbated silty sandstone with high trace fossil diversity. From well 7120/12-1, depth 2047 m. D) Very fine grained to silty sandstone with faint ripple lamination (lower arrows) and large coal fragment (upper arrow). From well 7120/12-1, depth 2046 m. Scale bars are 1 cm.*

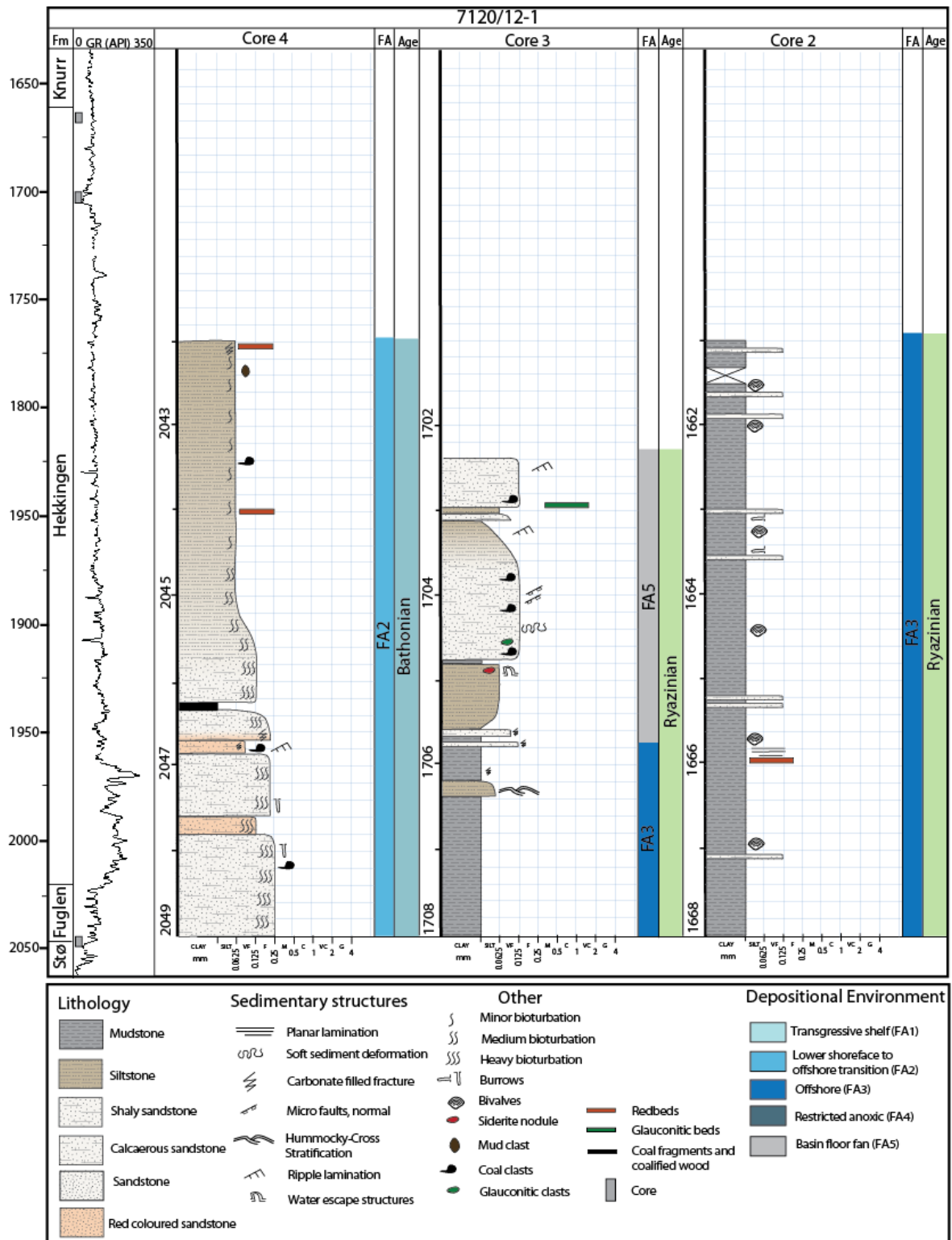


Figure 14: Core logs and the associated GR-log from well 7120/12-1 located on the southwestern basin margin. Ages are sourced from the final well report (NPD, 2018).

**Correlation with GR:**

FA2 displays a spiky to erratic well-log signature, with low to medium GR values (0-50 API) (Table 5; Figure 14). On the southwestern basin margin, FA2 shows an overall coarsening upwards trend, and the upper boundary is marked by a rapid increase in GR (Table 5; Figure 14). The basal contact represents a gradual change from clean sandstones to more silty, fine grained sandstones, and is represented as a minor fining upwards unit in the GR-log (Table 5; Figure 14 ). On the southern central basin margin, the basal contact of FA2 with FA1, is marked by an unconformity observed in cores (Figure 9). This unconformity is displayed as a rapid increase in GR-values from the well logs (Table 5; Figure 11). In this area, FA2 has a slightly higher silt to sand ratio, represented by higher GR-values for this association on the southern central margin. The well-log signature appears less serrated compared to the signature observed on the southwestern basin margin (Figure 11; Figure 14). Stacking patterns appear similar in the two locations, with an overall coarsening upwards trend, slightly aggradational and the upper contact marked at the start of a fining upwards unit (Table 5; Figure 11; Figure 14 ). FA2 is confidently defined from GR-logs on the southern basin margin (Figure 15), and tentatively interpreted on the northern basin margin based on similarities in well-log signatures, however, no core data was available for this association in the area for more accurate correlation.

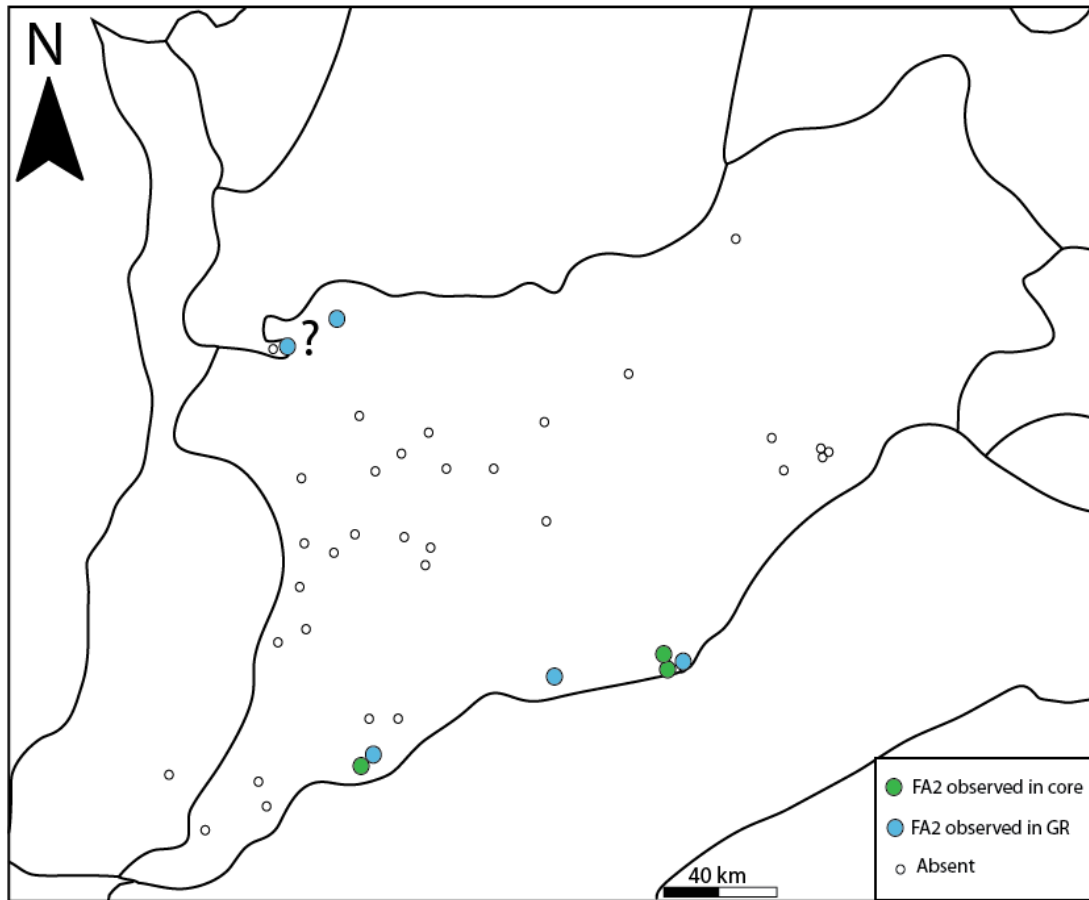


Figure 15: Distribution of FA2 observed from core data and well-logs.

### Interpretation

Based on the overall low grain sizes, fossil content, abundance of fossils and high degree of bioturbation, this association is interpreted as a well-oxygenated, medium to low energy marine environment. A shallow marine environment is inferred due to the intensity of bioturbation, as this is usually more abundant in sandy sediments in shallow waters, where the currents transporting sand also carry nutrients for benthic organisms (MacEachern and Bann, 2008; Nichols, 2009c). Rate of sediment supply is believed to be low, as low rates provide sufficient time for burrowing organisms to thoroughly rework the sediment (Wetzel, 1984; MacEachern and Bann, 2008; Morad et al., 2010). The presence of sub-vertical burrows witnesses to some degree of current influence, as

vertical escape traces occur more frequently under increasing energy levels (Nichols, 2009a). This is also supported by the low angle lamination and faint ripple lamination observed, indicating some influence of current activity. Siderite cemented intervals might indicate minor dysoxic episodes, caused by episodic restriction of the water circulation. FA2 is therefore inferred to have been deposited in a shelfal environment, below fair-weather wave base, and above storm wave base, possibly in the offshore transition zone, or a restricted lower shoreface environment. Furthermore, the abundance of coal clasts and well-preserved coal fragments within this low-energy unit could indicate that FA2 was deposited in close proximity to the paleo-shoreline.



### **4.1.3. FACIES ASSOCIATION 3 – OFFSHORE**

#### **Observations from core:**

FA3 is dominated by brown to dark black, micaceous, subfissile to blocky, highly bioturbated mudstones (F1; Table 3). Pyrite nodules, euhedral pyrite crystals and pyritized burrows are common (Figure 16). Carbonate filled fractures occur sporadically, but are generally not common. Siderite and glauconite is observed at the basal contact between FA2 or FA1 (Figure 9; Figure 10). Thin (1-5 cm) silty and sandy intervals occur sporadically and are generally more common towards the top of the Middle and Upper Jurassic successions (Figure 10; Figure 16). The coarser grained intervals are often parallel laminated and glauconitic or pyritic. Trace fossil diversity appears to be low, but is often quite difficult to observe within the clay dominated intervals due to little variation in grain size and composition. Trace fossils related to both the coarse and finer grained intervals are mainly horizontal to sub-horizontal (Figure 16). Burrows observed in the mudstones are often pyritized (Figure 16). Well-preserved bivalves are observed frequently, and are in some intervals very abundant (Figure 14; Figure 16; Figure 17).

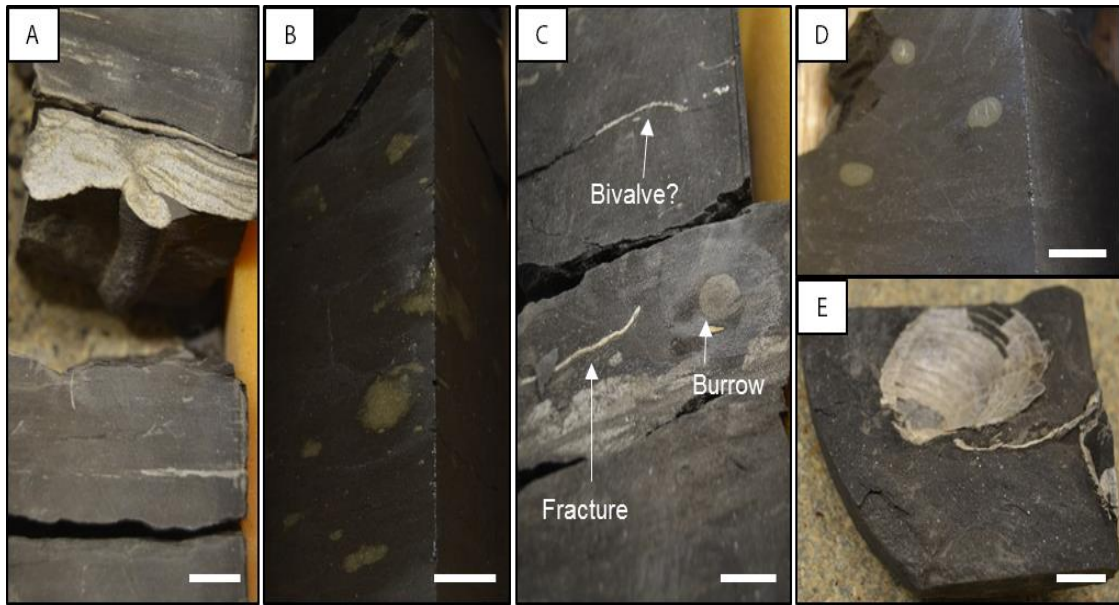


Figure 16: Facies observed in FA3. A) Horizontal burrow in a thin, very fine-grained light coloured sandstone. The sandstone is encased in a dark grey, micaceous and structureless mudstone. From well 7120/12-1, depth 1665.65 m. B and D) Dark grey to black, structureless mudstone with pyritized burrows. From well 7121/4-2 and 7120/6-1, depths 2473.7 m, and 2387.9 m., respectively. C) Dark grey micaceous mudstone with interbedded, very fine grained sandstone, sand-filled burrow, possible bivalve fossil and carbonate filled fractures. From well 7120/12-1, depth 1663.5 m. E) Very well preserved bivalve fossils in dark grey, micaceous mudstone. From well 7120/12-1, depth 1662 m. Scale bars are 1 cm.

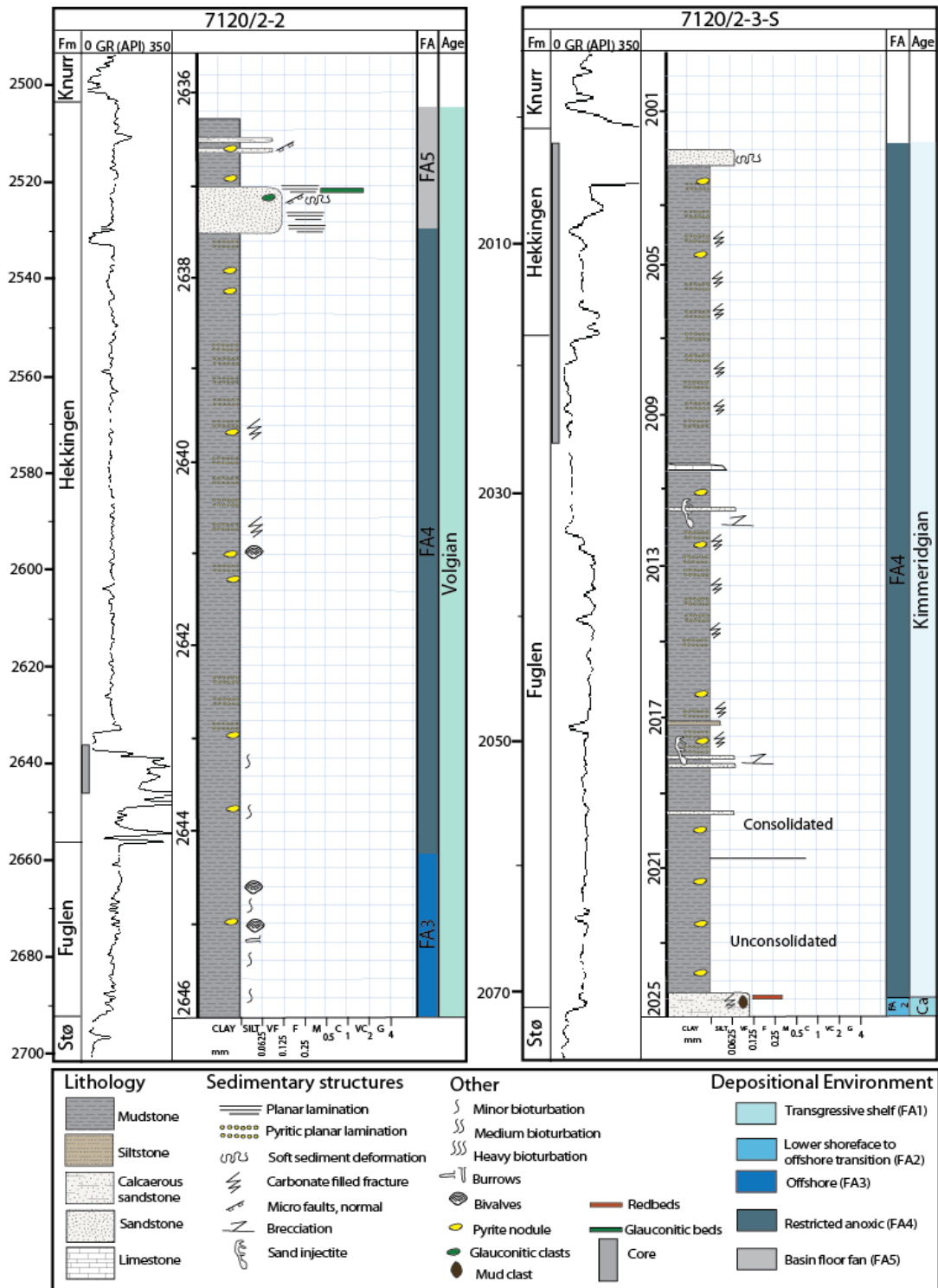


Figure 17: Core logs and gamma ray logs from wells 7120/2-2 and 7120/2-3-S located on the northern Hammerfest Basin margin. Ages for well 7120/2-2 is from the final well report (NPD). Ages for well 7120/2-3-S is from the biostratigraphic report available from the Petrobank database, conducted by Fugro Robertson Ltd. (2012). Ages for well 7120/2-2 is from the final well report (NPD, 2018).

### Correlation with GR:

FA3 displays an overall erratic well log signature, with high GR values. Stacking patterns are mainly aggradational, but show a coarsening upwards trend towards the top of the Middle and Upper Jurassic successions (Table 5; Figure 10; Figure 14; Figure 17). Both the upper and lower contacts are marked by a rapid increase in GR, going from clean sands to claystone, or a rapid decrease in GR, going from organic rich shales to mudstone (Table 5; Figure 10; Figure 14; Figure 17). FA3 has been observed in all the studied wells in the Hammerfest Basin (Figure 18), and it makes up the majority of the Middle to Upper Jurassic successions.

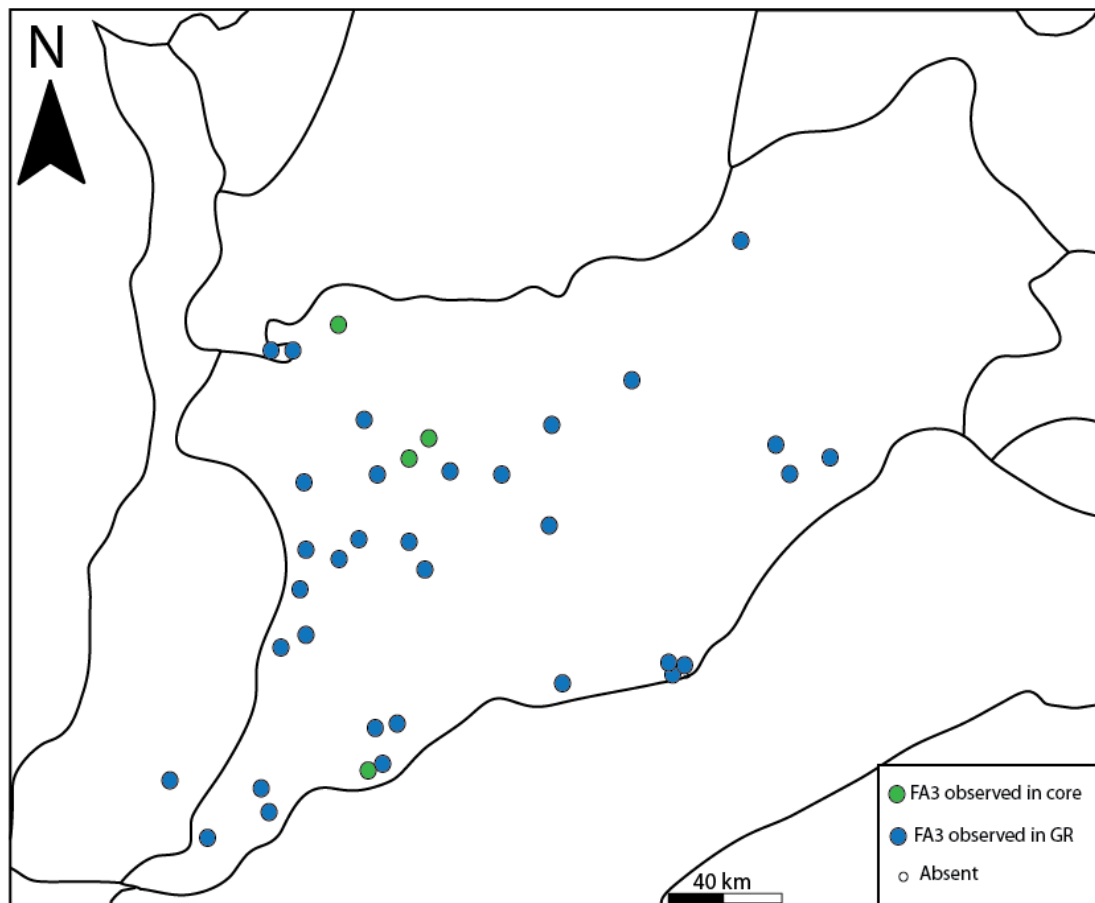


Figure 18: Distribution of FA3 observed in cores and well-logs.

## **Interpretation**

Based on the dominance of clay-sized sediments, types of fossils, intensity of bioturbation and the dominance of horizontal burrows within the trace fossil assemblage, FA3 is proposed to represent a more distal low-energy, marine environment compared to FA2. Pelagic and hemipelagic sedimentation was dominant, and the dark colour of the mudstones suggest good organic productivity. The intensity of bioturbation, abundance of fossils and absence of primary sedimentary structures suggests a well-oxidized setting. An offshore setting is further supported by the style of bioturbation, as in offshore areas, fluctuations of temperature and salinity and energy are low, and burrows are commonly horizontal and shallow (Blatt et al., 1972b). Moreover, the intensity of bioturbation and presence of authigenic minerals also suggest low rates of sediment supply (MacEachern and Bann, 2008; Morad et al., 2010). However, presence of pyrite and minor intervals of well-defined parallel laminated suggests sporadic episodes of anoxia or dysoxia. Lamination in mudstones is only preserved where the sea-bed is anoxic and hence, benthic organisms scarce, or where the sedimentation rates are particularly high (Johnson and Baldwin, 1996; Stow et al., 1996). The thin, sandy to silty intervals most likely reflect deposition from distal storm-generated flows or distal turbidity currents (Johnson and Baldwin, 1996).

#### **4.1.4. FACIES ASSOCIATION 4 – RESTRICTED ANOXIC**

##### **Observations from core:**

Facies association 4 is present in cores from the northern Hammerfest Basin margin in wells 7120/2-3-S and 7120/2-2 (Figure 8), and consists of dark brown to black, fissile to blocky, organic-rich mudstones (F2 and F3; Table 3). Towards the base of the core in well 7120/2-3-S, the mudstones are poorly consolidated, and no sedimentary structures are observed (Figure 17). The mudstones appear homogeneous, massive and devoid of both trace and body fossils. Parallel lamination occurs frequently, where the laminae often displays a faint greenish tint, and are occasionally silty in composition (Figure 19). Pyrite nodules and euhedral pyrite crystals are common throughout this facies association. The larger pyrite nodules (up to 5 cm) often display distinct zonation (Figure 19). Fractures filled with white, blocky carbonate occur frequently, and do not show any preferred orientation (Figure 17). Minor siltstone beds 2-5 cm thick with faint parallel lamination occur sporadically, with sharp, slightly erosive contacts with the overlying and underlying mudstones. Minor sandstones are present throughout this facies association in well 7120/2-3-S, appearing both as sub-horizontal, sharp-based beds, and as vertical, ptymatically folded bodies (as described by Dzulynski and Walton (1965)) (Figure 19). The sandstones are white to light grey, fine to medium grained, non-calcaerous, mainly structureless, and often well cemented. The sandstone intervals often contain very angular shale clasts (Figure 19).

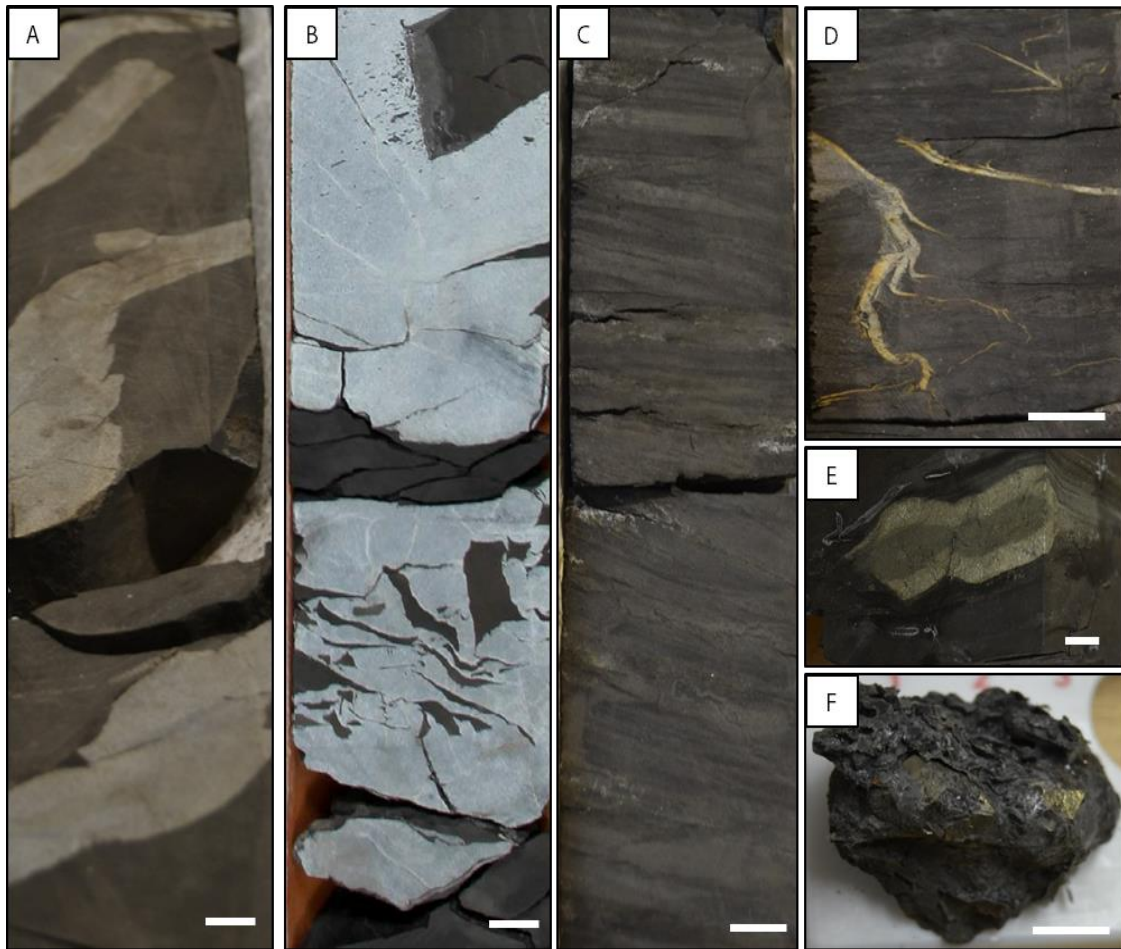


*Figure 19: Facies observed in FA4. A) Ptygmatically folded, vertical to sub-vertical sandstone beds encased in organic rich, black shale. From well 7120/2-3-S, depth 2017 m. B) Angular shale clasts in light grey, non-calcareous, well cemented sandstone. From well 7120/2-3-S, depth 2010 m. C and D) Parallel laminated to low-angle laminated dark coloured shales with carbonate filled fractures. From well 7120/2-3-S, depths 2004 m. E) Large pyrite nodule with well developed zonation in black shale. From well 7120/2-2, depth 2636.6 m. F) Poorly consolidated mudstone with euhedral pyrite crystals. From well 7120/2-2, depth 2023.5 m. Scale bars are 1 cm.*

### **Correlation with GR:**

FA4 is represented by extremely high GR values (>200 API) (Table 5; Figure 17). The lower contact is marked by a rapid increase in API values, and the upper contact is marked by a rapid decrease in API values (Table 5; Figure 17). This association also shows a wide range of well log signatures, ranging from erratic, spiky and slightly blocky. Stacking patterns of FA4 are also highly variable, ranging from aggradational, to fining or coarsening upwards (Table 5; Figure 17). FA4 is widely distributed in the

Hammerfest Basin, and are only absent from a few wells on the southwestern margin (Figure 20).

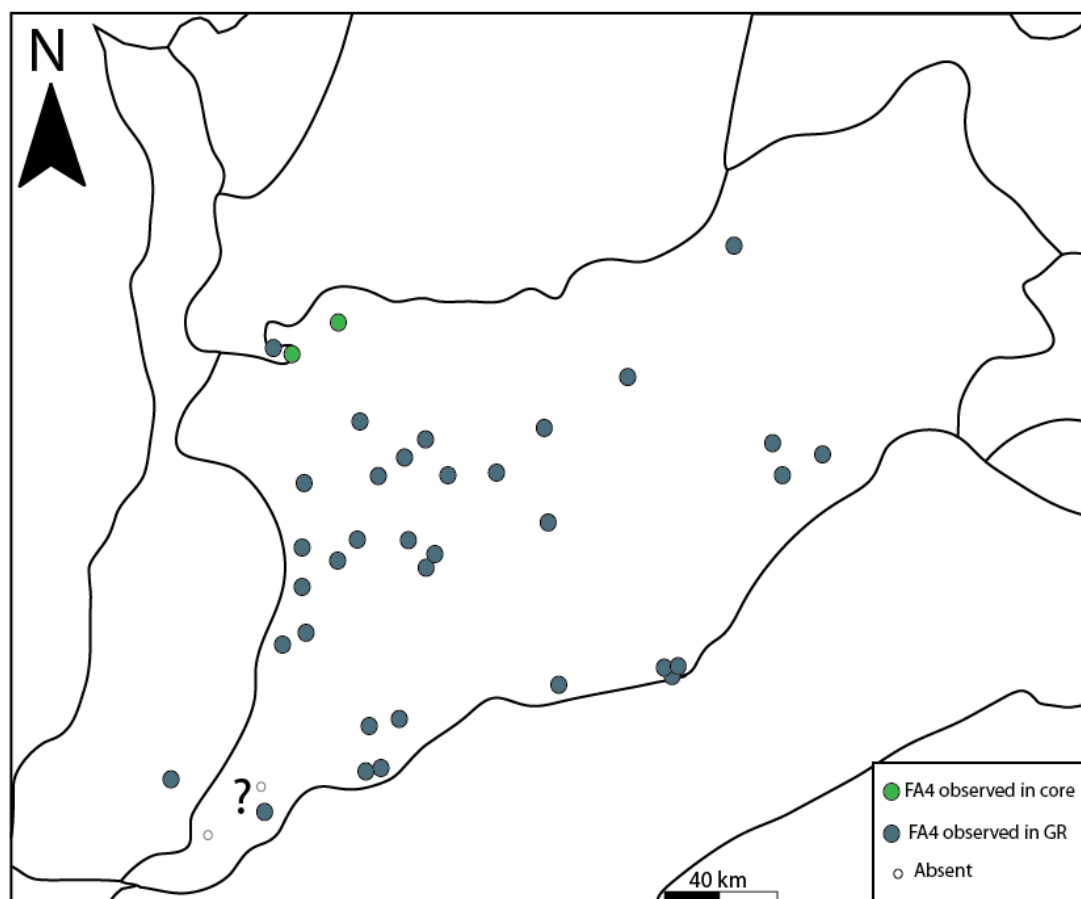


Figure 20: Distribution of FA4 based on observations from cores and well-logs.

### Interpretation:

FA4 shares several lithological characteristics with FA3, however, minor differences are observed. FA4 displays a lower silt to clay ratio compared to FA3, is darker in colour and contains no fossils or trace fossils. This is proposed to reflect a more restricted setting, higher levels of anoxia compared to FA3, and a stronger dominance of pelagic and hemipelagic sedimentation with good organic productivity. Laminations are more readily preserved during anoxic episodes, and an anoxic setting is also indicated by the abundance of pyrite observed within this facies association (Johnson



and Baldwin, 1996; Stow et al., 1996). Furthermore, a reducing environment is also inferred for the water column of FA4, based on the size and shapes of the pyrite crystals and complete absence of trace and body fossils (Wilkin et al., 1996). Moreover, pyrite formed together with calcite, and an absence of siderite commonly reflects depletion of iron, further supporting a restricted, anoxic setting (Potter et al., 2005). The sharp-based, sub-vertical and ptymatically folded sandstone bodies in well 7120/2-3-S are interpreted as sand injectites. This is based on the irregular, penecontemporaneous geometries and the presence of angular shale clasts derived from the underlying units within the sandstone bodies (Hurst et al., 2003). Sand injectites can form due to liquefaction from triggers such as earthquakes, slumps and slides, or due to rapid emplacement by mass flows (Boggs, 2006; Hurst et al., 2011). This is consistent with the close proximity to the Loppa High, and probably reflects a single or multiple episodes of fault movement along the AFC.

#### **4.1.5 FACIES ASSOCIATION 5 – MASS FLOW**

##### ***4.1.5.1 Sub-association 5a – Distal basin floor fan***

###### **Observations:**

Sub-association 1 occurs in well 7120/2-2 and comprises a relatively thin interval (1.5 m) of parallel laminated, very fine-grained sandstone with interbedded dark mudstones (Figure 17; Figure 21). The mudstones are subfissile to blocky, dark brown and slightly pyritic. The sandstones are very fine grained to silty, white to grey in colour, and occasionally contains authigenic and detrital glauconite (Figure 21). Laminae range in thickness from 1 mm to 1 cm. The base of the individual sandstone units are non-erosive to slightly erosive, and the laminae display a faint fining upwards trend (Figure 21). The top of the sandstone interval displays evidence of penecontemporaneous deformation, with micro-normal faults and convoluted bedding present (Figure 21). This sub-association shows no sign of bioturbation, and no fossils are observed within the unit.

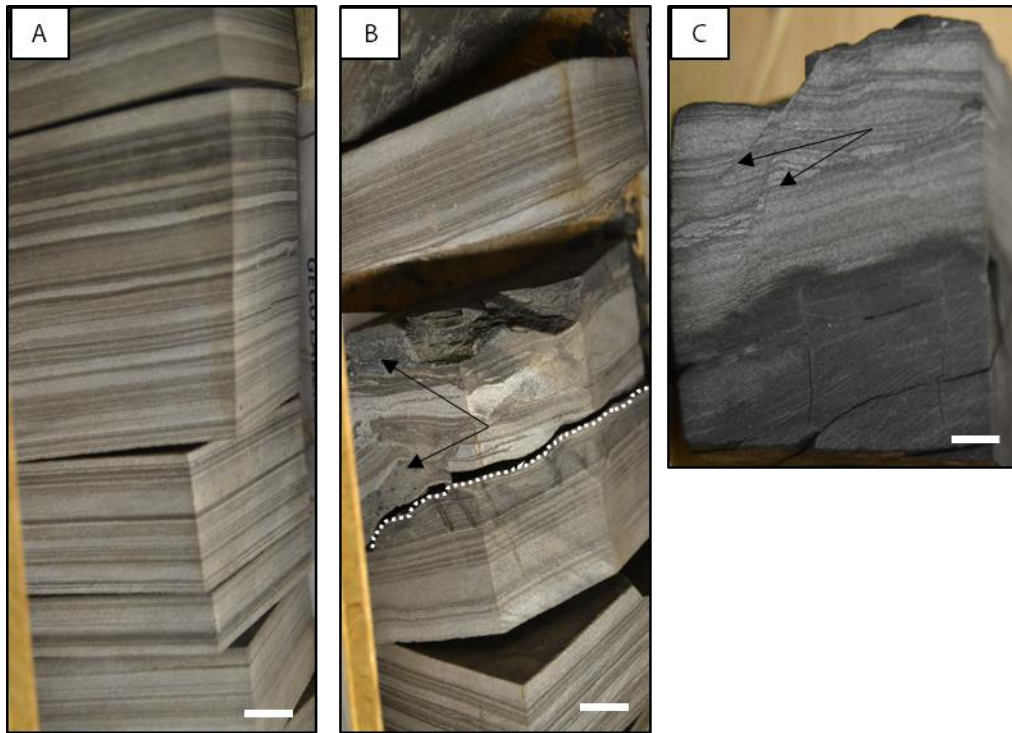


Figure 21: Facies observed in FA5a. A) Parallel laminated, very fine grained sandstone with interbedded mudstone and siltstone. B) Erosive contact in F11, overlain by soft sediment deformed sandstone and siltstone. A lithoclast with glauconite fragments (Lower arrow), and possibly authigenic glauconite (Upper arrow) is also observed. C) Parallel laminated, and ripple laminated sandstone and siltstone with micro-normal faults. All images are from well 7120/2-2, at depths 2637.5 m, 2637.1 m, and 2636.3 respectively. Scale bars are 1 cm.

### Correlation with GR:

The base of FA5a is marked by an abrupt decrease in API values, reflecting the change from mudstone to fine grained siltstone (Figure 14 Table 5). Stacking patterns are slightly aggradational to fining upwards (Figure 14). The upper contact is marked by a rapid increase in GR. FA5a is relatively thin (5-10 meters), and has an overall blocky GR signature. Overlying and underlying lithologies display relatively high API values, and appear as an aggradational sequence, interrupted by the minor packages of FA5a (Table 5; Figure 14).

**Interpretation:**

Sub-association FA5a displays evidence of deposition in an overall low energy environment, below fair-weather wave base, and possibly below storm-wave base, based on the dominance of clay sized sediments observed above and below this relatively thin unit. The interbedded mudstones are interpreted to be a result of background sedimentation, with deposition of clay-sized sediment from suspension fallout from the water column. The sandstone laminae are interpreted as a result of deposition from suspension from a waning, low density, turbiditic flow ( $T_d$ ) (Bouma, 1962) based on the cyclicity, fining upwards trend and absence of higher flow regime structures. The authigenic glauconite horizon towards the top of FA5a (Figure 21), both overlain and underlain by parallel laminated sandstones suggests an interval of slow rates of deposition, indicating that the deposition of sandstones was episodic rather than continuous (Cloud, 1955; Stow et al., 1996; Bonewitz, 2012). Moreover, the formation of glauconite reflects slightly reducing water conditions, most likely in a shallow marine environment (Cloud, 1955; Blatt et al., 1972a; Stow et al., 1996; Einsele, 2000c; Nichols, 2009c; Bonewitz, 2012). The soft sediment deformation structures (convoluted bed and micro-normal faults) towards the top of the facies association are most likely a result of shear stress exerted by flows moving above the recently deposited sediments (Blatt et al., 1972b). Based on the mentioned observations in combination with GR facies, FA5a is interpreted as deposited by turbiditic currents in an overall low-energy environment. The fine-grained sediments, turbidites and abundance of background sedimentation suggests a distal setting in a possible basin floor fan fringe environment (Mutti and Ricci Lucchi, 1978; Shanmugam et al., 1985).

#### ***4.1.5.1 Sub-association 5b – Proximal basin floor fan***

##### **Observations:**

FA5b is observed in well 7120/12-1 on the southern Hammerfest Basin margin, makes up a 3.5 m thick unit, and shows great internal variability (Figure 8Figure 14). This facies association is composed of sandstone, siltstone and mudstone, and is overall sandstone dominated. It makes up a succession of three fining upwards, sandstone units, bound by minor erosive surfaces (Figure 14Figure 22). The base of FA5b is reflected by a change from dark coloured mudstones containing thin (1 cm) vertical to sub-vertical ptymatically folded sandstones, to medium-grained sandstones (Figure 14). The contact between these units was not observed due to discontinuous core recovery. The lower sandstone unit is composed of medium grained, light to dark brown sandstone, grading into mudstone towards the top (Figure 14; Figure 22). The base of this unit is internally chaotic, containing abundant coal clasts, mud rip-up clasts and glauconitic clasts (Figure 22). Ripple lamination and soft sediment deformation structures are common towards the top of the lowermost unit. The two uppermost sandstone beds are thinner (Figure 14; 10 cm and 50 cm) and show ripple lamination with mudstone drapes. The lower boundary of the uppermost bed contains coal clasts, rip-up clasts and authigenic glauconite (Figure 14A). Bioturbation and body fossils are rare to absent within FA5b (Figure 22).

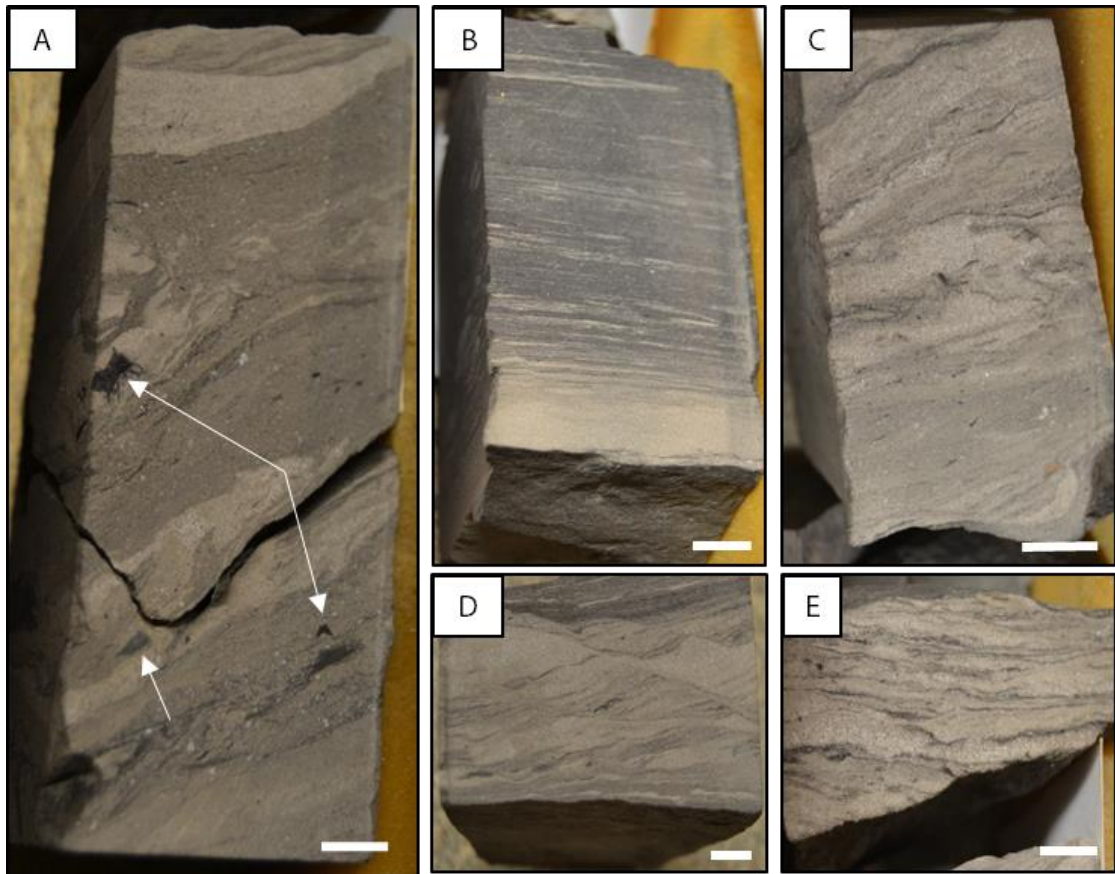


*Figure 22: Facies observed in FA5b. A) Chaotic medium grained sandstone with angular coal clasts (upper arrows) and glauconitic clast (lower arrow) (F8). B) Heterolithic bedding, fining upwards from medium grained sandstone to mudstone and slightly offset by micro-normal fault (F8 and F9). C) Ripple laminated, medium-grained sandstone (F9) D) Ripple laminated sandstone capped by dark brown mudstone, offset by micro-normal faults (F8 and F10) E) Medium-grained ripple laminated sandstone with erosive base and fining upwards (F9). All images are from well 7120/12-1 at depths, 1703.4 m, 1703 m, 1702 m, 1702.9 m, and 1703.2 m, respectively. Scale bars are 1 cm.*

### **Correlation with GR:**

FA5b show a gradual coarsening upwards trend, followed by a gradual fining upwards trend. The well-log signature is bell shaped and slightly spiky (Table 5; Figure 14). Both the upper and lower contacts are marked by relatively high API values. A rather thick unit comprising of stacked beds with a blocky GR signature, overall low API values and a fining upwards trend is observed in well 7120/1-2 (Figure 23), and is

tentatively correlated to belong to FA5. However, no core is available from this interval to confirm.

FA5a and FA5b was observed in two wells from core on the northern and southern basin margins, and in four additional wells from GR, also located along the northern and southern basin margins (Figure 23)

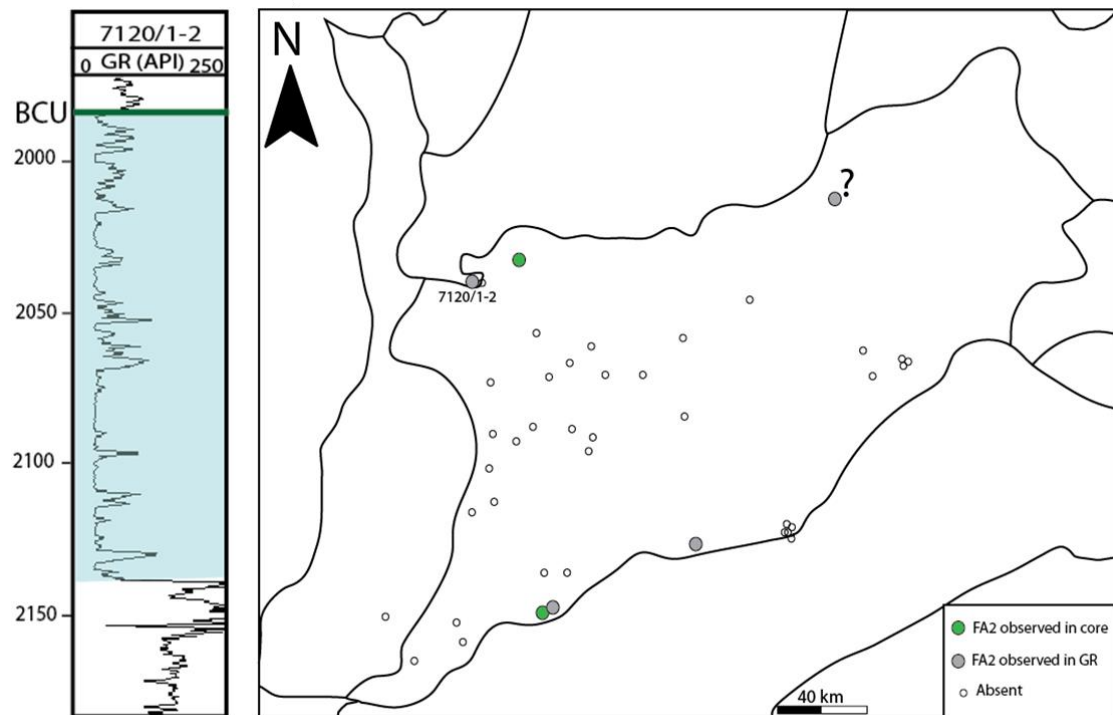


Figure 23: Left: Coarse-grained clastic packages observed in well 7120/1-2, possibly belonging to FA5. Right: Distribution of FA5 based on observations from cores and well logs.

### Interpretation:

The internal variability in sub-association FA5b, its absence of bioturbation and the presence of soft sediment deformation structures suggest a more rapid deposition of this unit compared to FA5a. Furthermore, the dominance of coarser grains and higher flow regime sedimentary structures reflects a higher depositional energy than that of FA5a, possibly reflecting a more proximal setting. The ripple lamination and normal

grading are interpreted as a result of a slightly higher density turbidity current compared to FA5a. The beds of FA5b are interpreted as T<sub>c</sub>, T<sub>d</sub> and T<sub>e</sub> units of the Bouma Sequence (Bouma, 1962). The abundance of coal clasts and mud rip up clasts suggest the flow was erosive. Presence of authigenic glauconite at the base of the uppermost bed suggests a time of low clastic influx prior to the deposition of the upper unit. Based on the assumed rapid emplacement of the individual units of FA5b, they are interpreted mass flow deposits, possibly resulting from gravitational failure along the slope of the TFFC, deposited as a basin floor fan in proximity to the slope.

Thus, FA5a and FA5b are both assumed deposited by turbiditic currents, however, under different flow regimes and at different locations within a similar depositional system. The clastic packages observed from the GR-log in well 7120/1-2 tentatively correlated to FA5a (Figure 23), and may represent the more proximal expression of the same event. FA5b is assumed to be a mass flow deposit resulting from slope failure, however, no classification is made for FA5a on delivery system due to lack of more proximal core data.



## **4.2 Genetic Sequences and Age Control**

Five genetic sequences (J1-J5) are defined to establish a sequence stratigraphic framework of the Middle to Upper Jurassic deposits in the Hammerfest Basin. The genetic sequences show an overall good correlation with the lithostratigraphy in the area, where sequence J1 and J2 roughly correspond to the Fuglen Formation, whereas sequences J3-J5 more or less correlate with the Hekkingen Formation (Figure 24). Figure 24 gives a general overview of the sequences, the ages, and their associated stacking patterns. The following sub-chapters provides descriptions of the different sequences, the associated bounding surfaces, and how they relate to the facies associations defined in Chapter 4.1.

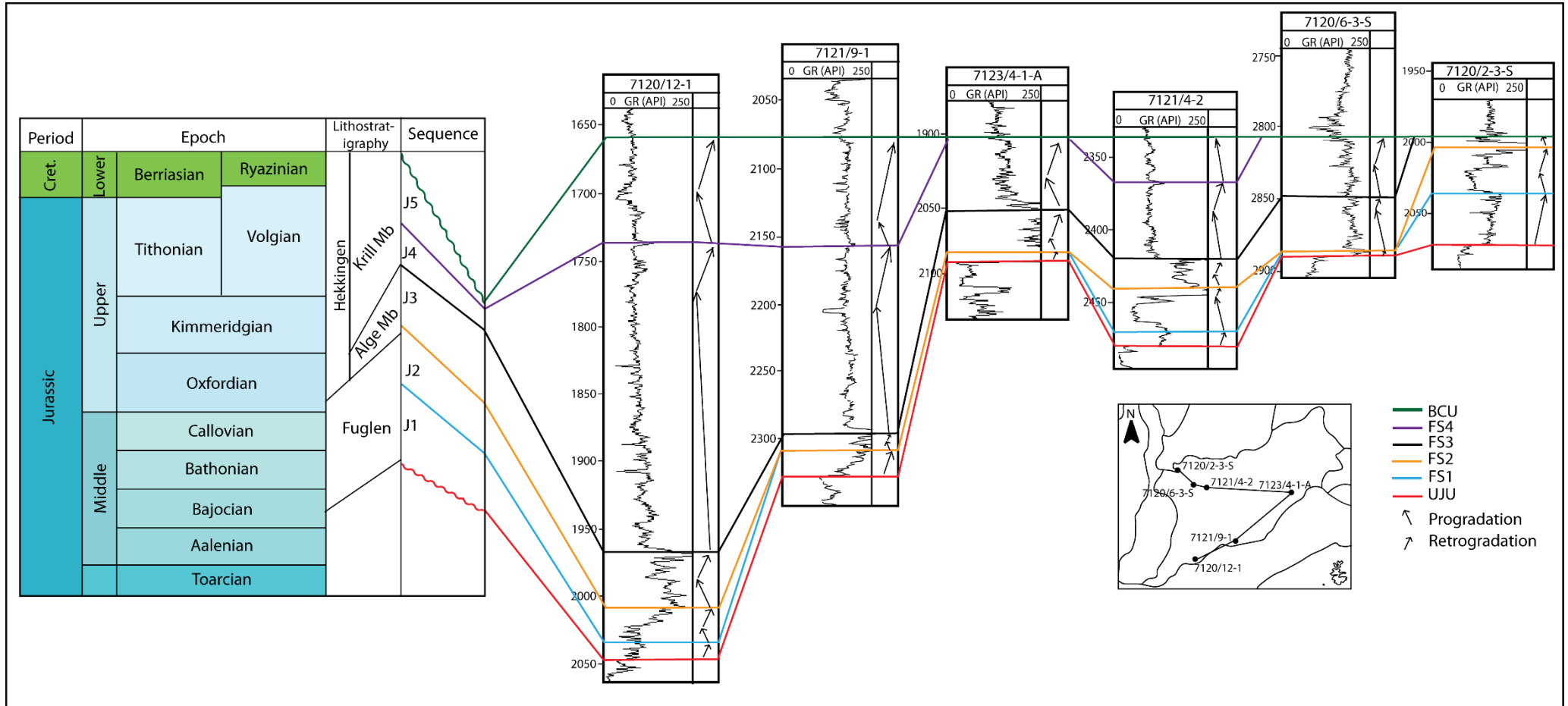


Figure 24: Six selected wells and their correlation across the Hammerfest Basin illustrating the five third order sequences (J1-J5). The sequences are bound by flooding surfaces (FS1-FS4). The base of J1 and top of J5 are bound by the regional unconformities, the Upper Jurassic Unconformity (UJU) and Base Cretaceous Unconformity (BCU) respectively. Note the time transgressive relationship between the different sequences and their respective bounding surfaces, and the correlation between the sequences and the lithostratigraphy. Abbreviations: Cret=Cretaceous. Mb=Member.

#### **4.2.1. SEQUENCE J1:**

Sequence J1 is bound at the base by the UJU and at the top by FS1 (Figure 24). The sequence range in age from early Bathonian to early Oxfordian. Lithologically, this sequence corresponds to the transition from the Stø Formation and the Lower part of the Fuglen Formation (Figure 24). Based on GR-facies correlation and observations from cores, sequence J1 comprises transgressive shelf facies (FA1), lower shoreface to offshore transition zone facies (FA2) and offshore facies (FA3) (Figure 25; Figure 26; Figure 27). On the southern margin, J1 is composed of proximal facies (FA1 and FA2). The sequence gradually thins towards the Goliat Anticline, and is absent in the eastern part of the Hammerfest Basin (Figure 26). Along the northern basin margin, sequence J1 is thicker and more continuous compared to the southern margin, and is composed of more distal facies (FA3) (Figure 25). J1 on the northern margin display a diachronous relationship, with an overall younging eastwards trend (Figure 25). The sequence pinches out towards the Central High both from the northern and southern margins (Figure 27).

#### **4.2.2. SEQUENCE J2:**

J2 is bound at the base by FS1, and by the UJU over structural highs where FS1 is absent (Figure 24). The top is represented by FS2. The sequence range in age from Late Bathonian to late Kimmeridgian, and corresponds to the uppermost part of the Fuglen Formation and the lower part of the Alge Member of the Hekkingen Formation (Figure 24). On the southwestern basin margin, J2 is dominated by proximal facies (F2), grading into more distal facies (F3 and F4) eastwards (Figure 26). This change in facies also corresponds with a younging eastwards trend of J2, going from Callovian in the southwest to Kimmeridgian in the northeast (Figure 26). Furthermore, the Kimmeridgian deposits within sequence J2 on the southern margin is observed to be

pinching out towards the Central High (Figure 27). On the northern margin, J2 is composed of offshore facies (FA3), and restricted anoxic facies (FA4) (Figure 25). J2 can be correlated basin wide, but show a gradual thinning towards the Central High and the southeastern part of the basin (Figure 26; Figure 27).

#### **4.2.3. SEQUENCE J3:**

Sequence J3 is bound at base by FS2 and at the top by FS3, or the BCU in well 7120/2-3-S located on the outer part of the AFC High. FS3 correlates well with the lithostratigraphic framework, and represents the top of the Alge Mb (Figure 24). J3 ranges from Middle Oxfordian to Early Volgian in age, and corresponds mainly to the Alge Mb, and locally to the Krill Mb (Figure 23). Sequence J3 represents the most widespread deposition of FA4, but locally reflects the deposition of FA3 (Figure 25; Figure 26; Figure 27). On the southwestern margin, the sequence displays a highly diachronous relationship, going from Oxfordian in the west, to Volgian age in the east (Figure 26). However, the opposite trend is observed from the northern margin, where J3 is younging westwards from Oxfordian to Kimmeridgian (Figure 25). The sequence show good lateral continuity, and can be correlated in all the studied wells.

#### **4.2.4. SEQUENCE J4:**

Sequence J4 is of Late Kimmeridgian to Middle Volgian age, and is bound at the base by FS3. The top of the sequence is represented by FS4, and locally the BCU. Sequence J4 shows a more aggradational stacking pattern compared to J1-J3. Lithologically this sequence corresponds to the lower part of the Krill Mb of the Hekkingen Formation, and reflects the deposition of offshore facies and mass flow facies (FA3 and FA5). The sequence is thickest on the southwestern margin, but gradually thins eastwards (Figure 26). This trend corresponds to a change from Kimmeridgian to Volgian age.

#### **4.2.5. SEQUENCE J5:**

Sequence J5 is bound at top by the BCU and at the base by FS4. It ranges in age from Late Kimmeridgian to Ryazinian, and correlates to the upper part of the Krill Mb. It comprises FA3 and FA5, and display an overall aggradational stacking pattern. It comprises the lithological facies associations FA3 and FA5, the sequence is not laterally continuous, and is better developed along the southern basin margin (Figure 25-Figure 27).

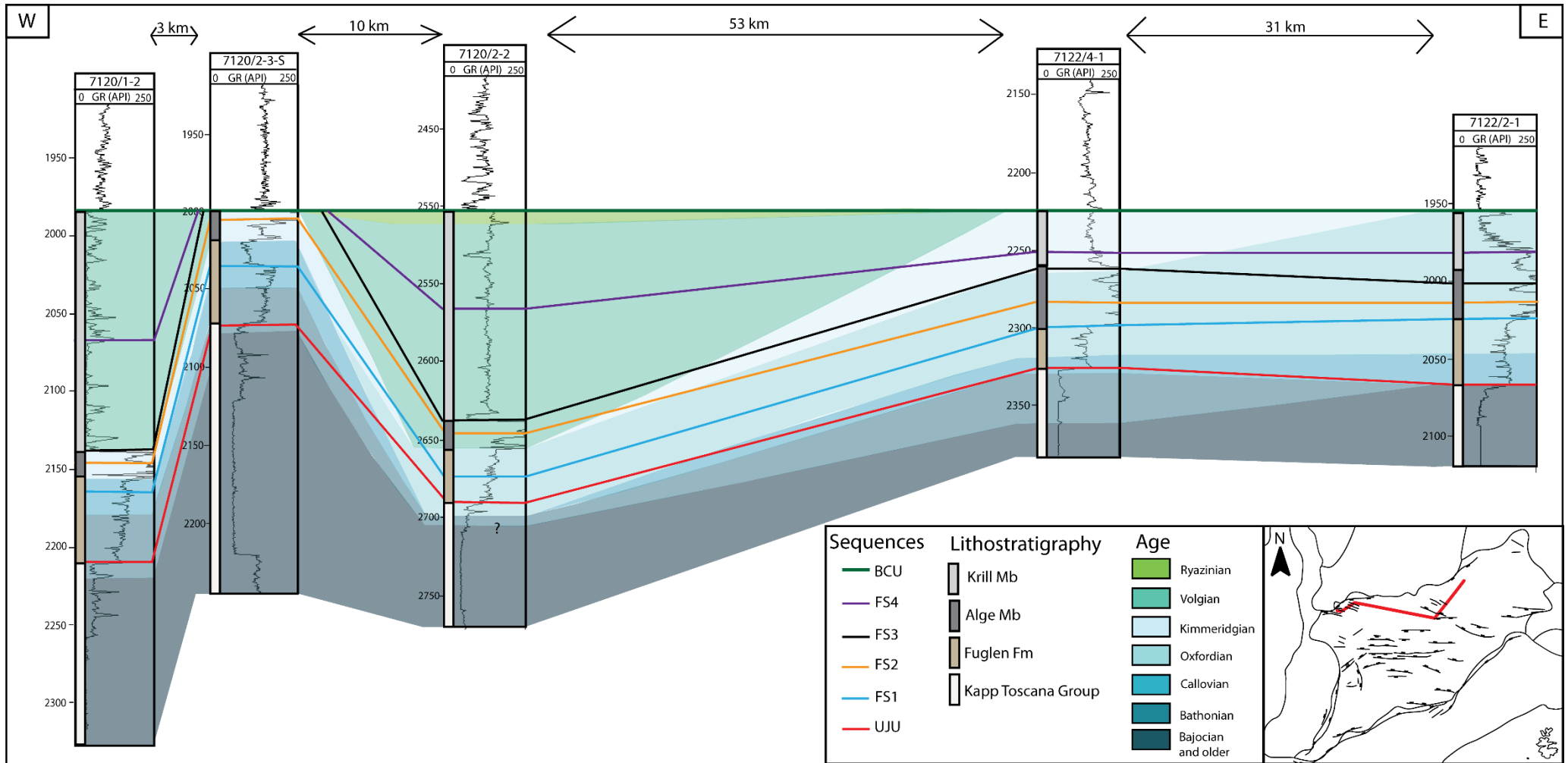


Figure 25: Chronostratigraphic correlation compared to the sequence stratigraphic framework and the lithostratigraphy along the northern Hammerfest Basin margin. Note the variability of ages within similar lithostratigraphic units.

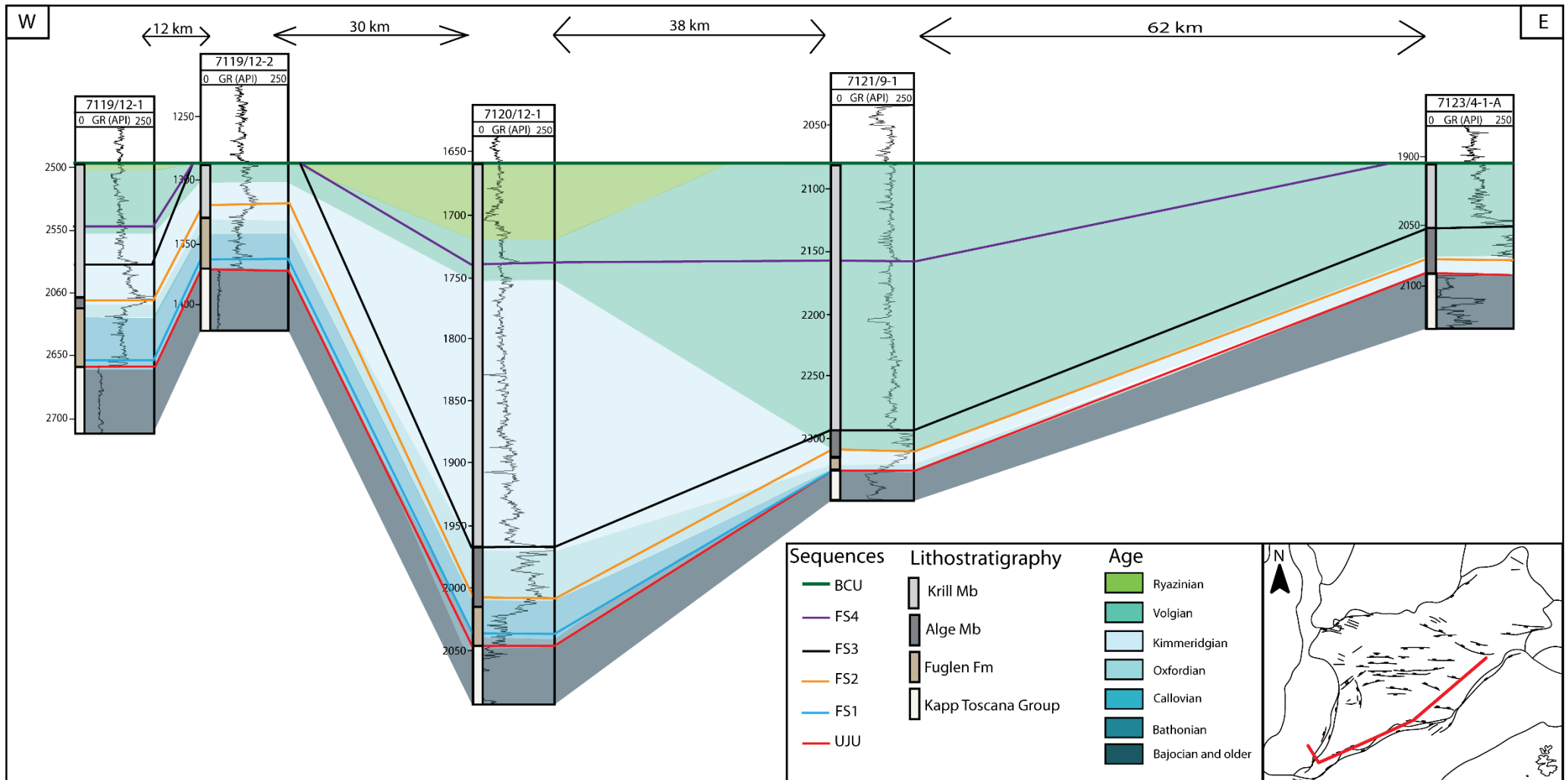


Figure 26: Chronostratigraphic correlation compared to the sequence stratigraphic framework and the lithostratigraphy along the northern Hammerfest Basin margin. Note the variability of ages within similar lithostratigraphic units.

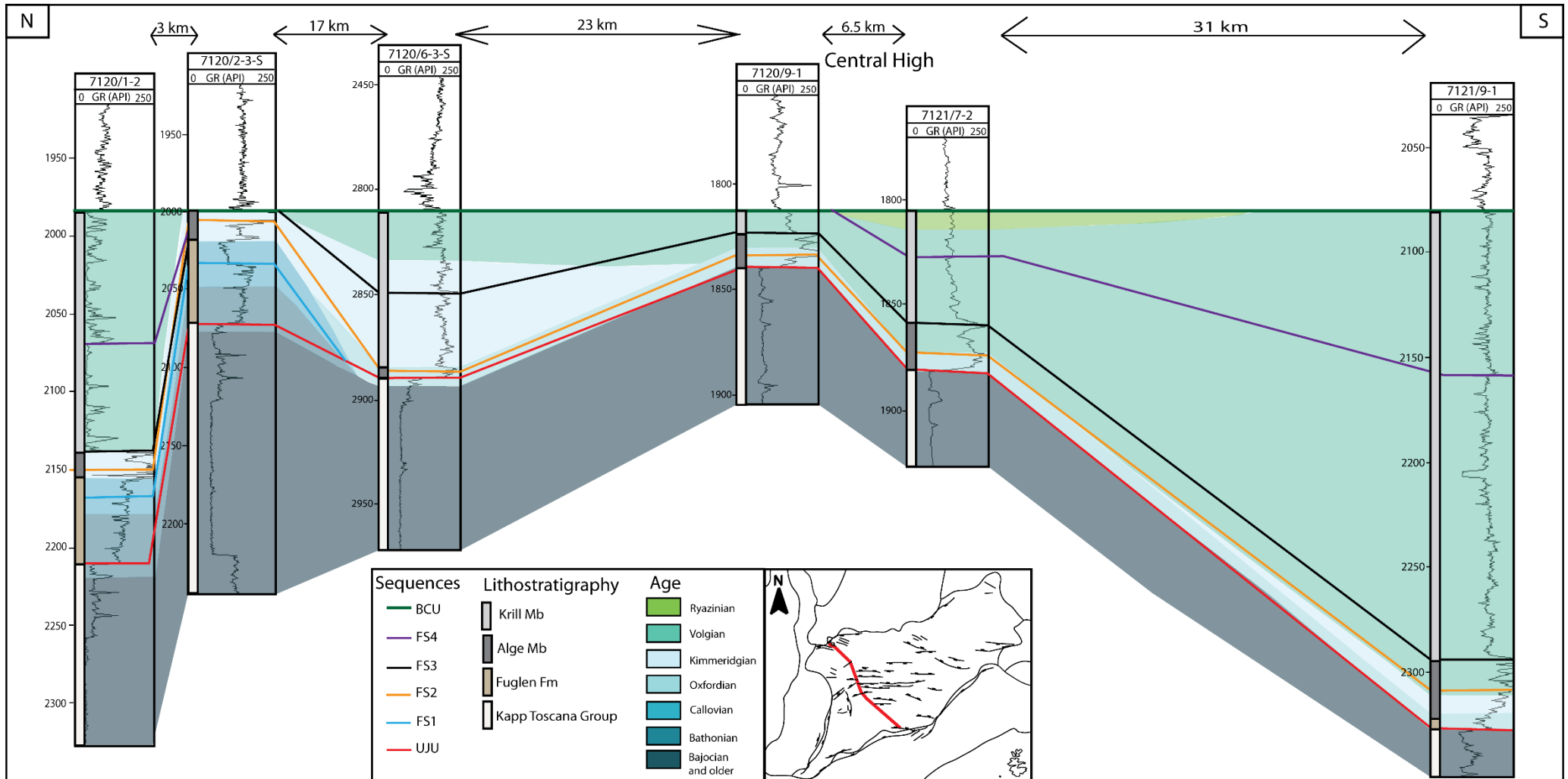


Figure 27: Chronostratigraphic correlation compared to the sequence stratigraphic framework and the lithostratigraphy across the Central High. Note the variability of ages within similar lithostratigraphic units.



### **4.3. Seismic Interpretation**

As mentioned in Chapter 3.2, the Middle to Upper Jurassic of the Hammerfest Basin is represented by a single seismic sequence, and the genetic sequences J1-J5 are below seismic resolution (Figure 6; Figure 7). Hence, the following chapter provides a general overview of the structural configuration of the Hammerfest Basin, and the lateral and vertical distribution of the Middle to Upper Jurassic interval as a single seismic unit.

#### **4.3.1 STRUCTURAL CONFIGURATION**

Four main fault families are identified within the study area, and are classified based on similar strikes and age (i.e. offset of the Middle to Upper Jurassic seismic sequence). The most prominent fault activity is observed along the southern margin and the central part of the basin (Figure 3; Figure 28). Fault activity decreases eastwards, and the eastern part of the basin show little to no fault activity (Figure 3). The characteristics of the individual fault families are described below, and their locations are illustrated in Figure 28.

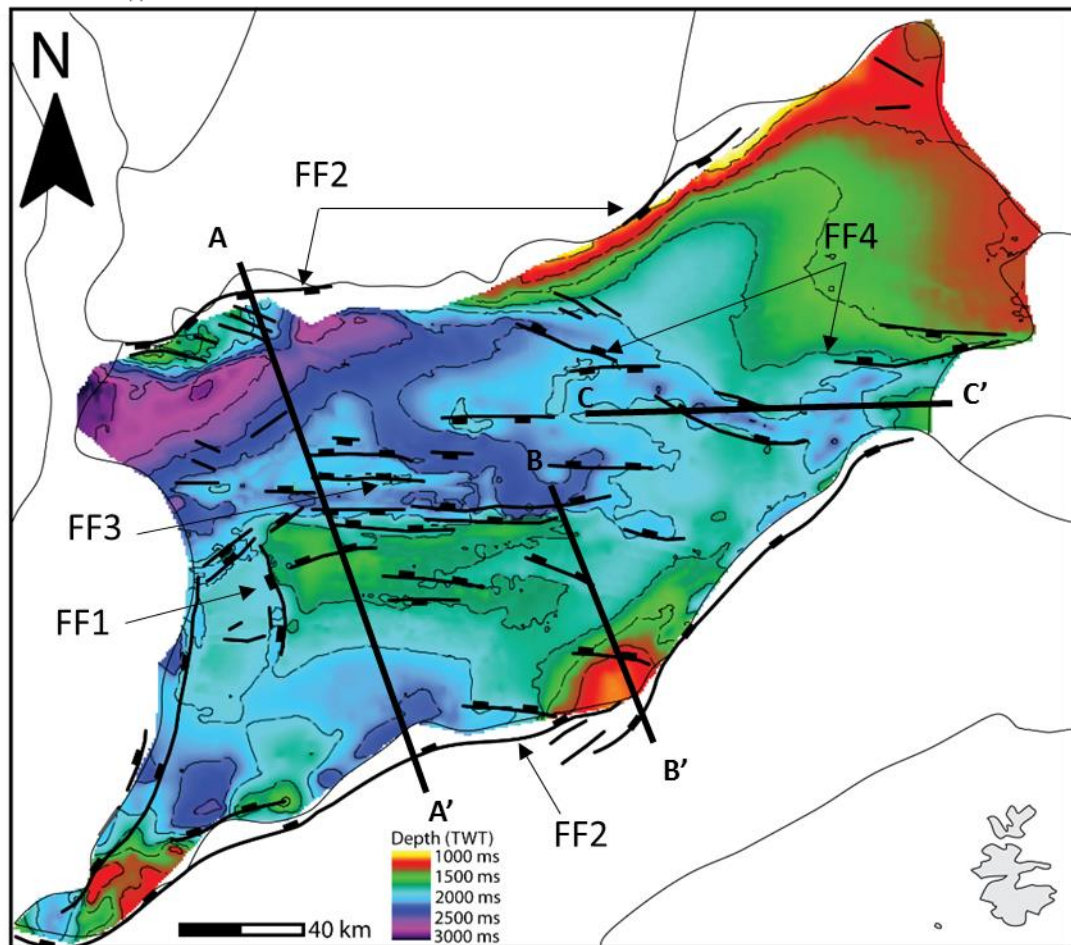


*Figure 28: Time structural map of the Upper Jurassic Unconformity and the four different fault families identified.*

### **Fault Family 1 (FF1).**

FF1 consists of NNE-SSW trending normal faults, located on the western margin of the basin (Figure 3; Figure 28). This fault family makes up part of the Ringvassøy-Loppa Fault complex (RLFC), and represents the western boundary of the study area. FF1 displays offset through the entire Middle to Upper Jurassic interval. Little to no growth strata was observed related with FF1 within the study area.

### **Fault Family 2 (FF2).**

FF2 is represented by NE-SW trending normal faults, located at the northern and southern Hammerfest Basin margin (Figure 3; Figure 28). The basin bounding faults to the north belong to the Asterias Fault Complex (AFC), separating the Hammerfest Basin from the Loppa High (Figure 3; Figure 28; Figure 29). The southern basin bounding faults represents the Troms-Finnmark Fault Complex (TFFC), consisting of a segmented system of listric normal faults (Figure 3; Figure 28; Figure 29; Figure 30). FF2 shows offset through the entire Middle to Upper Jurassic interval, and growth strata was observed in the hanging walls both on the northern and southern basin margins.

### **Fault Family 3 (FF3)**

FF3 is located in the central part of the Hammerfest Basin, and consists of E-W trending, planar normal faults. Most faults of FF3 offset the entire Middle to Upper Jurassic interval, whereas some terminate before the BCU reflector (Figure 29). Thinning of strata is common on the footwalls of the larger faults in FF3, as illustrated in Figure 29.

### **Fault Family 4 (FF4)**

Fault family 4 is represented by NW-SE striking normal faults, and are confined to the eastern part of the Hammerfest Basin (Figure 28; Figure 31). Growth strata was observed related to this fault family (Figure 31). Some faults of FF4 terminate at the BCU level, whereas some offset the entire Middle to Upper Jurassic seismic sequence (Figure 31).

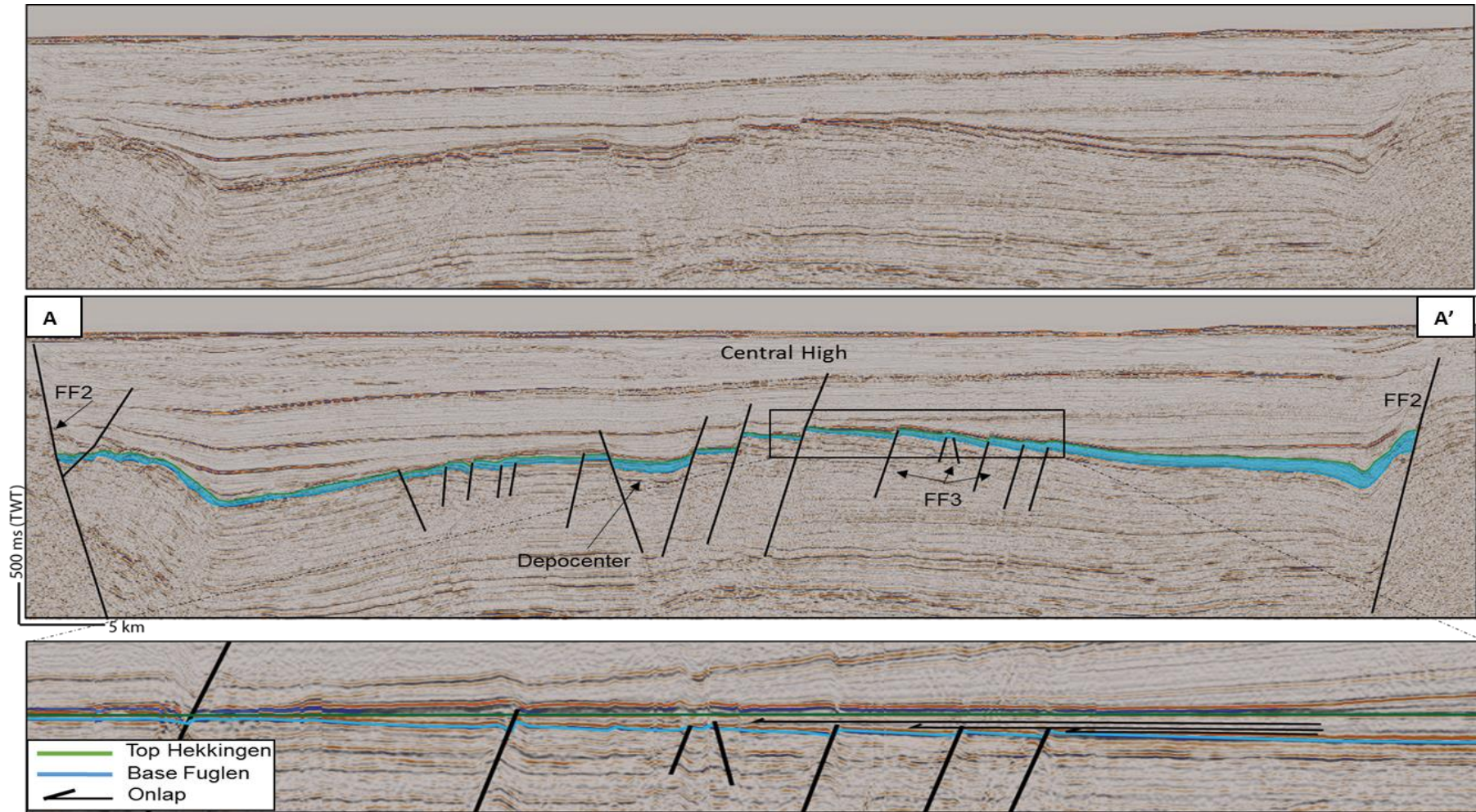


Figure 29: Upper: Un-interpreted NNW-SSE regional line. Middle: Interpreted NNW-SSE regional line illustrating the basin configuration of the southern central part of the study area. Note the diachronous fault activity and thinning of strata over the Central High. Lower: Close up of the Central High, where the line is flattened to the BCU surface. Internal reflectors of the Middle to Upper Jurassic seismic sequence are onlapping the structure. Location of the line is indicated in Figure 28.

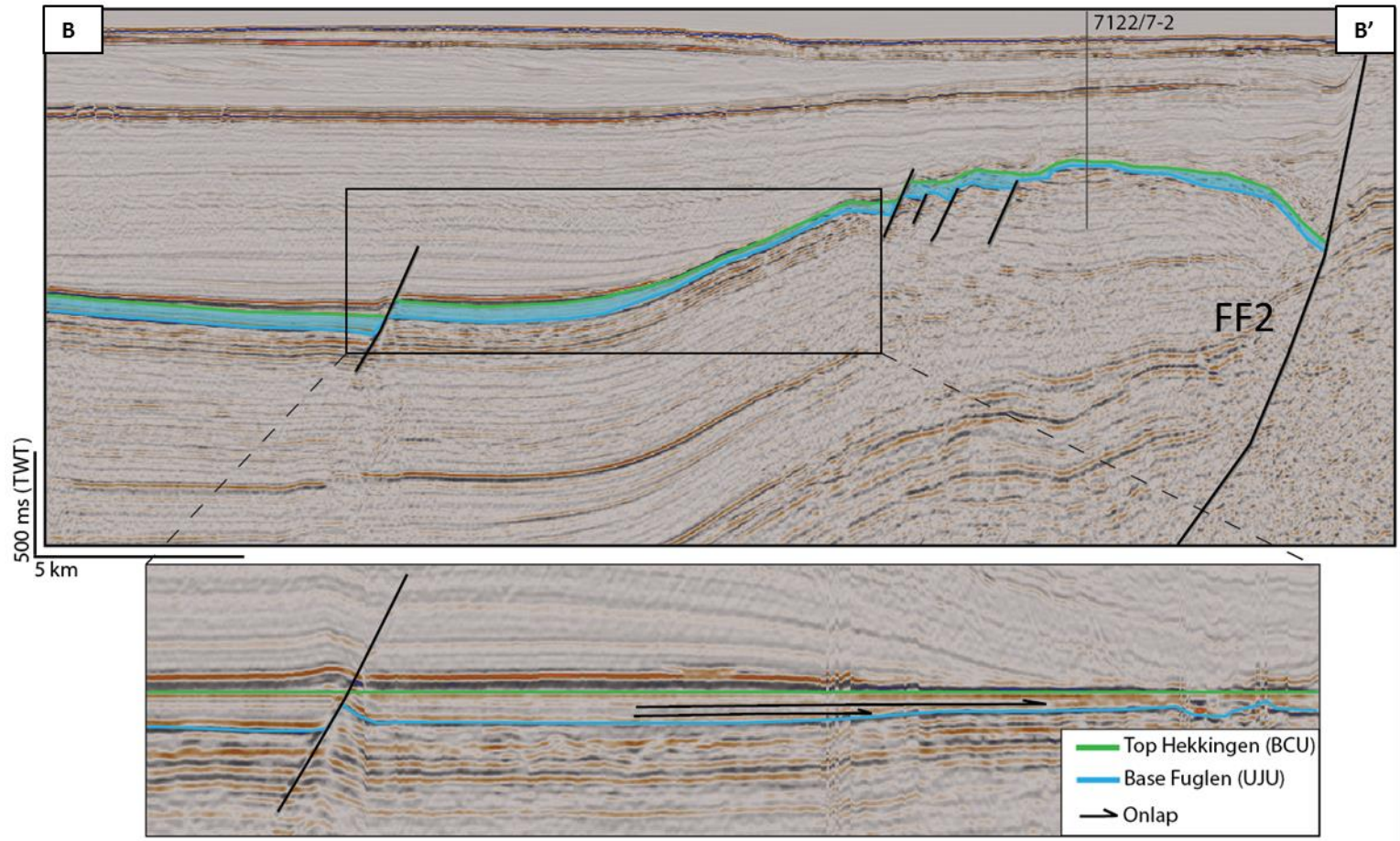


Figure 30: Upper: Interpreted NNW-SSE seismic line through the Goliat Anticline illustrating the structural configuration of the Goliat Anticline. Note the thinning of strata towards the structure. Lower: Close up of the flank of the Goliat Anticline flattened to the BCU surface, where the Middle to Upper Jurassic seismic sequence is seen onlapping the anticline. Location of the line is indicated in Figure 28.

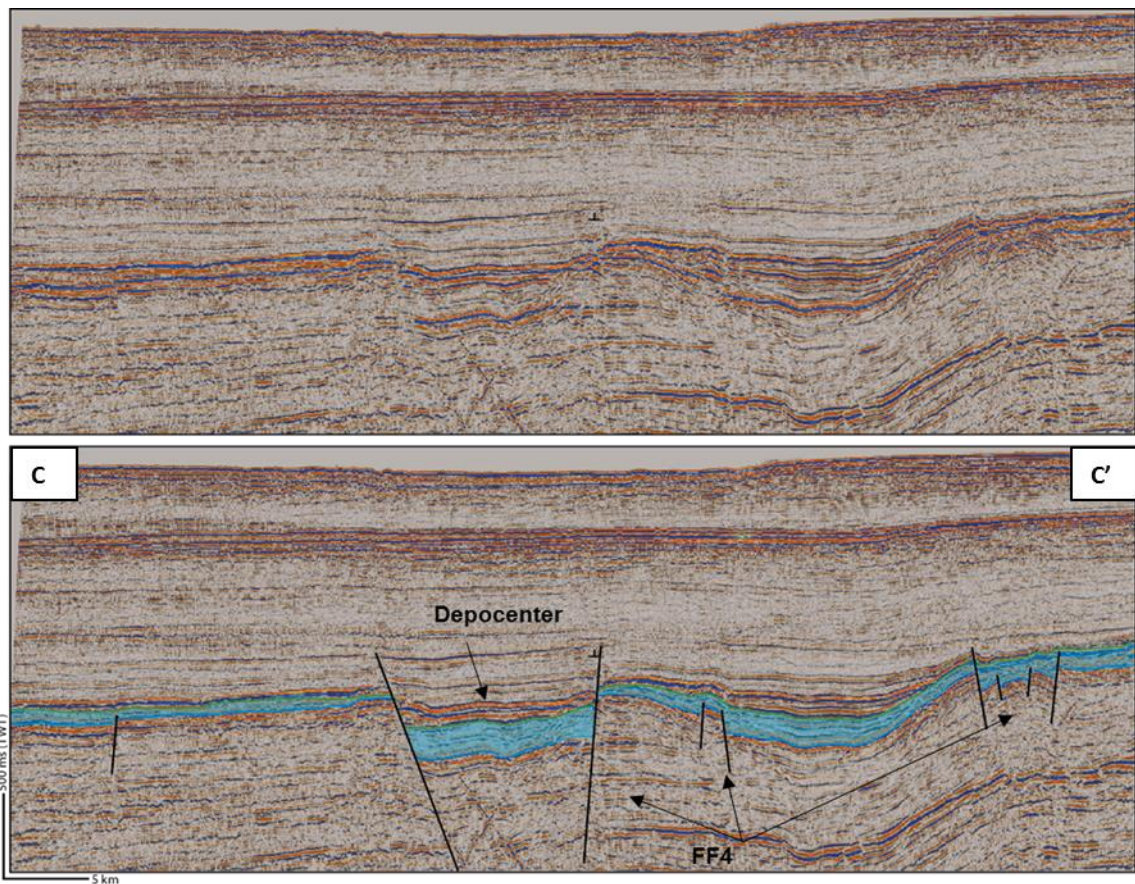
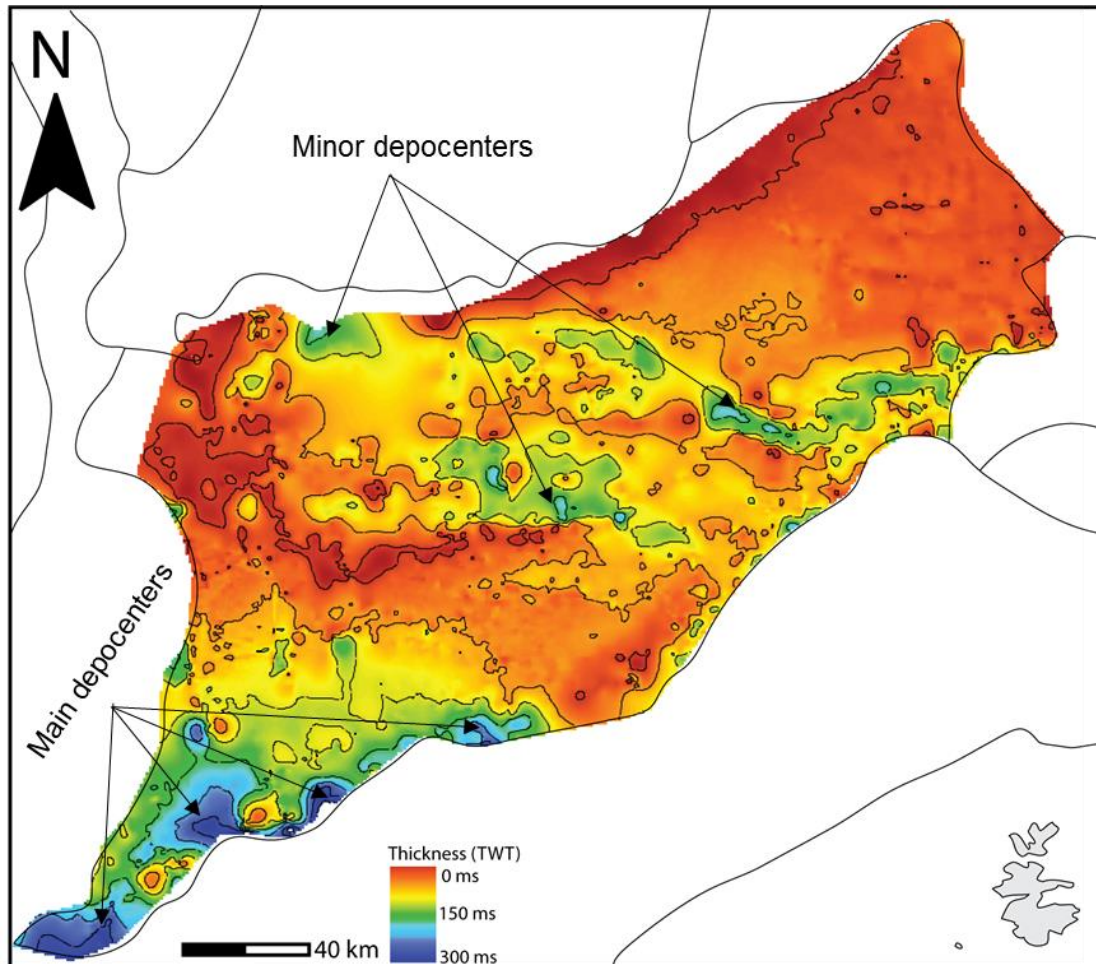


Figure 31: E-W regional line illustrating the basin configuration in southeastern part of the study area. Note the depocenter associated with FF4, and how some of the faults offset the entire seismic sequence, whereas others terminate before the BCU. Location of the line is indicated in Figure 28.

#### 4.3.2. VERTICAL AND LATERAL DISTRIBUTION

The Middle to Upper Jurassic seismic sequence shows a gradual thinning eastwards towards the Bjarmeland Platform and northward towards the Loppa High (Figure 3; Figure 32). An overall NW-SE thinning trend is observed in the western, central part of the Basin (Figure 32). The most prominent depocenters are located along the southwestern basin margin, in the hanging walls of FF2. The westernmost depocenters are separated by local highs (Figure 28; Figure 32). A minor depocenter is observed on the northern basin margin, east of the AFC high, and in the hanging-wall of FF2. Minor depocenters are also present in the central Hammerfest Basin, related to FF3, and in the

southeastern part of the study area, related to FF4 (Figure 29; Figure 31). Onlapping strata are observed over the Central High and on the flanks of the Goliat Anticline (Figure 29; Figure 30).



*Figure 32: Time thickness map of the Middle to Upper Jurassic seismic sequence. Note how the depocenters are isolated and restricted to areas of more fault activity.*

## **5. DISCUSSION**

### **5.1. Controlling Factors on Basin Fill**

The infill of sedimentary basins and the resultant architectural elements and facies associations are generally controlled by the interaction between several factors. Sediment supply, eustatic sea level change and rate of basin subsidence has been proposed to act as the main controlling variables for basin fill at various scales (Galloway, 1989; Myers and Milton, 1996; Einsele, 2000a; Catuneau, 2006). The following sub-chapters addresses each of these variables in order to analyse the main controls on sedimentation of the Middle to Upper Jurassic in the Hammerfest Basin.

#### **5.1.1. SEDIMENT SUPPLY:**

Sediment supply refers to the amount and type of sediments that is supplied from the source areas to the site of deposition, and plays an important role in terms of basin architecture (Galloway, 1989; Catuneau, 2006). Mud dominated marine settings are commonly associated with large fluvial systems drained from low-relief hinterlands (Johnson and Baldwin, 1996; Potter et al., 2005b), and the amount of sediments deposited is highly dependent on climatic controls and the lithology of the source area (Galloway, 1989; Catuneau, 2006).

The degree of bioturbation within a sedimentary unit is often a good reflection of the sediment influx within a site of deposition. Low rates of sediment supply are commonly associated with highly bioturbated units, as low rates of sediment input provides the burrowing organisms sufficient time to thoroughly rework the sediment (Wetzel, 1984; MacEachern and Bann, 2008; Morad et al., 2010). Hence, sequences J1 and J2, comprising the highly bioturbated units of FA2, are interpreted to have been deposited



during a time of relatively low sediment supply. Moreover, sequence J1 also comprises transgressive shelf deposits (FA1), where both omission surfaces and glauconite rich beds are present. The formation of glauconite occurs when sedimentation rates are extremely low (Galloway, 1989; Einsele, 2000b; Nichols, 2009c), whereas omission surfaces form during non-deposition (Reading and Collinson, 1996; Catuneau, 2006; MacEachern and Bann, 2008)

The formation and preservation of organic material within a marine basin is favoured by high organic productivity with little clastic dilution (Potter et al., 2005c; Nichols, 2009a). These conditions are consistent with the interpreted depositional setting of FA4, which makes up large parts of sequence J3 and correlates with the organic rich Alge Mb. Thus, a low rate of clastic input to the basin during the deposition of J3 was a prerequisite for the formation of the present day source rock. Moreover, Galloway (1989) noted that widespread radioactive mudstone units, comparative to the high API values as noted from the Alge Mb, reflected slow sedimentation and concentration of organic matter. J1-J3 all indicate low rates of sedimentation from the Bathonian to Lower Volgian times in the Hammerfest Basin

The overall aggradational stacking patterns observed in sequences J4 and J5 could indicate a slight increase in sediment supply towards the end of the Jurassic. The introduction of the sand rich FA5, and the lack of FA4 within these sequences further support this assumption. However, lack of very coarse grained sediments along the northern and southern margins suggests that the rejuvenation of the source area was low (Catuneau, 2006).

### 5.1.2. EUSTASY

Eustasy represents the absolute global sea-level relative to the center of the earth. Eustasy can be influenced by either changing the ocean-basin volume (tectono-eustasy), or the ocean water volume (glacioeustasy). The Jurassic of the southwestern Barents Sea has been noted as a time of regional transgression by several authors (Dalland et al., 1988; Mørk et al., 1999; Worsley, 2008; Henriksen et al., 2011). The transgressional event is inferred based on the widespread deposition of fine-grained sediments, as the initial stages of transgression trap coarse clastic material inshore (Steel and Ravnås, 1998; Potter et al., 2005b), only allowing for the finer sediment fractions to be deposited basinwards.

Figure 33 illustrates the estimated long-term and short-term sea level curves for European basins during the Jurassic and Lower Cretaceous (Haq et al., 1988), together with the estimated sea-level curve based on outcrop mapping and detailed biostratigraphy of the Jurassic of the Jameson Land, Greenland (Surlyk, 1990). The transgressive-regressive cycles of Hardenbol et al. (1998) indicates the magnitude of the maximum flooding surfaces for fourth order cycles. A good correlation is observed between sequences J1-J5 and the eustatic sea level curves, with the best fit with the curve of Surlyk (1990). Figure 33 indicates a time of regional sea-level rise, with a minor fall towards the Lower Cretaceous. This is consistent with the observations from this study, where the lithological facies associations indicates a change shallow marine shelf to a more distal, low energy environment. Thus, the transgressional nature observed from the data utilized in this study, coincides with a regional sea-level rise. However, the effects of this sea-level rise could also have been amplified by accommodation creation from local tectonics, and hence, increasing basin volume on a local scale in addition to the regional eustatic effects.

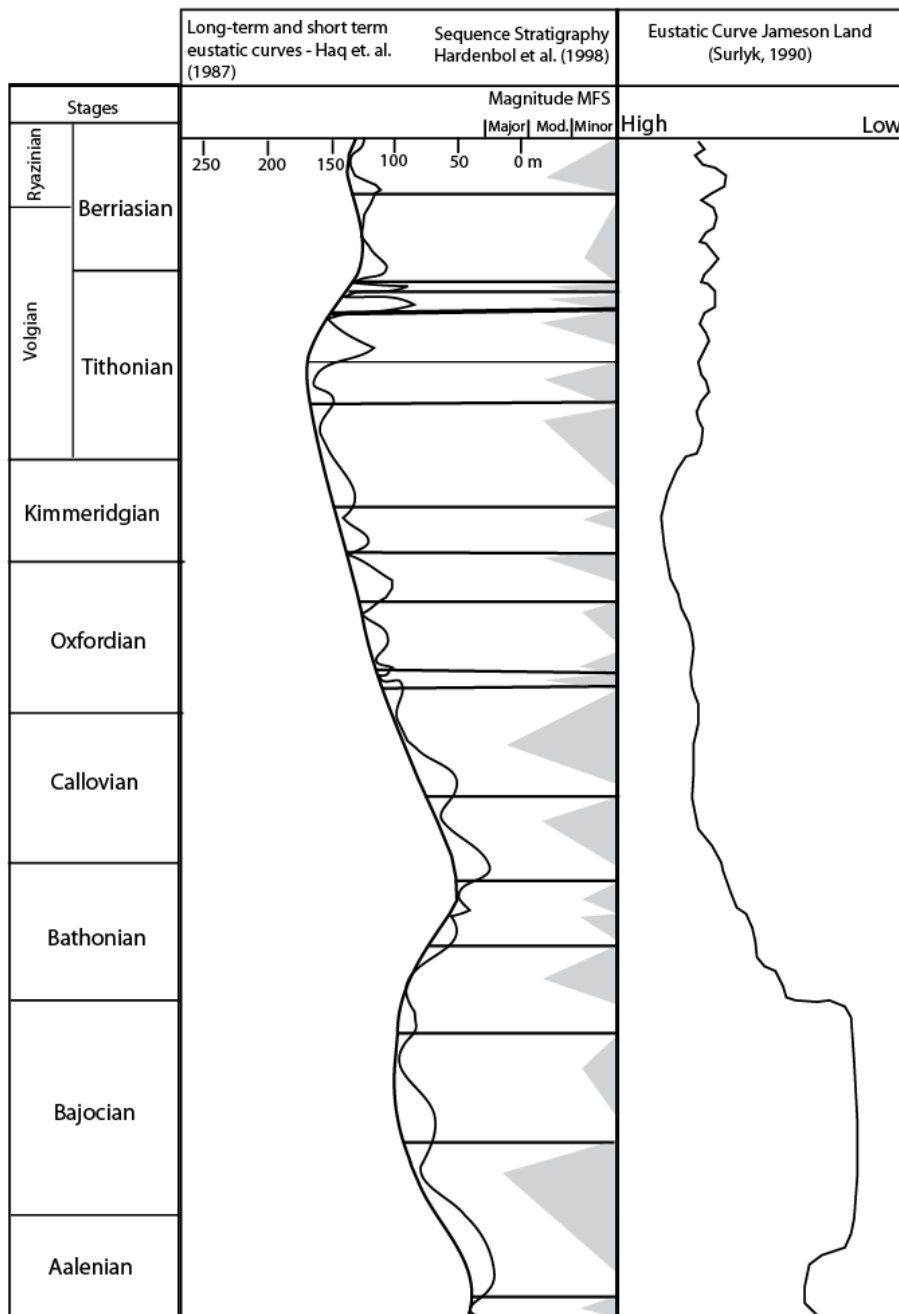


Figure 33: Composite sea level charts of the Jurassic to Lower Cretaceous, including transgressive-regressive cycles from Hardenbol et al. (1998). Modified from Haq et al. (1988), Surlyk (1990), and Hardenbol et al. (1998).

### 5.1.3. SUBSIDENCE

Subsidence is responsible for the accommodation creation, allowing for sediments to accumulate within a basin. The time thickness map (Figure 32) revealed several isolated depocenters located in the northern, central eastern and southern parts of the basin. The dominant depocenters were found to be related to FF2, whereas the minor depocenters are related to FF3 and FF4, suggesting a dominant tectonic control on the accommodation creation within the study area.

Figure 34 shows subsidence plots generated for the Jurassic and Lower Cretaceous intervals to gain a better understanding of the accommodation creation through time. On the AFC High (well 7120/2-3-S) a slight deflection of the subsidence curve is observed in the Middle Jurassic (Figure 34), most likely reflecting the rift initiation on the northern margin. This event of accommodation creation is consistent with the more continuous sequences of J1 and J2 observed on the northern basin margin (Figure 25Figure 26Figure 27). The Upper Jurassic in this area is characterized by relatively constant subsidence rates, and no major influence from subsidence is seen until the Lower Cretaceous. The same trends are present further basinwards, in wells 7120/6-3-S and 7121/4-2. The Middle to Upper Jurassic show more or less constant rates of subsidence, with no major deflections until the Lower Cretaceous. Wells 7120/9-1 and 7120/12-1 on the southern margin reveals a different trend. Well 7120/9-1 show low subsidence rates until the Early Oxfordian, which is followed a marked deflection in the curve. This deflection most likely reflects an episode of rifting related to FF2. Well 7121/12-1 shows high subsidence rates during the entire studied time interval, with rapid increases occurring in the Late Middle Jurassic and Late Upper Jurassic. This suggests that the more continuous sedimentation in this area due to more accommodation creation along FF2.

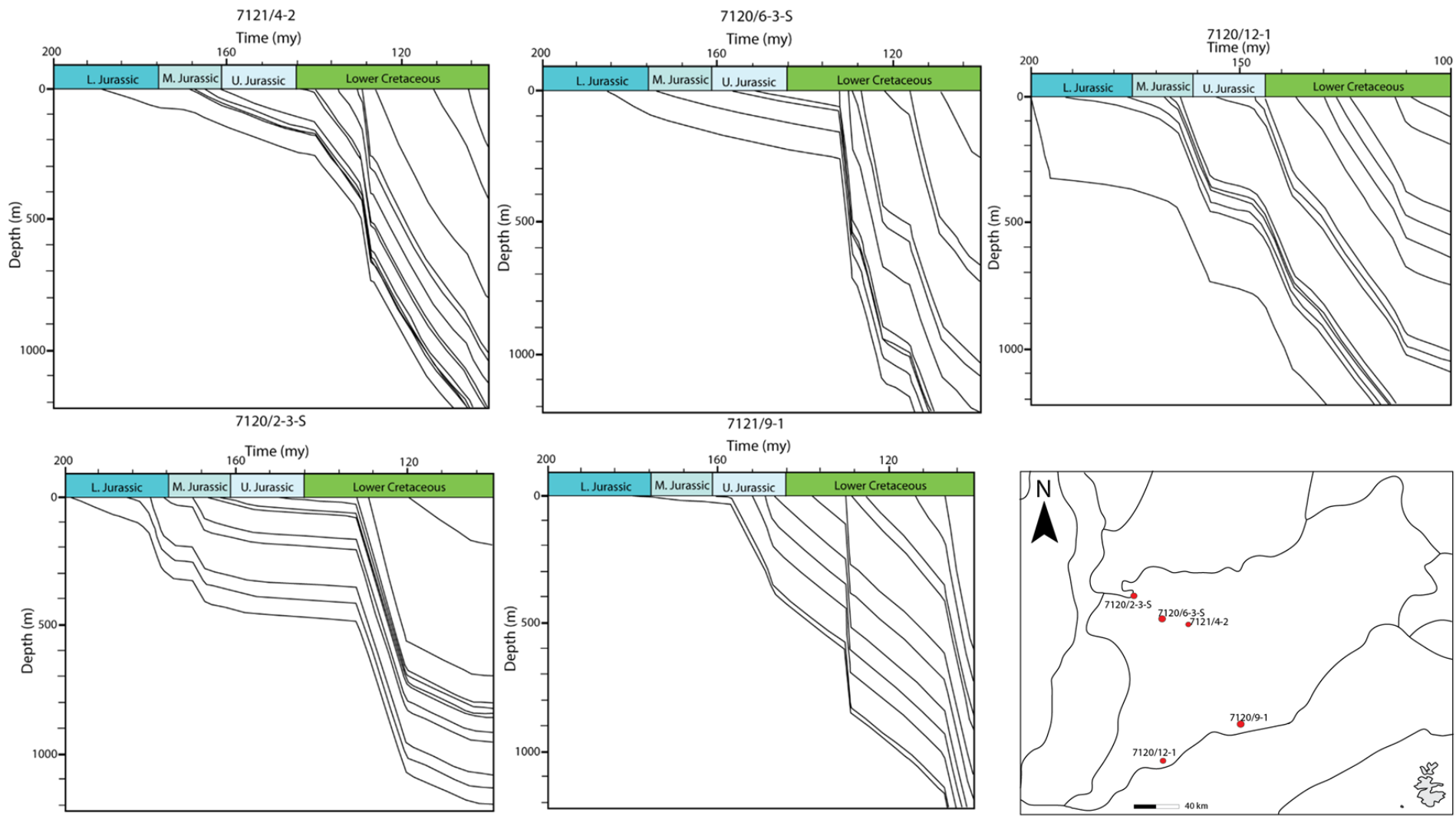


Figure 34: Subsidence plots generated for wells 7121/4-2, 7120/6-3-S, 7120/12-1, 7120/2-3-S and 7121/9-1. Note the large variability in subsidence at different locations. Locations of wells are indicated in insert map.

The subsidence curves together with the assumed low sediment supply suggest the subsidence is controlled by tectonics rather than isostatic loading. Accommodation creation due to fault activity along FF2 was more prominent on the northern margin during the deposition of J1 and J2 compared to the southern margin. However, a shift is noted during the deposition of J3-J5, where more accommodation was created on the southern margin during these times. Moreover, subsidence appears more prominent towards the southwest, indicating differential subsidence across the segmented FF2. Subsidence was however less prominent on the northern margin, which could reflect the onset of uplift of the Loppa High. The fact that the depocenters are located in the hangingwalls of major faults and are isolated from each other could suggest that the fault systems of FF2, FF3 and FF4 were discontinuous during this stage, and that the segmented fault system led to differential subsidence and consequently diachronous deposition of the different sequences and the associated depositional facies.

## **5.2. Depositional Evolution**

### **5.2.1. STAGE 1: LATE BATHONIAN – OXFORDIAN (SEQUENCES J1 AND J2)**

The lithological characteristics combined with biostratigraphic data indicates that the southwestern margin during sequences J1 and J2 was dominated by shallow marine processes in an overall low-energy lower shoreface to offshore environment (Figure 35). Age control reveals that deposition of organic rich facies (FA4) was initiated during this stage, represented by the upper unit of J2, and was related to local restrictions along FF2, FF3 and FF4 (Figure 35).

Omission surfaces observed from cores in the vicinity of the Central High suggest times of low sedimentation rates, possibly related to uplift of the structure from the Bathonian to Oxfordian. Uplift would lead to topographic differences, exposing this area for erosional processes, or leading to condensed sections or non-deposition. Erosion and non-deposition in this area are further supported by the onlap relationship observed in seismic (Figure 29) and the absence of Bathonian and Callovian strata over the high (Figure 27). Omission surfaces are also noted on the Goliat Anticline, together with onlapping of the Middle to Upper Jurassic seismic sequence towards the high (Figure 30). FA2 lacks age control on the Goliat High, but based on the overall younging eastwards trend, FA2 in this area is tentatively correlated from GR-logs of nearby wells to be of late Oxfordian to Kimmeridgian age, suggesting that this area was dominated by erosion and non deposition during deposition of sequences J1 and J2. The minor coarse grained intervals (FA1) observed at the base of sequence J1 is believed to be a result of reworking of previously deposited sediments.

The GR facies observed on the northern margin suggest more dominance of offshore processes, further supported by the subsidence plots where accommodation creation

was more prominent on the northern margin during J1 and J2. The dominance of fine-grained sediments deposited during this stage, suggests an absence of a major clastic source-areas northwards and southwards. Due to the possible fault activity along FF2 on the northern margin indicated by the subsidence plots, the Loppa High is interpreted as slightly uplifted comprising more paralic facies, and not as a dominant clastic sediment source (Figure 35).

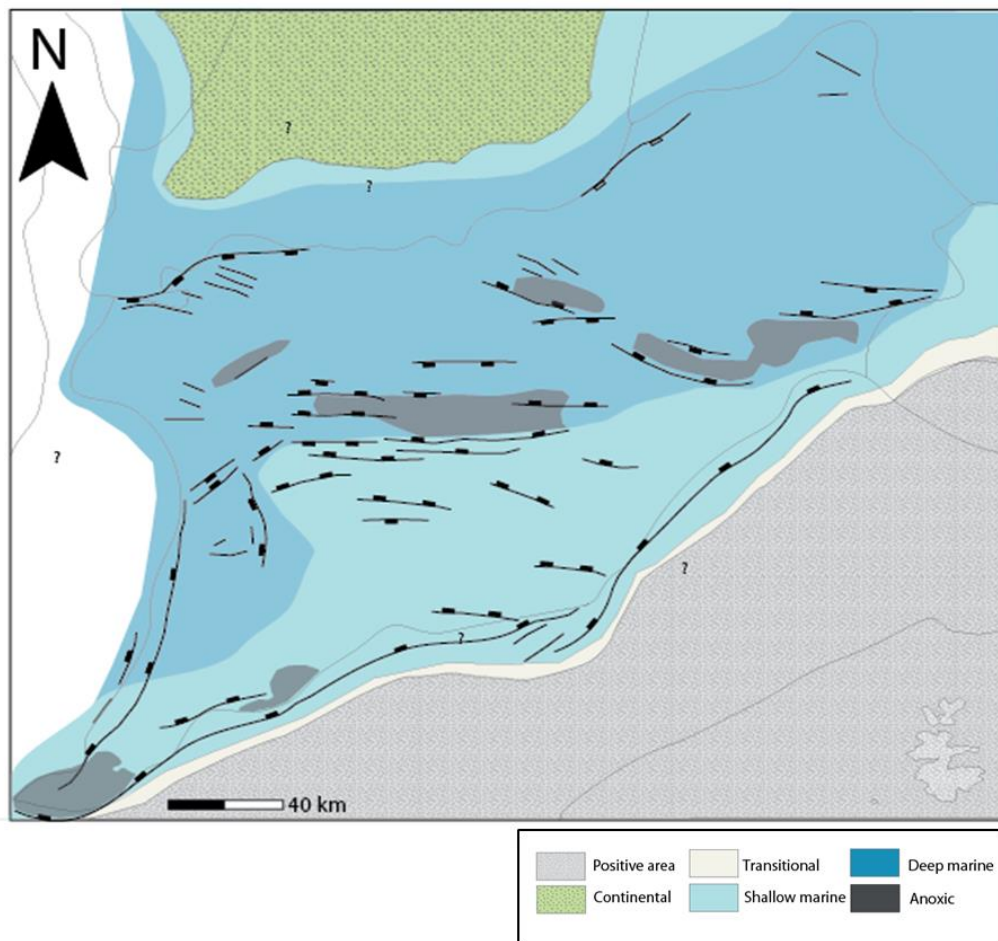


Figure 35: Paleogeographic interpretation of sequences J1 and J2.



### **5.2.2. STAGE 2: KIMMERIDGIAN – RYAZINIAN (SEQUENCES J3-J5)**

From sequences J3-J5 the Hammerfest Basin experienced more widespread deposition of organic rich facies (FA4), and offshore processes were more dominant across the entire study area (Figure 36). Still, deposition of FA4 is believed to be controlled by accommodation creation and restriction related to FF2, FF3 and FF4, but not as dominant as in sequence J1-J2.

The thin units and absence of younger sediments (Kimmeridgian – Ryazinian) in the eastern part of the Hammerfest Basin (Figure 25; Figure 26) indicates that this area was a site of low sedimentation rates, and possibly exposed to erosion or non-deposition during this stage. Thus, a more shallow marine environment is inferred (Figure 36). The aggradational stacking patterns and presence of FA5 within this stage indicates a slight increase in sedimentation rates, resulting from rejuvenation of distal source areas both in the northern and southern areas. However, the absence of coarse-grained conglomerates along the basin margins suggest that the rejuvenation and subsequent erosion of the hinterlands was not particularly prominent.

The deposition of sand-rich sediments are restricted to the northern and southern basin margins, and confined to sequences J4 and J5 (Figure 36). The absence of sand rich deposits further basinwards suggests that the intra-basinal highs (AFC High, Central High and Goliat Anticline) did not serve as sites for widespread erosion. However, the onlap relationship (Figure 29) and absence of Kimmeridgian strata suggests that the Central High was an area of erosion or non-deposition during this stage, thus, a higher energy, shallow marine environment is inferred for this area (Figure 37).

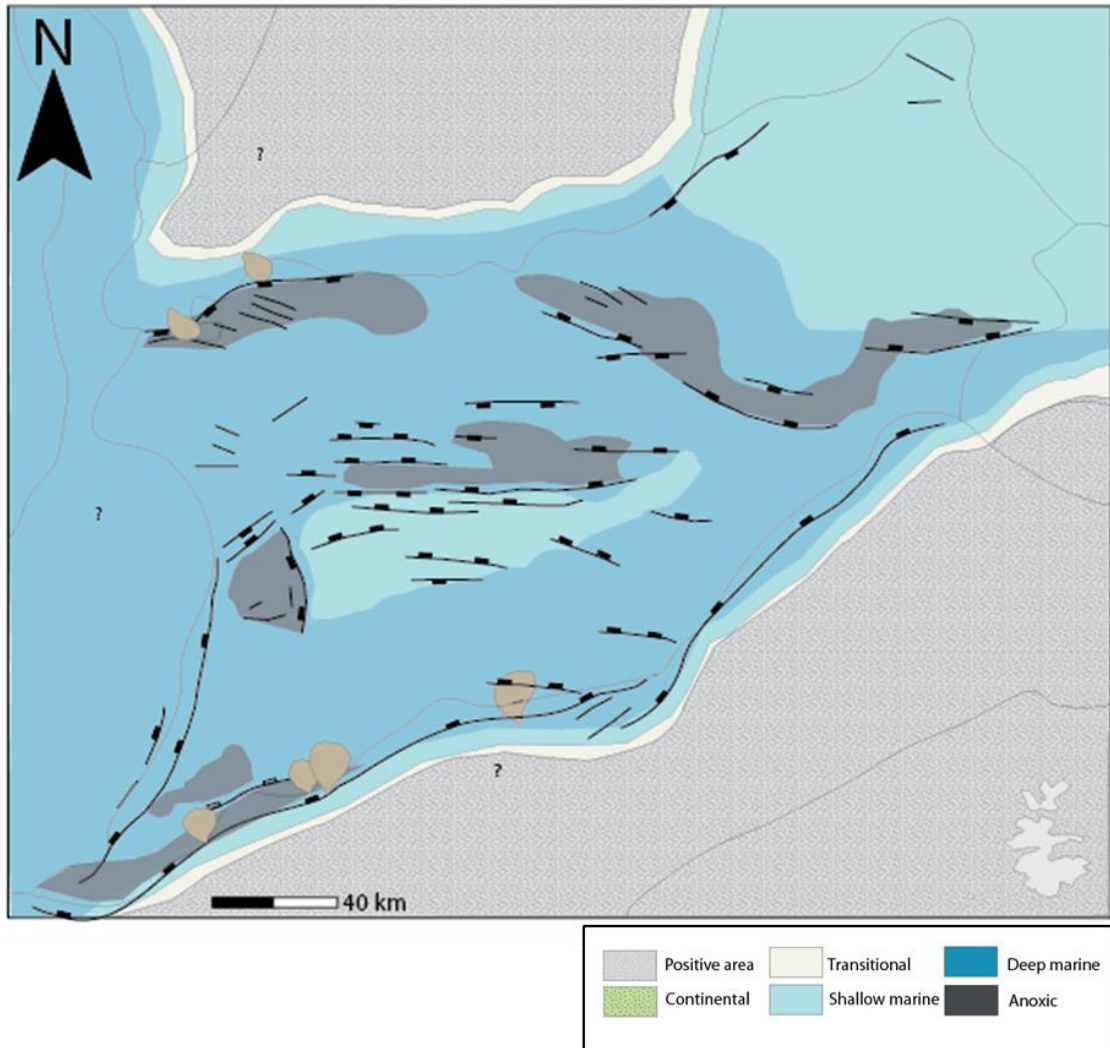


Figure 36: Paleogeographic interpretation of sequences J3-J5. Note the more widespread deposition of offshore and anoxic facies during this stage.

## 6. CONCLUSIONS

This study of the Middle to Upper Jurassic of the Hammerfest Basin using core-, seismic-, and petrophysical proves that the depositional setting comprised a more complex system than previously described. The main findings and contributions are summarised below:

- Five facies associations (FA1-FA5) comprising transgressive shelf deposits, lower shoreface to offshore transition zone deposits, offshore deposits, restricted anoxic and mass flow facies.
- Five genetic sequences (J1-J5) bounded by unconformities and flooding surfaces are defined based on ages and stacking patterns. The genetic sequences have time significance, and show a good correlation with the existing lithostratigraphic framework. Moreover, the sequences also show a good correlation with the defined facies associations.
- Four fault families (FF) are defined based on similar strikes and ages. The fault families comprises the NNW-SSE striking FF1 on the western basin margin, the NW-SE basin bounding faults of FF2 on the northern and southern margins, the E-W trending FF3 in the central part of the basin, and lastly the NW-SE striking FF4 located in the eastern part of the study area.
- Rate of sediment supply was extremely low during the deposition of sequences J1-J3 due to a lack of source area. Sequence J3 represents the time of maximum flooding and widespread deposition of organic rich facies. A slight increase in sediment supply is noted during the deposition of J4 and J5, due to minor hinterland rejuvenation to the north and south.
- The deposition of sequences J1-J5 correlates to a regional event of sea level rise, and the transgressive effects were further amplified due to local tectonics.

- Local tectonics acts as the main controlling factor on sedimentation throughout the Middle to Upper Jurassic interval. Diachronous fault activity along FF2, FF3 and FF4 led to the formation of isolated depocenters, where water circulation was restricted, and conditions were optimal for deposition of organic rich facies (FA4). Moreover, differential subsidence related to the individual fault segments of FF2, FF3 and FF4 controlled the accommodation creation and the subsequent depositional facies.
- Sand-rich intervals are confined to sequences J4 and J5, restricted to the basin margins and controlled by FF2.

## REFERENCES:

- BERGLUND, L. T., AUGUSTSSON, J., FÆRSETH, R., GJELBERG, J. & RAMBERG-MOE, H. 1986. The evolution of the Hammerfest Basin. *In: SPENCER, A. M. (ed.) Habitat of hydrocarbons on the Norwegian Continental Shelf*. London: Graham & Trotman for the Norwegian Petroleum Society, pp. 319-338.
- BLATT, H., MIDDLETON, G. & MURRAY, R. 1972a. Facies Models. *In: BLATT, H., MIDDLETON, G. & MURRAY, R. (eds.) Origin of Sedimentary Rocks*. New Jersey: Prentice-Hall Inc, pp. 185-211.
- BLATT, H., MIDDLETON, G. & MURRAY, R. 1972b. Sedimentary Structures. *In: BLATT, H., MIDDLETON, G. & MURRAY, R. (eds.) Origin of Sedimentary Rocks*. New Jersey: Prentice-Hall, pp. 111-184.
- BOGGS, S. 2006. Sedimentary Structures. *In: LYNCH, P. (ed.) Principles of Sedimentology and Stratigraphy*. 4 ed. London: Pearson Prentice Hall, pp. 74-116.
- BONEWITZ, R. L. 2012. Minerals. *In: FRANCES, P. (ed.) Rocks and Minerals*. London: Dorling Kindersley Limited, pp. 166-246.
- BOUMA, A. H. 1962. Sedimentology of Some Flysch Deposits: A Graphic Approach to Facies Interpretations. *Elsevier*, 168.
- BUGGE, T., ELVEBAKK, G., FANAVOLL, S., MANGERUD, G., SMELROR, M., WEISS, H. M., GJELBERG, J., KRISTENSEN, S. E. & NILSEN, K. 2002. Shallow stratigraphic drilling applied in hydrocarbon exploration of the Nordkapp Basin, Barents Sea. *Marine and Petroleum Geology*, 19, 13-37.
- CATTANEO, A. & STEEL, R. J. 2003. Transgressive deposits: a review of their variability. *Earth-Science Reviews*, 62, 187-228.
- CATUNEAU, O. 2006. Methods of Sequence Stratigraphic Analysis. *In: CATUNEAU, O. (ed.) Principles of Sequence Stratigraphy*. 1 ed. Oxford: Elsevier, pp. 17-40.
- CLOUD, P. E. 1955. Physical limits of glauconite formation. *AAPG Bulletin*, 39, 484-492.
- DALLAND, A., WORSLEY, D. & OFSTAD, K. 1988. A lithostratigraphic scheme for the mesozoic and cenozoic and succession offshore mid-and northern Norway. *NPD Bulletin*, 65.
- DENGO, C. A. & RØSSLAND, K. G. 1992. Extensional tectonic history of the western Barents Sea. *In: LARSEN, R. M., BREKKE, H., LARSEN, B. T. & TALLERAAS, E. (eds.) Structural and tectonic modelling and its application to petroleum geology*. Norwegian Petroleum Society special publication 1. Amsterdam: Elsevier, pp. 91-108.
- DORÉ, A. G. 1995. Barents Sea geology, petroleum resources and commercial potential. *The Arctic Institute of North America*, 48, 207-221.
- DORÉ, A. G. & JENSEN, L. N. 1996. The impact of late Cenozoic uplift and erosion on hydrocarbon exploration: offshore Norway and some other uplifted basins. *Global and Planetary Change*, 12, 415-436.
- DZULYNSKI, S. & WALTON, E. K. 1965. *Sedimentary features of flysch and greywackes*, Elsevier.

- EINSELE, G. 2000a. The Interplay Between Sediment Supply, Subsidence, and Basin Fill. *In: EINSELE, G. (ed.) Sedimentary Basins: Evolution, Facies and Sediment Budget*. 2 ed. Berlin: Springer, pp. 480-536.
- EINSELE, G. 2000b. Sequences, Minor Cycles, and Event Stratigraphy. *In: EINSELE, G. (ed.) Sedimentary Basins: Evolution, Facies and Sediment Budget*. 2 ed. Berlin: Springer, pp. 292-384.
- EINSELE, G. 2000c. Special Depositional Environments and Sediments. *In: EINSELE, G. (ed.) Sedimentary Basins: Evolution, Facies and Sediment Budget*. 2 ed. Berlin: Springer, pp. 249-290.
- FALEIDE, J., VÅGNES, E. & GUDLAUGSSON, S. Late Mesozoic–Cenozoic evolution of the southwestern Barents Sea. Geological Society, London, Petroleum Geology Conference series, 1993a. Geological Society of London, 933-950.
- FALEIDE, J. I., BJØRLYKKE, K. & GABRIELSEN, R. H. 2010. Geology of the Norwegian Continental Shelf. *In: BJØRLYKKE, K. (ed.) Petroleum Geoscience. From Sedimentary Environments to Rock Physics*. Berlin: Springer, pp. 467-499.
- FALEIDE, J. I., TSIKALAS, F., BREIVIK, A. J., MJELDE, R., RITZMANN, O., ENGEN, O., WILSON, J. & ELDHOLM, O. 2008. Structure and evolution of the continental margin off Norway and the Barents Sea. *Episodes*, 31, 82-91.
- FALEIDE, J. I., VÅGNES, E. & GUDLAUGSSON, S. T. 1993b. Late Mesozoic–Cenozoic evolution of the south-western Barents Sea in a regional rift-shear tectonic setting. *Marine and Petroleum Geology*, 10, 186-214.
- GABRIELSEN, R. H., FÆRSETH, R. B., JENSEN, L. N., KALHEIM, J. E. & RIIS, F. 1990. Structural elements of the Norwegian continental shelf. *NPD Bulletin*, 6, 33.
- GALLOWAY, W. E. 1989. Genetic stratigraphic sequences in basin analysis I: architecture and genesis of flooding-surface bounded depositional units. *AAPG bulletin*, 73, 125-142.
- GLØRSTAD-CLARK, E. 2010. *Basin analysis in the western Barents Sea area: The interplay between accommodation space and depositional systems*. Ph.D., University of Oslo.
- GUDLAUGSSON, S., FALEIDE, J., JOHANSEN, S. & BREIVIK, A. 1998. Late Palaeozoic structural development of the south-western Barents Sea. *Marine and Petroleum Geology*, 15, 73-102.
- HAQ, B., HARDENBOL, J. & VAIL, P. R. 1988. Mesozoic and Cenozoic chronostratigraphy and cycles of sea-level change. *In: WILGUS, C., HASTINGS, B., KENDALL, C., POSAMENTIER, C., ROSS, H. & WAGONER, J. V. (eds.) Sea level changes: An integrated approach*. Special Publication 42. Society of Economic Paleontologists and Mineralogists, pp. 3-17.
- HARDENBOL, J., THIERRY, J., FARLEY, M., DE GRACIANSKY, P.-C. & VAIL, P. 1998. Mesozoic and Cenozoic Sequence Chronostratigraphic Framework of European Basins. *In: DE GRACIANSKY, P.-C., HARDENBOL, J., THIERRY, J. & VAIL, P. (eds.) Mesozoic and Cenozoic Sequence Chronostratigraphic Framework of European Basins*. Special Publication 60. Society of Economic Paleontologists and Mineralogists, pp. 783.

- HENRIKSEN, E., RYSETH, A. E., LARSSSEN, G. B., HEIDE, T., RØNNING, K., SOLLID, K. & STOUPAKOVA, A. V. 2011. Tectonostratigraphy of the greater Barents Sea: implications for petroleum systems. *In*: SPENCER, A. M., EMBRY, A. F., GAUTIER, D. L., STOUPAKOVA, A. V. & SØRENSEN, K. (eds.) *Arctic Petroleum Geology*. 35. London: Geological Society, pp. 163-195.
- HURST, A., CARTWRIGHT, J. & DURANTI, D. 2003. Fluidization structures produced by upward injection of sand through a sealing lithology. *Geological Society, London, Special Publications*, 216, 123-138.
- HURST, A., SCOTT, A. & VIGORITO, M. 2011. Physical characteristics of sand injectites. *Earth-Science Reviews*, 106, 215-246.
- INDREVÆR, K., GABRIELSEN, R. H. & FALEIDE, J. I. 2016. Early Cretaceous synrift uplift and tectonic inversion in the Loppa High area, southwestern Barents Sea, Norwegian shelf. *Journal of the Geological Society*, 174, 242-254.
- JAKOBSSON, M., MAYER, L., COAKLEY, B., DOWDESWELL, J. A., FORBES, S., FRIDMAN, B., HODNESDAL, H., NOORMETS, R., PEDERSEN, R. & REBESCO, M. 2012. The international bathymetric chart of the Arctic Ocean (IBCAO) version 3.0. *Geophysical Research Letters*, 39.
- JOHNSON, H. D. & BALDWIN, C. T. 1996. Shallow clastic seas. *In*: READING, H. G. (ed.) *Sedimentary Environments: Processes, Facies and Stratigraphy*. Oxford: Blackwell Publishing, pp. 232-280.
- LARSSSEN, G. B., ELVEBAKK, G., HENRIKSEN, L. B., KRISTENSEN, S., NILSSON, I., SAMUELSBERG, T. J., SVÅNÅ, T. A., STEMMERIK, L. & WORSLEY, D. 2002. Upper Palaeozoic lithostratigraphy of the Southern Norwegian Barents Sea. *NPD Bulletin*, 9, 76.
- LEITH, T. L., WEISS, H. M., MØRK, A., ÅRHUS, N., ELVEBAKK, G., EMBRY, A. F., BROOKS, P. W., STEWART, K. R., PCHELINA, T. M., BRO, E. G., VERBA, M. L., DANYUSHEVSKAYA, A. & BORISOV, A. V. 1993. Mesozoic hydrocarbon sourcerocks of the Arctic region. *In*: VORREN, T. O., BERGSAGER, E., DAHL-STAMNES, Ø. A., HOLTER, E., JOHANSEN, B., LIE, E. & LUND, T. B. (eds.) *Arctic Geology and Petroleum Potential: Norwegian Petroleum Society Special Publication*. 2. Amsterdam: Elsevier, pp. 1-25.
- LINJORDET, A. & OLSEN, R. G. 1992. The Jurassic Snohvit Gas Field, Hammerfest Basin, Offshore Northern Norway. *In*: HALBOUTY, M. T. (ed.) *Giant Oil and Gas Fields of the Decade 1978-1988*. AAPG Memoir 54. Tulsa: American Association of Petroleum Geologists, pp. 349-370.
- MACEACHERN, J. A. & BANN, K. L. 2008. The role of ichnology in refining shallow marine facies models. *In*: HAMPSON, G. J., STEEL, R. J., BURGESS, P. M. & DALRYMPLE, R. W. (eds.) *Recent Advances in Models of Siliciclastic Shallow-marine Stratigraphy*. Society for Sedimentary Geology, Special Publications 90, pp. 73-116.
- MACEACHERN, J. A., RAYCHAUDHURI, I. & PEMBERTON, S. G. 1992. Stratigraphic applications of the Glossifungites ichnofacies: delineating discontinuities in the rock record. *In*: PEMBERTON, S. G. (ed.) *Applications of Ichnology to Petroleum Exploration: A Core Workshop*. 17. SEPM Society for Sedimentary Geology.

- MARÍN, D. 2017. *Tectonostratigraphic evolution of the southwestern Barents Sea during the Early Cretaceous*. PhD, University of Stavanger.
- MORAD, S., AL-RAMADAN, K., KETZER, J. M. & DE ROS, L. 2010. The impact of diagenesis on the heterogeneity of sandstone reservoirs: A review of the role of depositional facies and sequence stratigraphy. *AAPG bulletin*, 94, 1267-1309.
- MULROONEY, M. J., LEUTSCHER, J. & BRAATHEN, A. 2017. A 3D structural analysis of the Goliat field, Barents Sea, Norway. *Marine and Petroleum Geology*, 86, 192-212.
- MULROONEY, M. J., RISMYHR, B., YENWONGFAI, H. D., LEUTSCHER, J., OLAUSSEN, S. & BRAATHEN, A. 2018. Impacts of small-scale faults on continental to coastal plain deposition: Evidence from the Realgrunnen Subgroup in the Goliat field, southwest Barents Sea, Norway. *Marine and Petroleum Geology*.
- MUTTI, E. & RICCI LUCCHI, F. 1978. Turbidites of the northern Apennines: introduction to facies analysis. *International geology review*, 20, 125-166.
- MYERS, K. & MILTON, N. 1996. Concepts and Principles of Sequence Stratigraphy. In: EMERY, D. & MYERS, K. (eds.) *Sequence Stratigraphy*. Oxford: Blackwell Science, pp. 11-45.
- MØRK, A., DALLMANN, W., DYPVIK, H., JOHANNESSEN, E., LARSSSEN, G., NAGY, J., NØTTVEDT, A., OLAUSSEN, S., PCHELINA, T. & WORSLEY, D. 1999. Mesozoic Lithostratigraphy. In: DALLMANN, W. K. (ed.) *Lithostratigraphic lexicon of Svalbard: review and recommendations for nomenclature use: Upper Palaeozoic to Quaternary bedrock*. Tromsø: Norsk Polarinstitut, pp. 127-214.
- NICHOLS, G. 2009a. The Marine Realm: Morphology and Processes. In: NICHOLS, G. (ed.) *Sedimentology and Stratigraphy*. 2 ed. Oxford: Wiley-Blackwell, pp. 163-178.
- NICHOLS, G. 2009b. Processes of Transport and Sedimentary Structures. In: NICHOLS, G. (ed.) *Sedimentology and Stratigraphy*. 2 ed. Oxford: Wiley-Blackwell, pp. 44-68.
- NICHOLS, G. 2009c. Shallow Sandy Seas. In: NICHOLS, G. (ed.) *Sedimentology and Stratigraphy*. 2 ed. Oxford: Wiley-Blackwell, pp. 215-224.
- NPD. 2018. *Norwegian Petroleum Directorate Factpages* [Online]. Available: <http://factpages.npd.no/factpages/Default.aspx?culture=en> [Accessed July 2018].
- NØTTVEDT, A., CECCHI, M., GJELBERG, J. G., KRISTENSEN, S. E., LØNØY, A., RASMUSSEN, A., RASMUSSEN, E., SKOTT, P. H. & VEEN, P. M. V. 1993. Svalbard-Barents Sea correlation: a short review. In: VORREN, T. O., BERGSAGER, E., DAHL-STAMNES, Ø. A., HOLTER, E., JOHANSEN, B., LIE, E. & LUND, T. B. (eds.) *Arctic Geology and Petroleum Potential: Norwegian Petroleum Society Special Publication*. 2. Amsterdam: Elsevier, pp. 363-375.
- NØTTVEDT, A. & JOHANNESSEN, E. P. 2008. The source of Norway's oil wealth. In: RAMBERG, I. B., BRYHNI, I., NØTTVEDT, A. & RANGNES, K. (eds.) *The Making of a Land, Geology of Norway*. Trondheim: Norsk Geologisk Forening, pp. 387-417.



- NØTTVEDT, A. & JOHANNESSEN, E. P. 2013. Grunnlaget for Norges oljerikdom. *In: RAMBERG, I. B., BRYHNI, I., NØTTVEDT, A. & RANGNES, K. (eds.) Landet blir til - Norges geologi. 2 ed. Trondheim: Norsk Geologisk Forening, pp. 386-422.*
- OHM, S. E., KARLSEN, D. A. & AUSTIN, T. 2008. Geochemically driven exploration models in uplifted areas: Examples from the Norwegian Barents Sea. *AAPG bulletin*, 92, 1191-1223.
- OLAUSSEN, S., DALLAND, A., GLOPPEN, T. G. & JOHANNESSEN, E. 1984. Depositional environment and diagenesis of Jurassic reservoir sandstones in the eastern part of Troms I area. *In: SPENCER, A. M. (ed.) Petroleum Geology of the North European Margin. London: Springer, pp. 61-79.*
- POTTER, P. E., MAYNARD, J. B. & DEPETRIS, P. J. 2005a. Burial. *In: POTTER, P. E., MAYNARD, J. B. & DEPETRIS, P. J. (eds.) Mud and Mudstones. New York: Springer, pp. 127-155.*
- POTTER, P. E., MAYNARD, J. B. & DEPETRIS, P. J. 2005b. Muddy Basins. *In: POTTER, P. E., MAYNARD, J. B. & DEPETRIS, P. J. (eds.) Mud and Mudstones. New York: Springer, pp. 175-222.*
- POTTER, P. E., MAYNARD, J. B. & DEPETRIS, P. J. 2005c. Muddy Depositional Systems. *In: POTTER, P. E., MAYNARD, J. B. & DEPETRIS, P. J. (eds.) Mud and Mudstones. New York: Springer, pp. 75-124.*
- POTTER, P. E., MAYNARD, J. B. & DEPETRIS, P. J. 2005d. Role of Oxygen. *In: POTTER, P. E., MAYNARD, J. B. & DEPETRIS, P. J. (eds.) Mud and Mudstones. New York: Springer, pp. 55-73.*
- PUCHKOV, V. 2013. Structural stages and evolution of the Urals. *Mineralogy and Petrology*, 107, 3-37.
- PUCHKOV, V. N. 2009. The evolution of the Uralian orogen. *Geological Society, London, Special Publications*, 327, 161-195.
- READING, H. G. & COLLINSON, J. D. 1996. Clastic Coasts. *In: READING, H. G. (ed.) Sedimentary Environments: Processes, Facies and Stratigraphy. 3 ed. Oxford: Blackwell Publishing, pp. 154-228.*
- REY, P., BURG, J.-P. & CASEY, M. 1997. The Scandinavian Caledonides and their relationship to the Variscan belt. *Geological Society, London, Special Publications*, 121, 179-200.
- RIIS, F., LUNDSCHIEN, B. A., HØY, T., MØRK, A. & MØRK, M. B. E. 2008. Evolution of the Triassic shelf in the northern Barents Sea region. *Polar Research*, 27, 318-338.
- RIIS, F., VOLLSET, J. & SAND, M. 1986. Tectonic development of the western margin of the Barents Sea and adjacent areas.
- ROBERTS, D. & LIPPARD, S. J. 2005. Inferred Mesozoic faulting in Finnmark: current status and offshore links. *Norges geologiske undersøkelse Bulletin*, 443, 55-60.
- SHANMUGAM, G., MOIOLA, R. & DAMUTH, J. 1985. Eustatic control of submarine fan development. *In: BOUMA, A. H., NORMARK, W. R. & BARNES, N. E. (eds.) Submarine fans and related turbidite systems. New York: Springer, pp. 23-28.*

- SMELROR, M., PETROV, O., LARSSSEN, G. B. & WERNER, S. 2009. *Atlas: Geological history of the Barents Sea*, Trondheim, Norges Geologiske Undersøkelse.
- STEEL, R. J. & RAVNÅS, R. 1998. Architecture of marine rift-basin successions. *AAPG bulletin*, 82, 110-146.
- STEWART, D. J., BERGE, K. & BOWLIN, B. 1991. Exploration trends in the Southern Barents Sea. In: HANSLIEN, S. (ed.) *Petroleum Exploration and Exploitation in Norway*. 4. Amsterdam: Elsevier, pp. 253-276.
- STOW, D. A. V., READING, H. G. & COLLINSON, J. D. 1996. Deep Seas. In: READING, H. G. (ed.) *Sedimentary Environments: Processes, Facies and Stratigraphy*. 3 ed. Oxford: Blackwell Publishing, pp. 395-453.
- SUND, T., SKARPNES, O., JENSEN, L. N. & LARSEN, R. M. 1986. Tectonic development and hydrocarbon potential offshore Troms, northern Norway. In: HALBOUTY, M. T. (ed.) *Future petroleum provinces of the world*. 40. AAPG Memoir, pp. 615-627.
- SURLYK, F. 1990. A Jurassic sea-level curve for East Greenland. *Palaeogeography, Palaeoclimatology, Palaeoecology*, 78, 71-85.
- TAYLOR, A. M. & GOLDRING, R. 1993. Description and analysis of bioturbation and ichnofabric. *Journal of the Geological Society*, 150, 141-148.
- WETZEL, A. 1984. Bioturbation in deep-sea fine-grained sediments: influence of sediment texture, turbidite frequency and rates of environmental change. *Geological Society, London, Special Publications*, 15, 595-608.
- WILKIN, R. T., BARNES, H. L. & BRANTLEY, S. L. 1996. The size distribution of framboidal pyrite in modern sediments: an indicator of redox conditions. *Geochimica Cosmochimica Acta*, 60, 3897-392.
- WOOD, R. J., EDRICH, S. P. & HUTCHINSON, I. 1989. Influence of North-Atlantic Tectonics on the Large-Scale Uplift of the Stappen High and Loppa High, Western Barents Shelf. In: TANKARD, A. J. & BALKWILL, H. R. (eds.) *Extensional Tectonics and Stratigraphy of the North Atlantic Margins*. American Association of Petroleum Geologists Memoir 46, pp. 559-556.
- WORSLEY, D. 2008. The post-Caledonian development of Svalbard and the western Barents Sea. *Polar Research*, 27, 298-317.
- ZIEGLER, W. H., DOERY, R. & SCOTT, J. 1986. Tectonic Habitat of Norwegian oil and gas. In: SPENCER, A. M. (ed.) *Habitat of Hydrocarbons on the Norwegian Continental Shelf*. London: Graham and Trotman for the Norwegian Petroleum Society, pp. 3-21.